creative commons
COMMONS DEED

저작자표시-비영리-변경금지 2.0 대한민국

이용자는 아래의 조건을 따르는 경우에 한하여 자유롭게

- 이 저작물을 복제, 배포, 전송, 전시, 공연 및 방송할 수 있습니다.

다음과 같은 조건을 따라야 합니다:

저작자표시. 귀하는 원저작자를 표시하여야 합니다.

비영리. 귀하는 이 저작물을 영리 목적으로 이용할 수 없습니다.

변경금지. 귀하는 이 저작물을 개작, 변형 또는 가공할 수 없습니다.

- 귀하는, 이 저작물의 재이용이나 배포의 경우, 이 저작물에 적용된 이용허락조건을 명확하게 나타내어야 합니다.
- 저작권자로부터 별도의 허가를 받으면 이러한 조건들은 적용되지 않습니다.

저작권법에 따른 이용자의 권리는 위의 내용에 의하여 영향을 받지 않습니다.

이것은 이용허락규약(Legal Code)을 이해하기 쉽게 요약한 것입니다.

Disclaimer

dCollection

공학박사학위논문

멀티히트펌프시스템 내의 오일 축적과 오일분리기 성능에 관한 연구

Studies on the Oil Retention and Performance of Oil Separator in Multi Heat Pump System

2015 년 2 월

서울대학교 대학원

기계항공공학부

김 학 수

Abstract

Studies on the Oil Retention and Performance of Oil Separator in Multi Heat Pump System

Hak Soo Kim
Department of Mechanical and Aerospace Engineering
The Graduate School
Seoul National University

This paper presents analytical and experimental studies on the oil retention and performance of oil separator in multi heat pump system.

To suggest the proper charge amount of oil in a compressor of heat pump system, the prediction of oil retention amount in each component of heat pump system is necessary. This study proposed analytical models for predicting the oil retention amount in gas, liquid and two phase regions of refrigerant. Based on the proposed models, oil retention amount in each component of multi heat pump system was predicted. From the simulation results, it was confirmed that the oil retention amount decreases 26.1% and 67.3% as the mass flux of refrigerant rises from 100 $kgm^{-2}s^{-1}$ to 250 $kgm^{-2}s^{-1}$

and oil circulation ratio diminishes from 0.9% to 0.1%, respectively. Among 6 components which include condenser, horizontal and vertical liquid lines of refrigerant, evaporators, horizontal and vertical gas lines of refrigerant, large amount of oil is retained in the gas lines of refrigerant.

Because most of discharged oil is in the gas lines of refrigerant, prediction of oil retention amount in gas lines of refrigerant is important. To verify the model for predicting the oil retention amount in gas lines of refrigerant, experiment was conducted to measure the oil retention amount in horizontal and vertical gas lines of refrigerant. The oil retention amount and pressure drop were measured with respect to the mass flux of refrigerant, oil circulation ratio and pipe diameter. Flow visualization was also conducted for horizontal line. The oil retention amount tends to decrease as mass flux becomes higher or oil circulation ratio diminishes. As pipe diameter increases, the oil retention amount goes up. Generally, the oil retention amount in vertical line was higher than that in horizontal line due to the effect of gravity force. As mass flux of refrigerant rises, however, the effect of gravity force becomes negligible, so the oil retention amounts in horizontal and vertical lines were similar. Based on the experimental results, the model of oil retention amount in gas lines of refrigerant was verified. The mean absolute percentage error of predicted and experimental results was 15.0%.

From the analytical and experimental studies on the oil retention in each components of heat pump system, it was confirmed that the oil circulation ratio highly affects the oil retention amount and pressure drop. Reduction of oil circulation ratio is required to enhance the system performance and reduce the initial charge amount of oil in compressor. In order to reduce the oil circulation ratio, high performance oil separator is necessary. This study measured the separation efficiency of oil separator and pressure drop at the oil separator. Separation efficiency and pressure drop were measured with respect to body diameter, body height and inlet configuration. Based on the experimental results, empirical models for predicting the separation efficiency and pressure drop were suggested. Different empirical models were proposed based on the inlet configuration. In case of inlet configuration of type 1, the mean absolute percentage errors of the models for efficiency and pressure drop were 0.4% and 7.8%. In case of type 2, those were 0.3% and 7.6%.

Keywords: Oil retention, Pressure drop, Oil separator, Multi heat pump system, R410A, PVE oil

***Identification Number*: 2011-31291**

Contents

List of Figures

List of Tables

Nomenclature

A	Area [m^2]
BD	Body diameter [m]
BH	Body height [m]
Co	Inlet loading [-]
CoL	Limit loading [-]
D	Diameter [m]
DS	Design
d	Droplet diameter [m]
dP	Pressure difference [Pa]
f	friction factor
G	Mass flux [$kgm^{-2}s^{1}$]
g	Gravitational acceleration [ms^{-2}]
H	Horizontal
HP	Horizontal pipe
h	heat transfer coefficient [$W\ m^{-2}K^{-1}$]
IC	Inlet configuration
IP	Injection position
INP	Inlet position [m]
ID	Inner diameter [m]
IID	Inlet inner diameter [m]
k	thermal conductivity [$Wm^{-1}K^{-1}$]
L	Length [m]
LCR	Liquid circulation ratio
MF	Mass fraction

MFR	Mass flow rate
MG	Model for gas phase region
ML	Model for liquid phase region
m	Mass [kg]
$\dot{m}$	Mass flow rate [kgs^{-1}]
OCR	Oil circulation ratio [-]
OD	Outer diameter [m]
OH	Outlet height [m]
OID	Outlet inner diameter [m]
P	Pressure [Pa]
Pr	Prandtl number
Q	Volumetric flow rate [m^3s^{-1}]
r	Length of radial direction [m]
R	Inner radius of pipe [m]
Re	Reynolds number
Refer	Reference
T	Temperature [K]
Tp	Type
u	Velocity [ms^{-1}]
V	Vertical
VP	Vertical pipe
Vol	Volume [m^3]
WT	Weight
x	Quality [-]

Greek symbols

ρ	Density [kg m^{-3}]
μ	Dynamic viscosity [Pa·s]
ɳ	Efficiency
ε	Error
v	Kinematic viscosity [m^2s^{-1}]
τ	Shear stress [Pa]
δ	Thickness [m]
α	Void fraction

Subscript

1	Location for the pipe length of 1 m
2	Location for the pipe length of 2 m
3	Location for the pipe length of 3 m
c	Core
cal	Calculated
comp	Compressor
EOS	Efficiency of oil separator
g	Gas
i	Interfacial
in	Inlet
l	Liquid
mm	Mass mean
OR	Oil retention
sh	Degree of superheat

tp	Two phase
TEO	Total extracted oil
TIO	Total injected oil

Chapter 1. Introduction

1.1 Background of the study

The energy consumption has been increased. According to the IEA (International Energy Agency), use of primary energy and electrical energy increased about 83.3% and 161.8% from 1973 to 2004. Specific information is shown in Table 1.1. This increment has depleted energy resources and caused environmental problems which include global warming, climate change and ozone layer depletion. So, save and reduction of energy consumption are required to slow down and prevent those problems. Pe´rez-Lombard *et al.* (2008) investigated the energy consumptions of various devices in mid and large size buildings. Fig. 1.1 shows the energy consumption ratio by end use for various building types in USA. As shown in Fig. 1.1, the energy consumption for heating and air conditioning is about 40 to 50% of total energy consumptions in mid and large size buildings. So effective method for heating and cooling of the building is necessary. There are many methods for heating and cooling of the building. Among them, heat pump shows high efficiency. So demand for multi heat pump system in mid and large size building has increased to save the energy consumption in the

Table 1.1 Global energy indexes increment from 1973 to 2004

Parameter	1973	2004	Ratio (%)
Population (millions)	3,938	6,352	61.3
Primary energy (Mtoe)	6,034	11,059	83.3
Electrical energy (Mtoe)	525	1,374	161.8
Per capita primary energy (toe)	1.53	1.77	15.7
Per capita CO_2 emissions (ton)	3.98	4.18	5.0

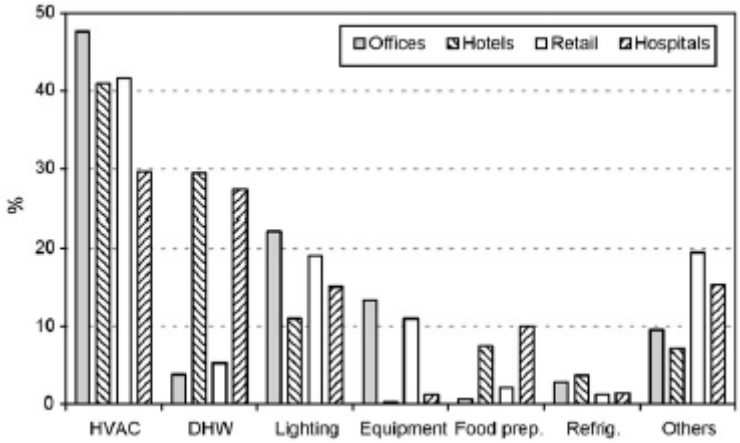

Fig. 1.1 Energy consumption ratio with respect to the end use for various building type

building. R410A is widely used in multi heat pump system because R410A does not contribute to ozone depletion and allows for high efficiency. There are many lubricants and lubricant is usually choosen based on the refrigerant. Polyvinylether (PVE) oil is used as a lubricant in heat pump system which uses R410A as a refrigerant because of good lubricity, good solubility and no hydrolysis.

A heat pump system consists of compressor, condenser, evaporator, expansion device and pipe line. Among these components, compressor has a moving part and the moving part of compressor typically needs a lubrication oil to reduce friction between metal moving parts and prevent possible damage of the compressor. Although the lubrication oil can enhance the compressor performance, small amounts of oil in compressor is discharged by the refrigerant which passes through the compressor. Generally, oil separator is installed at the outlet of the compressor to return the discharged oil to the compressor. Fig. 1.2 shows the ideal and real cases of pipe flow at the outlet of oil separator. If the efficiency of oil separator is 100%, all of the discharged oil from the compressor is separated and returns to the compressor. So only refrigerant comes out from the oil separator and circulates the heat pump system. Unfortunately, the efficiency of oil separator is not 100% in real system, so small amount of oil is unseparated at

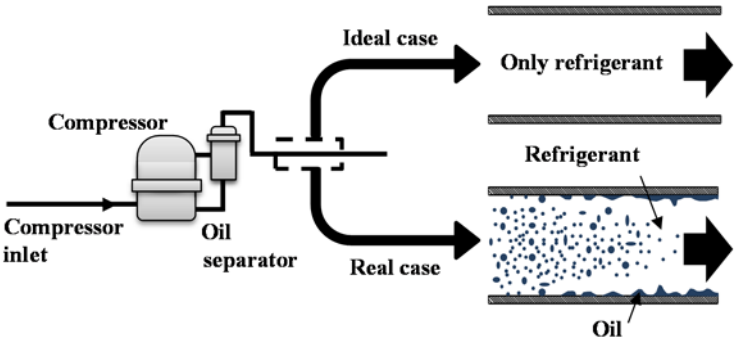

Fig. 1.2 Pipe flow patterns for ideal and real cases

the oil separator and circulates the heat pump system with refrigerant. Compare to the ideal case which only refrigerant circulates the system, small amount of unseparated oil causes increment of pressure drop, reduction of heat transfer effect and the durability problem of the compressor.

To predict the performance of heat pump system accurately, pressure drop and heat transfer effect of refrigerant and oil mixture should be considered. Pressure drop and heat transfer effect usually are predicted by the empirical correlations which are proposed based on the experimental data of refrigerant and oil mixture. However, the empirical correlations have limitations which include experimental conditions, working fluids and so on. So if there's no empirical correlation for specific operating conditions or working fluids, development of new correlation or verification of existing correlation under new operating conditions or working fluids are necessary.

In case of the durability problem of the compressor, it can be prevented by charging the proper amount of oil in the compressor. Proper charge amount of oil in the compressor is the summation of the amount of oil for lubrication inside a running compressor and the amount of the unseparated oil which circulates the whole system with refrigerant. The proper amount of oil for lubrication inside a running compressor can be provided by the manufacturer. However, the amount of unseparated oil which circulates the

whole system changes with the system operating conditions which include mass flow rate of refrigerant, efficiency of oil separator and so on and system installation conditions which include diameter and length of pipe line, number of heat exchanger, size of heat exchanger and so on. So numerical models for calculating the oil retention amount in each component of heat pump system are required to predict the amount of oil which circulates the system.

The efficiency of heat pump system increases as the amount of oil which circulates the system with refrigerant decreases. So development of high performance of oil separator is required to enhance the efficiency of heat pump system. There are many kinds of gas-liquid separators, and among them, a cyclone gas-liquid separator is widely used in heat pump system because of its simple design and high efficiency. Against its simple design, the flow characteristics in cyclone separator is very complex and hard to predict. Fig. 1.3 shows basic cyclone separator. As shown in Fig. 1.3, there are many design factors which include diameter and height of separator, diameter of inlet and outlet pipe, length of outlet pipe and so on. These design factors affect the performance of oil separator, so the model for predicting the performance of oil separator with respect to these design

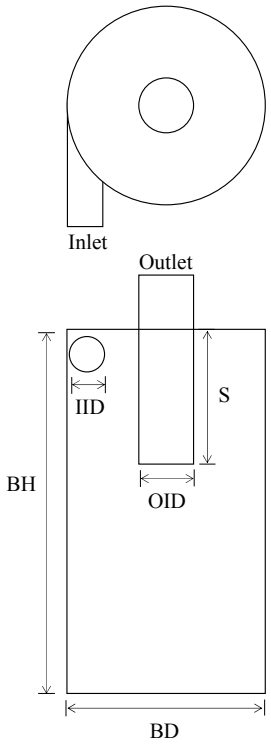

Fig. 1.3 Basic design of cyclone separator

factors and operating condition is required to develop the optimal oil separator.

1.2 Literature survey

Prediction of oil retention amount in heat pump system is required to decide the initial charge amount of oil in the compressor. The oil retention amount in heat pump system changes with the operating conditions and installation conditions. So the oil retention amount under various operating conditions and installation conditions has to be predicted. To calculate the oil retention amount in each component of heat pump system, modeling for each component of heat pump system is necessary. For the compressor and expansion device, performance can be calculated based on the performance data provided by the manufacturer. For the heat exchanger and refrigerant flow lines, the heat transfer coefficient and pressure drop in pipe under various operating conditions can be calculated using empirical correlations based on past studies. There have been many studies on heat transfer coefficient and pressure drop in the pipe flow, where the former can be calculated using the proposed empirical Nusselt number correlations. Dittus-Boelter (1930) suggested the local Nusselt number correlation of single

phase for turbulent flow in a smooth circular tube. This suggested an empirical correlation with the cooling and heating process. Winterton (1998) discussed historical origins of the Dittus-Boelter (1930) equation. Gnielinski (1976) proposed a new Nusselt number correlation of single phase flow for large Reynolds number range, including the transition region. Gungor and Winterton (1986) suggested an empirical Nusselt number correlation of boiling flow, then modified and suggested a simpler correlation (1987). Chen *et al.* (1987) proposed an experimental Nusselt number correlation for condensation flow based on analytical and empirical results, and compared calculation results from the new correlation to existing data. Wang *et al.* (1998), Wang and Chi (2000), Wang *et al.* (2000) and Wang *et al.* (2001) studied and proposed empirical correlations for air side heat transfer coefficient of a finned tube heat exchanger.

Similar to studies on the heat transfer coefficient, studies on pressure drop in pipe flow have been conducted. There are three states that include gas, liquid and two phase of refrigerant in the heat pump system. The pressure drop of single phase can be predicted based on the friction factor, which is calculated by using the Moody diagram or Petukhov's friction factor correlation. Incropera *et al.* (2007) discussed Petukhov's friction factor.

For the two phase flow pressure drop, there are several empirical

correlations. Lockhart and Martinelli (1949), Bankoff (1960), Grőnnerud (1972), Friedel (1979), and Műller-Steinhagen and Heck (1986) suggested empirical two phase pressure drop correlations in different forms. Thome (2004) summarized these correlations. Ould Didi *et al.* (2002) discussed the accuracy of each correlation and concluded that the correlations of Grőnnerud (1972) and Műller-Steinhagen and Heck (1986) are more accurate than those of the others.

Other studies proposed interfacial friction factor correlation for predicting the pressure drop of two phase flow. Wallis (1969) proposed an interfacial friction factor correlation as a function of liquid film thickness and pipe inner diameter. Fore *et al.* (2000) conducted an experiment using nitrogen and water in concurrent upward annular flow and obtained the film thickness and the pressure gradient data. Based on the experimental data, their research proposed a correlation for interfacial friction factor. The form of correlation from their research was quite similar to that of Wallis's correlation (1969). However, unlike Wallis's correlation, the gas phase Reynolds number was added to the correlation. Wongwises and Kongkiatwanitch (2001) also proposed a correlation for interfacial friction factor based on the experimental data which was obtained from air-water system. The correlation from this research was relatively simple. The

interfacial friction factor was expressed in terms of gas phase Reynolds number, liquid film thickness and pipe inner diameter. Ben (2002) conducted an experiment on air-oil and air-water systems and presented the empirical correlation for interfacial friction factor. The interfacial friction factor can be calculated from some variables including the roughness of pipe, the thickness of liquid film and Reynolds numbers of liquid and gas phase. Lee (2003) also suggested an empirical correlation for interfacial friction factor. The form of the correlation from this research is similar to that of Wongwise and Kongkiatwanitch (2001) but the coefficient and exponents are different. In this research, an experiment using carbon dioxide and PAG was conducted using an air conditioning system. Cremaschi (2004) suggested an empirical interfacial friction factor correlation for various refrigerant and oil mixtures, with the correlation given as a function of gas phase Reynolds number, liquid film thickness, inner pipe diameter and Weber number of mixture.

There have been many studies on the prediction or measurement of flow characteristics of refrigerant and oil mixture. Several studies have suggested void fraction correlations to predict the gas or liquid amount in a two phase pipe flow. Zivi (1964) suggested an analytical void fraction model that minimized the total kinetic energy of gas and liquid phase. Levi (1967)

derived an analytical momentum void fraction model. Smith (1969) and Chisholm (1972) proposed empirical void fraction equations.

Shedd and Newell (1997) suggested a new optical method for measuring the oil film thickness. Their method is a non-intrusive, automated procedure for various fluids and flow configurations. Crompton *et al.* (2004) conducted an experiment with various refrigerant and oil mixtures. They showed the oil retention amount with respect to the refrigerant quality and mass flux. They also suggested two models for predicting the oil retention amount in the heat exchanger of high and low quality regions. Sheth and Newell (2005) used R22 as a refrigerant in their study and collected oil hold-up data for an air-conditioning system. They showed the experimental oil hold up and refrigerant mass data in a compressor, a condenser, a liquid line, an evaporator and a compressor suction line. Zoellick and Hrnjak (2010) measured the oil retention amount and pressure drop at the compressor suction line with respect to refrigerant mass flux, oil circulation ratio (OCR) and pipe diameter. They used R410A and POE oil and considered the horizontal and vertical pipe configurations. They measured oil retention amount by weighing the mass of oil directly. Ramakrishnan and Hrnjak (2012) investigated the oil retention amount and pressure drop in the compressor suction line. The experimental setup and method of this research

were similar to those of Zoellick and Hrnjak (2010). Unlike Zoellick and Hrnjak (2010), Ramakrishnan and Hrnjak (2012) focused on the low refrigerant mass flux condition and used R134a, R1234yf and R410A as refrigerants and POE oil as a lubricant.

Mehendale and Radermacher (2000) studied the oil transport with vapor, liquid and two phase refrigerant. This research showed, both experimentally and theoretically, critical mass flow rate for preventing oil film flow reversal in a vertical pipe. An experiment on flow visualization was also conducted as well. The momentum equation for a liquid film of the annular flow and an empirical correlation for interfacial friction factor were used to conduct theoretical analysis. The results of the experiment and the theoretical analysis were compared and the accuracy of theoretical model was good. Hwang *et al.* (2000) presented an experimental method to measure the oil film thickness and to observe the flow pattern in a vertical upward pipe. The flow pattern of refrigerant and oil mixture was churn or annular flow in the vertical upward flow and the oil film thickness data was presented. Lee (2003) presented experimental oil retention data and theoretical models for computing the oil retention amount in each component of air conditioning system. Carbon dioxide and polyalkylene glycol (PAG) were used as refrigerant and oil, respectively. The oil retention amount was measured by

an oil injection and extraction device. Cremaschi (2004) also presented experimental oil retention data and theoretical models for computing the oil retention amount in each component of an air conditioning system. The experimental setup was similar to Lee's experiment (2003). An oil injection and extraction device was used for measuring oil retention. R22/BWMO (Blended white mineral oil), R410A/BWMO, R410A/POE, R134a/POE and R134a/PAG were used as refrigerant and oil mixtures.

Lebreton and Vuillame (2001) calibrated an ultrasonic device to measure the real time oil concentration in the liquid phase refrigerant. This research compared the oil concentration measurement from a sampling method with that from an ultrasonic probe. Luz III (2005) proposed a design of an oil concentration sensor using ultraviolet absorption spectroscopy. This research suggested an analytical model and calibration methods to develop a high accuracy oil concentration ratio sensor. Fukuta *et al.* (2006) developed a refractive index sensor for measuring oil circulation ratio in the liquid line. This research conducted a transient measurement of oil circulation ratio (OCR) in a real system by using the developed sensor and showed that the sensor works nicely. Guo *et al.* (2012) developed a criterion for oil return in various types of suction pipes. Cho (2013) suggested an optical method to measure the liquid film thickness in an annular flow regime. An experiment

was conducted and the results of the liquid film thickness measurements using the optical method and the sampling method were compared. The relative measurement error was about ±20%.

Cyclone separator has been widely used in various industries and mechanical machines to separate liquid or solid particle from gas stream, and many studies on the cyclone separator have been conducted. Some of the studies focused on the gas-solid cyclone separator. Gil *et al.* (2002) presented the effects of solid loading on the performance of cyclone separator. Matsuzaki *et al.* (2006) conducted numerical investigation on the particle motions in the cyclone separators with respect to the height of inserted pipe. Wang *et al.* (2006) studied on the gas-solid flow in a typical Lapple cyclone separator by using commercial software package, and they verified the model by comparing the simulation results with measured results in term of gas pressure and flow field, solid flow pattern and collection efficiency. Brennan *et al.* (2009) conducted CFD (computational fluid dynamics) predictions of flow characteristics in two different cyclone separators and compared the results to the measured data from previous research. Azadi *et al.* (2010) examined the effect of cyclone size on performance parameters and suggested flow field behaviour by numerical modeling. Safikhani *et al.* (2010) suggested results from numerical

simulations of the three types of standard cyclone separators. Elsayed and Lacor (2011) investigated on the effect of increasing width and height of cyclone inlet on the pressure drop and cut-off diameter and suggested flow filed pattern and velocity profiles in separator by using numerical analysis. Other studies focused on the gas-liquid cyclone separator. Murakami *et al.* (2006) suggested a model for predicting the efficiency of cyclone separator, and verified the models based on the experimental data. They insisted that separation in cyclone consists of gravity separation and centrifugal separation, and effect of centrifugal separation increases as the mass flow rate of gas phase goes up. Gao *et al.* (2012) developed a 3-D model and established experimental system to study the effect of the breakup of oil droplets to the performance of gas-oil cyclone separators. There is an ASHRAE (American society of heating, refrigerating and air-conditioning engineers) standard which suggested a method for measuring the efficiency of oil separator in air conditioning system. In this paper, the efficiency of oil separator was defined as a ratio of the mass flow rate of separated oil at the oil separator to mass flow rate of oil at the inlet of oil separator.

Hoffmann and Stein (2007) summarized the principles, design and operation characteristics of cyclone separators. They mentioned that the particle size distribution is one of main parameter to predict the separation

efficiency of gas-liquid separator. In case of gas-liquid separator, there are a few studies on the droplet size distribution in separator. Murakami *et al.* (2006) conducted an experiment with nitrogen and oil to measure the droplet size distribution with respect to the mass flow rate of gas phase. They proposed an empirical correlation based on the experimental data. Gao *et al.* (2012) also measured a droplet size distribution. However, they did not proposed correlation but showed the experimental results as a graph.

1.3 Objectives and scopes

There have been many studies on the flow characteristics of refrigerant and oil mixture in a heat pump system. In case of the flow characteristics in the pipe, there has been little study which considered R410A with PVE oil which are commonly used for multi heat pump system. In addition, there has been little study which considered the flow characteristics with respect to the pipe diameter. So verification or new modeling for predicting the flow characteristics of these working fluids and various pipe diameter conditions is required. In case of the flow characteristics in the oil separator, there has been little experimental data of the performance of oil separator. So it's not appropriate to use previous models for predicting the performance of the oil

separator because working fluids and operating conditions of heat pump system vary. Therefore, based on the experimental data, suggestion of new model or verification of previous model is necessary.

The objective of this study is to analyse and verify the flow characteristics of refrigerant and oil mixture in a heat pump system. This study focused on the flow of refrigerant and oil mixture in the pipe and oil separator of a heat pump system.

In chapter 2, numerical modeling for calculating the oil retention amount in each component of a heat pump system suggested. Modeling was proposed for three regions based on the phase of refrigerant. Based on the modeling of oil retention, the oil retention amount in each component of multi heat pump system was calculated. This study predicted the oil retention amount in a condenser, four indoor units, horizontal and vertical gas lines, and horizontal and vertical liquid lines with respect to the mass flux of refrigerant, oil circulation ratio and length of horizontal and vertical pipe lines.

From the numerical study in chapter 2, it was predicted that the oil retention amount in gas line of refrigerant is much higher than that in other component. Therefore, experimental study on the oil retention and pressure drop in compressor suction line was conducted in chapter 3. From the

experimental results, the numerical study was verified.

In chapter 4, the experimental results of efficiency and pressure drop of oil separator were presented. Seven different oil separators were used to confirm the separation efficiency and pressure drop with respect to the size of oil separator and inlet configuration. Based on the experimental results, the model for predicting the separation efficiency and pressure drop were proposed.

The main points and conclusion of this study are summarized in the last chapter.

Chapter 2. Numerical study on the oil retention in a heat pump system

2.1 Introduction

Because refrigerant passes through the compressor, lubrication oil is discharged from the compressor and circulates the entire system with the refrigerant. So total amount of oil which is initially charged the compressor should be the sum of oil for lubrication inside a running compressor and discharged oil from the compressor. To determine the appropriate charge amount of oil in the compressor, the amount of discharged oil under various operating conditions is required, which can be calculated by numerical simulation of a heat pump system with precise calculation of oil retention amount in each component.

In case of multi heat pump system, R410A and polyvinylether (PVE) oil are used as the refrigerant and lubricant, respectively. Multi heat pump systems and single heat pump systems are different in the length of pipe line which connects indoor and outdoor units, and the number of indoor units. There are many experimental and analytical studies on the oil retention amount in a heat pump system. However, there is little research on multi

heat pump system with R410A and PVE oil. To suggest a proper charge amount of oil in compressor of multi heat pump system, a numerical study on the prediction of oil retention amount in each component is necessary. In case of multi heat pump system, the installation features which include length of pipe line and number of indoor units should be considered.

In this chapter, analytical models for predicting the oil retention amount in gas, liquid and two phase regions of heat pump system were proposed. In addition, the oil retention amount in each component of multi heat pump system under various operating conditions was predicted and analysed. Based on the numerical results, the proper charge amount of oil in the compressor of a multi heat pump system under specific operating condition was suggested. .

2.2 Simulation methodology

2.2.1 Modeling of oil retention in gas and liquid phase regions

Oil exists in a liquid phase in all components of a heat pump system, and refrigerant exists as a gas phase in the superheat region of evaporator and condenser, and gas line of refrigerant. Refrigerant and oil mixture engage in a two phase flow, with flow patterns that vary with the mass flux of

refrigerant. There have been many studies on the flow visualization of refrigerant and oil mixture with various refrigerant and oil mixture in the gas phase region. Mehendale and Radermacher (2000), Hwang *et al.* (2000), Sethi (2011) and Ramakrishnan and Hrnjak (2012) performed related studies. This study also checked the flow pattern of R410A and PVE oil mixture in horizontal gas line of refrigerant, and flow visualization is explained in chapter 3. From these studies, it is possible to know that the flow patterns in horizontal line are usually stratified wavy flow and annular flow under low and high mass flux conditions. The flow pattern is annular flow when the superficial velocity of gas phase refrigerant is higher than 3 ms^{-1}. For the vertical line, flow patterns is also annular flow when superficial velocity of gas phase refrigerant is higher than 3 ms^{-1}. When the flow pattern is annular flow, the equation for predicting the oil film thickness can be derived based on some assumptions and basic fluid dynamic equations which include continuity and momentum equations. Fig 2.1 shows the schematic of annular flow, and the following assumptions are applied.

(1) Flow is fully developed, incompressible, steady state, adiabatic and axisymmetric.

(2) Film thickness in a section is uniform.

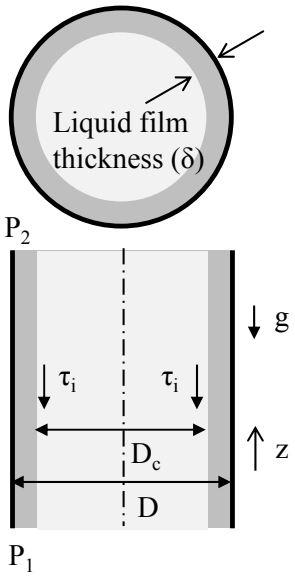

Fig. 2.1 Annular flow in the pipe

(3) The fraction of liquid entrained as droplets is zero.

(4) Gas and liquid phases in a section have uniform properties.

(5) Liquid film behaves as a Newtonian fluid.

With these assumptions, the continuity and momentum equations for z-direction of liquid film are described in the following equations.

$$\frac{\partial(ru_r)}{\partial r} = 0 \tag{2.1}$$

$$\frac{\mu_l}{r}\frac{\partial}{\partial r}\left(r\frac{\partial u}{\partial r}\right) = \frac{dP}{dz} + \rho_l g \tag{2.2}$$

By integrating equations (2.1) and (2.2) with boundary conditions that include $u_r(r=R)=0$ and $\tau_i = \tau(r = R-\delta)$, the following equations (2.3) and (2.4) are obtained.

$$u_r = 0 \quad \left(R-\delta \le r \le R\right) \tag{2.3}$$

$$\tau = \tau_i \frac{(R-\delta)}{r} - \frac{1}{2}\left(\frac{dP}{dz} + \rho_l g\right)\left(\frac{r^2-(R-\delta)^2}{r}\right) \tag{2.4}$$

From the assumption that liquid film behaves as a Newtonian fluid, it is understood that $\tau = -\mu_l \frac{du}{dr}$. Inserting this into equation (2.4), the following equation is obtained.

$$-\mu_l \frac{du}{dr} = \tau_i \frac{(R-\delta)}{r} - \frac{1}{2}\left(\frac{dP}{dz} + \rho_l g\right)\left(\frac{r^2-(R-\delta)^2}{r}\right) \tag{2.5}$$

Integrating equation (2.5) with respect to r and using the no slip boundary condition that is $u_{r=R} = 0$, an equation for velocity of liquid film

is derived.

$$u_l = \frac{1}{\mu_l}\left[\left(\tau_i(R-\delta)+\frac{(R-\delta)^2}{2}\left(\frac{dP}{dz}+\rho_l g\right)\right)\cdot\ln\left(\frac{R}{r}\right)-\frac{1}{4}\left(\frac{dP}{dz}+\rho_l g\right)(R^2-r^2)\right] \quad (2.6)$$

Volume flow rate of liquid film is obtained by integrating equation (2.6) into the film cross section area, and the mass flow rate is calculated by multiplying the density of liquid film with volume flow rate. Equation (2.7) provides the expression of mass flow rate of liquid film.

$$\dot{m}_l = \frac{2\pi\rho_l}{\mu_l}\left[\tau_i(R-\delta)+\frac{(R-\delta)^2}{2}\left(\frac{dP}{dz}+\rho_l g\right)\right]\cdot\left[\frac{R^2-(R-\delta)^2}{4}-\frac{(R-\delta)^2}{2}\ln\frac{R}{R-\delta}\right]$$

$$-\frac{\pi\rho_l}{8\mu_l}\left(\frac{dP}{dz}+\rho_l g\right)\left[R^2-(R-\delta)^2\right]^2 \quad (2.7)$$

Mass flow rate of the liquid film, the pressure gradient and the interfacial shear stress are necessary to calculate the liquid film thickness in equation (2.7). Here, the mass flow rate of liquid film is treated as an input variable. The relationship between the pressure gradient and interfacial shear stress is derived by applying the momentum equation to the gas core.

$$\frac{dP}{dz}+\rho_g g+\frac{\tau_i D_c \pi}{A_c}=0 \quad (2.8)$$

Interfacial shear stress between the gas core and liquid film is given as;

$$\tau_i = \frac{1}{2} f_i \rho_g (u_g - u_l)^2 \quad (2.9)$$

Velocity of liquid film is negligible, as it is far smaller than velocity of

the gas core. Therefore, interfacial shear stress is a function of the interfacial friction factor, and density and velocity of the gas phase. For the interfacial friction factor, this study used the correlation which was proposed by Wallis (1969). This correlation is shown in following equation (2.10)

$$f_i = 0.005 \cdot (1 + 300 \cdot \delta / D) \tag{2.10}$$

Liquid film thickness can be calculated using equations (2.7) ~ (2.10) and the mass flow rate of liquid film. Then, volume of liquid film can be calculated after obtaining liquid film thickness. Using solubility data and liquid density, the mass of the oil in gas lines of refrigerant is calculated.

Liquid phase refrigerant exists in the subcooled region of the condenser and liquid line of refrigerant. In this case, it was assumed that the oil and refrigerant are totally mixed. Then, the oil mass in a segment can be calculated using equation (2.11).

$$m_o = OCR \cdot Vol \cdot (1 - \alpha) \cdot \rho_l \tag{2.11}$$

The α in equation (2.11) denotes a void fraction, and the value is equal to zero because all refrigerant exists as a liquid phase.

2.2.2 Modeling of oil retention in two phase region

The condenser can be divided into three sections which include superheat, subcooled and two phase regions. In case of superheat and subcooled regions, as mentioned above, the oil retention amount can be calculated by two different models. In case of two phase region, however, it is inappropriate to use only one model. Fig. 2.2(a) shows a result that model for gas phase region is applied on the whole two phase region of condenser. Volume fraction of oil is defined as a ratio of volume of oil to that of pipe in each segment. In this case, the volume fraction of oil diminishes as the quality decreases and there is a discontinuity point when the quality is equal to zero. As the amount of liquid phase refrigerant becomes higher, the accuracy of model for gas phase region diminishes so discontinuity occurs. Fig. 2.2(b) shows a result that model for liquid phase region is used to calculate the volume fraction of oil in the whole two phase region of condenser. In this case, void fraction is not equal to zero so an analytical void fraction model which is proposed by Zivi (1964) was used.

$$\alpha = \frac{1}{1 + \frac{1-x}{x}\left(\frac{\rho_g}{\rho_l}\right)^{2/3}} \tag{2.12}$$

There is a discontinuity point when the quality is equal to one because the accuracy of model for liquid phase region diminishes as the amount of liquid

phase refrigerant diminishes. Fig. 2.2(c) shows the volume fractions of oil from each model in two phase region. There is a point that the volume fractions of oil from each model are the same. A quality of this point is defined as a reference quality. When the quality is equal to one, it is appropriate to use the model for gas phase region to calculate the volume fraction of oil. When the quality is equal to zero, it is reasonable to use the model for liquid phase region. Under reference quality, the effects of both models are the same. That is, the weights of model for gas phase region are 1, 0.5 and 0 when the quality is equal to one, reference quality and zero, respectively. In case of model for liquid phase region, the weights are 0, 0.5 and 1 when quality is equal to one, reference quality and zero, respectively. As quality decreases the weight of model for gas phase region also reduces and that for liquid phase region increases. The summation of weights for each model is equal to one. The volume fraction of oil in two phase region was predicted based on the results from each model with a consideration of weights, and this is described in equation (2.13)

$$m_{oil\_two-phase} = m_{oil\_MG} \cdot WT_{MG} + m_{oil\_ML} \cdot (1 - WT_{MG}) \tag{2.13}$$

Volume fraction of oil in two phase region of evaporator was calculated by the same method. The reference quality is varied with operating condition, and the reference quality was varied from 0.92 to 0.98 during the simulation.

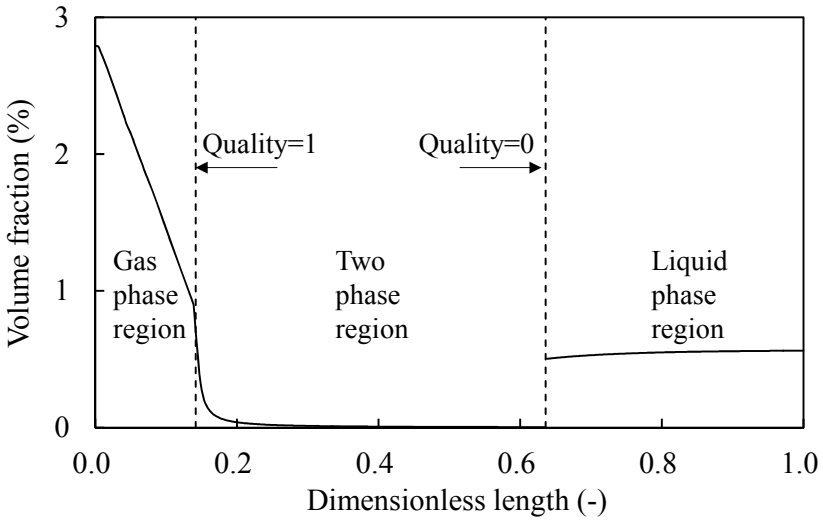

(a) Volume fraction of oil in condenser from the model for gas phase region

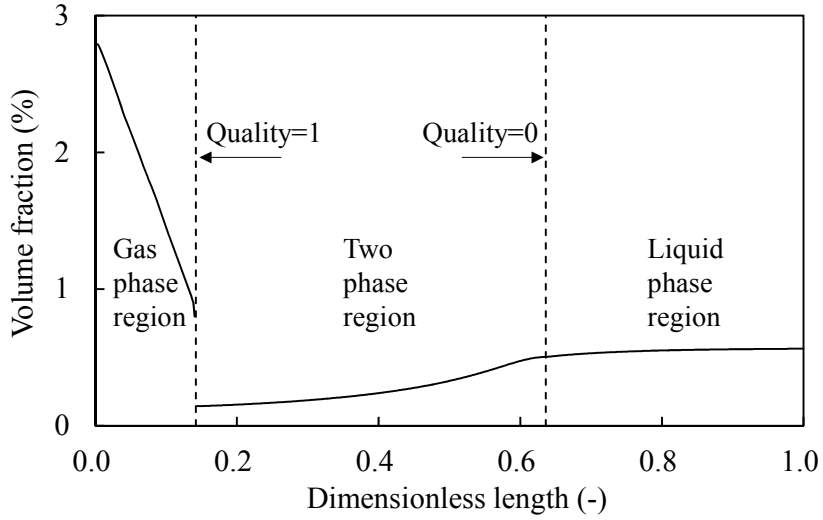

(b) Volume fraction of oil in condenser from the model for liquid phase region

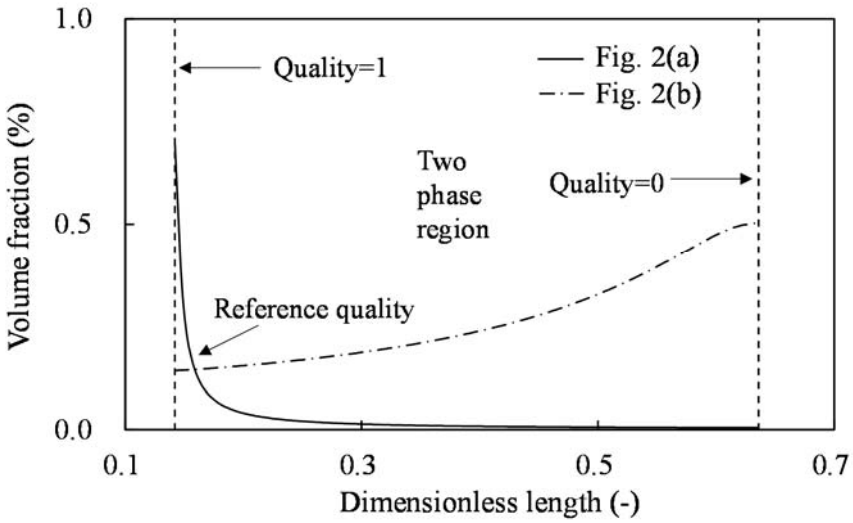

(c) Volume fractions of oil in two phase region from each model

Fig. 2.2 Volume fraction of oil in condenser from two different models

2.2.3 Overall heat pump system simulation

This study considered a multi heat pump system of 29 kW with one outdoor unit and four indoor units. Following assumptions are applied to conduct the simulation of multi heat pump system.

- The outdoor unit is installed at the top of the building.
- Indoor units are installed in the same floor and the refrigerant is equally divided.
- Refrigerant which comes out from indoor units flows the vertical line, and then passes through the horizontal line.

Fig. 2.3 shows a schematic of the multi heat pump system. This research considered a cooling mode. During cooling mode, the outdoor unit and indoor units works as condenser and evaporators, respectively. Isentropic efficiency of compressor was assumed as 0.9. Condensing and evaporating pressures were set as 3000 kPa and 800 kPa, respectively. The degree of superheat at the compressor suction was set as 10℃ and inner diameters of gas and liquid lines of refrigerant were set as 26.58 and 14.08 mm, respectively. Fig. 2.4 shows a flow chart of the whole simulation. To conduct the simulation, temperature and pressure of refrigerant at the compressor inlet were assumed. Then, the temperature and pressure at the

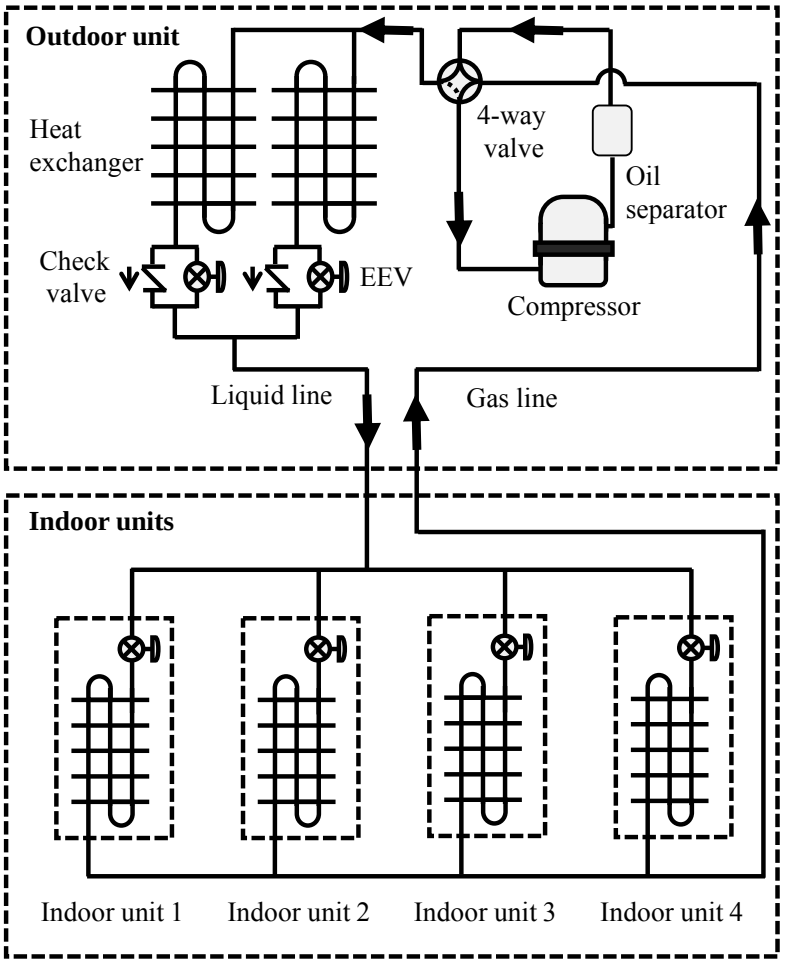

Fig. 2.3 Schematic of multi heat pump system

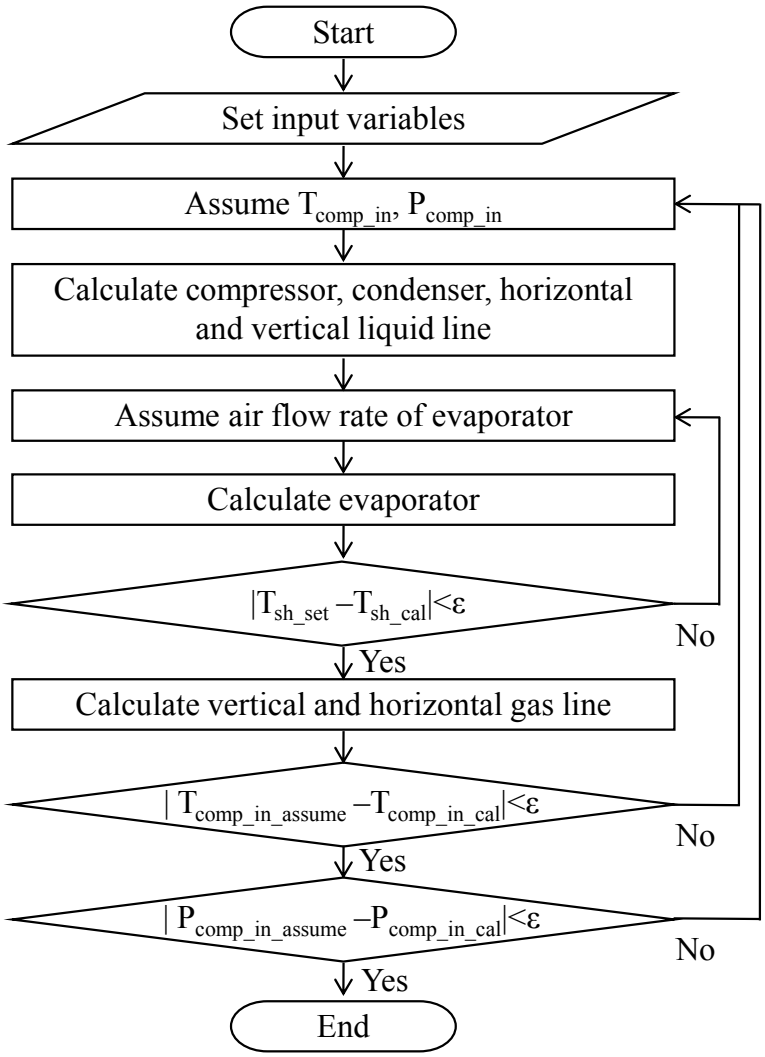

Fig. 2.4 Flow chart of the simulation

compressor outlet were calculated based on the isentropic efficiency. The mass flow rate of refrigerant was calculated by the compressor mapping data from manufacturer. As shown in the Fig. 2.3, condenser which is heat exchanger in outdoor unit is close to the compressor, so the temperature and pressure at condenser inlet were assumed as those at the compressor outlet. In condenser, the refrigerant changes from gas phase to liquid phase while temperature of secondary fluid in condenser increases. Secondary fluid of condenser is air and the temperature of the air was assumed as 30℃. Finned-tube heat exchanger was considered as a condenser. Air side heat transfer coefficient was calculated by an empirical correlation which was proposed by Wang *et al.* (2000). Wang *et al.* (2000) suggested empirical correlation of colburn j-factor, and the correlation is described as equation (2.14)

$$j = 0.086\,\mathrm{Re}_{Dc}^{P3}\,N^{P4}\left(\frac{F_P}{D_C}\right)^{P5}\left(\frac{F_P}{D_h}\right)^{P6}\left(\frac{F_P}{P_t}\right)^{-0.93} \tag{2.14}$$

P3, P4, P5, P6 and D_h in equation (2.14) are calculated from following equations.

$$P1 = 1.9 - 0.23\log_e(\mathrm{Re}_{D_c}) \tag{2.15}$$

$$P3 = -0.361 - \frac{0.042N}{\log_e(\mathrm{Re}_{D_c})} + 0.158\log_e\left(N\left(\frac{F_P}{D_c}\right)^{0.41}\right) \tag{2.16}$$

$$P4 = -1.224 - \frac{0.076\left(\frac{P_l}{D_h}\right)^{1.42}}{\log_e(\mathrm{Re}_{D_c})} \tag{2.17}$$

$$P5 = -0.083 + \frac{0.058N}{\log_e(\mathrm{Re}_{D_c})} \tag{2.18}$$

$$P6 = -5.735 + 1.21\log_e\left(\frac{\mathrm{Re}_{D_c}}{N}\right) \tag{2.19}$$

$$D_h = \frac{4A_cL}{A_0} \tag{2.20}$$

$$F1 = -0.764 + 0.739\frac{P_t}{P1} + 0.177\frac{F_P}{D_c} - \frac{0.00758}{N} \tag{2.21}$$

$$F2 = -15.689 + \frac{64.021}{\log_e(\mathrm{Re}_{D_c})} \tag{2.22}$$

$$F3 = 1.696 - \frac{15.695}{\log_e(\mathrm{Re}_{D_c})} \tag{2.23}$$

The heat transfer coefficient of air can be obtained by using colburn j-factor, and the relation between heat transfer coefficient and colburn j-factor is shown in equation (2.24).

$$h_{air} = \frac{j\rho u_{\max} C_p}{\mathrm{Pr}^{\frac{2}{3}}} \tag{2.24}$$

Surface efficiency is defined as equation (2.25) and fin efficiency is calculated by the Schmidt's method which is described in following equations.

$$\eta_o = 1 - \frac{A_t}{A_o}(1-\eta) \tag{2.25}$$

$$\eta = \frac{\tanh(mr\phi)}{mr\phi} \tag{2.26}$$

$$m = \sqrt{\frac{2h_o}{k_f \delta_f}} \tag{2.27}$$

$$\phi = \left(\frac{\mathrm{Re}_{eq}}{r} - 1 \right) \left[1 + 0.35 \ln \left(\frac{\mathrm{Re}_{eq}}{r} \right) \right] \tag{2.28}$$

$$\frac{\mathrm{Re}_{eq}}{r} = 1.27 \frac{X_M}{r} \left(\frac{X_L}{X_M} - 0.3 \right)^{\frac{1}{2}} \tag{2.29}$$

In case of single phase regions of condenser, the heat transfer coefficient of refrigerant was calculated by Dittus-Boelter's correlation (1930) which is described in equation (2.30). The heat transfer coefficient of refrigerant in two phase region was calculated by the empirical correlation of Chen *et al.* (1987), which is shown in equation (2.31).

$$\frac{h_r D_h}{k} = 0.023 \mathrm{Re}^{0.8} \mathrm{Pr}^n \tag{2.30}$$

$$\frac{h_r D_h}{k} = 0.018 \left(\frac{\mu_v}{\mu_l} \right)^{0.078} \left(\frac{\rho_l}{\rho_v} \right)^{0.39} \mathrm{Re}_l^{0.2} (\mathrm{Re}_{lo} - \mathrm{Re}_l)^{0.7} \mathrm{Pr}_l^{0.65} \tag{2.31}$$

Pressure drop at gas phase and high quality section of two phase region was calculated by the equations (2.8) ~ (2.10). Pressure drop at low quality section of two phase region was computed by the empirical correlation of Műller-Steinhagen and Heck (1986), and the correlation is described in equations (2.32) ~ (2.37).

$$\left(\frac{dp}{dz}\right) = G(1-x)^{\frac{1}{3}} + Bx^3 \tag{2.32}$$

$$C = A + 2(B-A)x \tag{2.33}$$

$$A = f_l \frac{2G_{total}^2}{D_i \rho_l} \tag{2.34}$$

$$B = f_g \frac{2G_{total}^2}{D_i \rho_g} \tag{2.35}$$

$$f_l = \frac{0.079}{\mathrm{Re}_l^{0.25}} \tag{2.36}$$

$$f_g = \frac{0.079}{\mathrm{Re}_g^{0.25}} \tag{2.37}$$

Pressure drop at subcooled region was calculated by following equation (2.38).

$$\Delta P = \frac{2fG^2L}{\rho D_i} \tag{2.38}$$

f in equation (2.38) was obtained by the correlation of Petukhov.

There's no heat exchange at the horizontal and vertical liquid lines, so only pressure drop was concerned in these sections. The pressure drop in liquid lines was calculated by equation (2.38). Refrigerant enters the indoor units which work as an evaporator. The heat transfer coefficient of air in evaporator was calculated by equations (2.14) ~ (2.24). In case of the heat transfer coefficient of refrigerant in superheat region, equation (2.30) was used. Correlation of Gungor and winterton (1987) was used to calculate the

heat transfer coefficient of refrigerant at two phase region, and the correlation is described in equations (2.39) ~ (2.42).

$$h_{tp} = Eh_l \tag{2.39}$$

$$h_l = \frac{0.023k\,\mathrm{Re}^{0.8}\,\mathrm{Pr}^{0.3}}{D_h} \tag{2.40}$$

$$E = 1 + 3000Bo^{0.86} + 1.12\left(\frac{x}{1-x}\right)^{0.75}\left(\frac{\rho_l}{\rho_g}\right)^{0.41} \tag{2.41}$$

$$Bo = \frac{q''}{h_{fg}G} \tag{2.42}$$

Equations (2.8) ~ (2.10) and (2.32) ~ (2.37) were used to calculate the pressure drop at superheat region and high quality section and low quality section. After evaporator, the refrigerant passes through the gas lines, and equations (2.8) ~ (2.10) were used to calculate the pressure drop at gas lines.

This study calculated the oil retention amount in each component with respect to refrigerant mass flux in gas line of refrigerant, oil circulation ratio (OCR), length of horizontal and vertical lines. From the flow visualization, it was shown that the flow patterns in horizontal and vertical lines are annular flow when superficial velocity is higher than about 3 ms^{-1} which is about mass flux of 100 kg $m^{-2}s^{-1}$ in gas lines of refrigerant. Usually the OCR is less than 1% under almost all operating conditions in real system. The pipe line length is different with the construction of building. Sometimes distance

between outdoor unit and indoor units is close and sometime the distance is far. Based on these features of multi heat pump system, the operating conditions for the simulation is decided. Refrigerant mass flux in gas line of refrigerant, oil circulation ratio (OCR), length of horizontal and vertical line were varied from 100 to 250 kg/m^{2}s, 0.1 to 0.9% and 20 to 100 m, respectively.

2.3 Results and discussion

One of the purposes of this study was to analyse the oil retention amount in a multi heat pump system under various operating conditions. The reference operating condition is shown in Table 2.1, while Figs. 2.5 ~ 2.8 show the volume fraction of oil in each component under the reference operating condition. In case of condenser and evaporator, 0 and 1 correspond to inlet and outlet of each component, respectively. For liquid lines, 0 and 1 denote the inlet of horizontal line and outlet of vertical line, respectively, while 0.5 denotes the outlet of horizontal line and the inlet of vertical line. For gas lines, 0 and 1 refer to the inlet of vertical line and the outlet of horizontal line, respectively, while 0.5 refers to the outlet of vertical line and the inlet of horizontal line. The volume fraction of oil in condenser reduces as the refrigerant passes through the gas phase region and high

Table 2.1 Reference operating condition

Parameter	Value
Mass flux in gas line ($kgm^{-2}s^{-1}$)	175
OCR (%)	0.5
Length of horizontal line (m)	60
Length of vertical line (m)	60

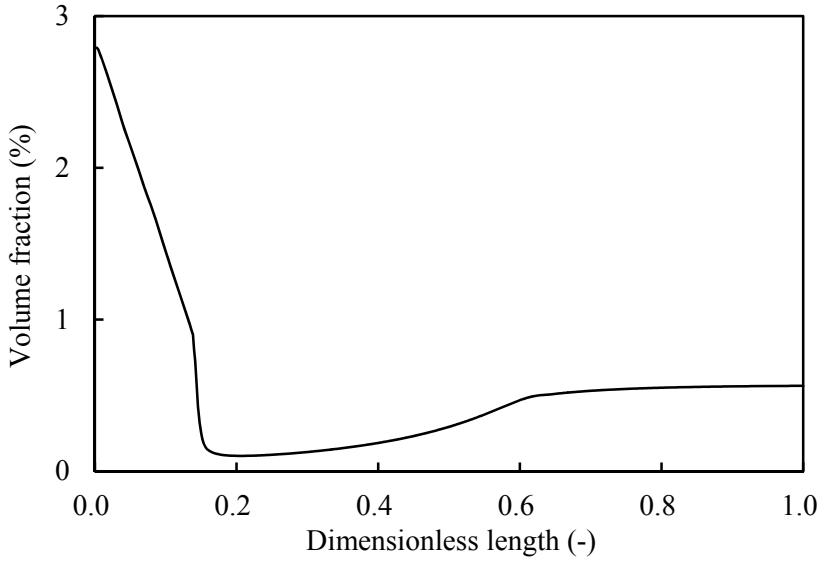

Fig. 2.5 Volume fraction of oil in condenser

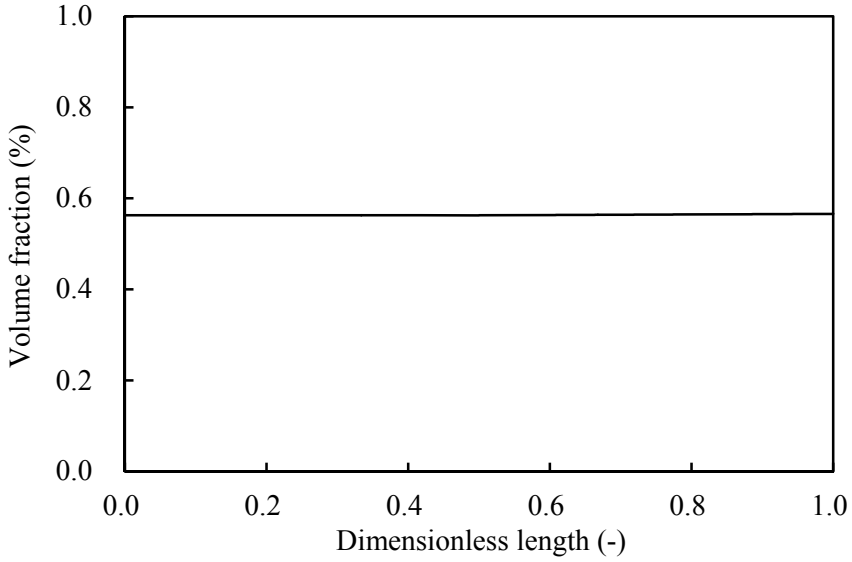

Fig. 2.6 Volume fraction of oil in horizontal and vertical liquid lines

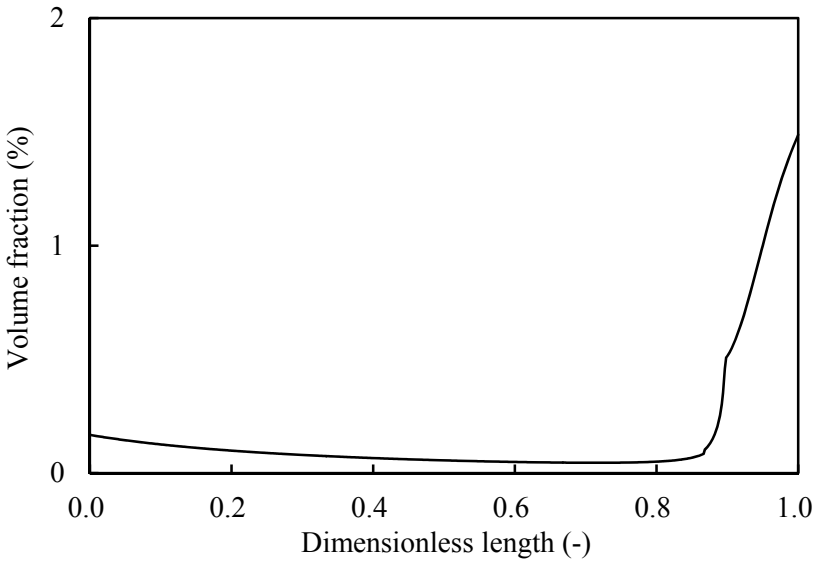

Fig. 2.7 Volume fraction of oil in evaporator

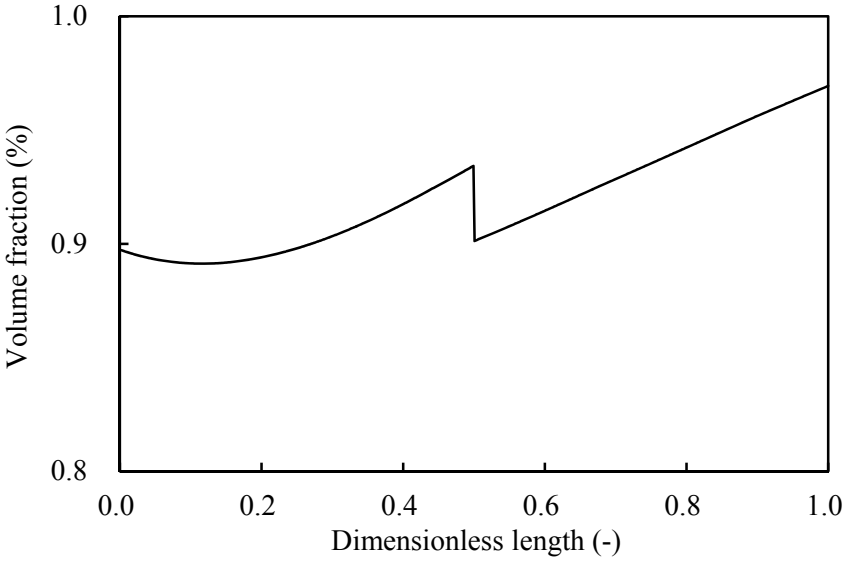

Fig. 2.8 Volume fraction of oil in horizontal and vertical gas lines

quality region of condenser, attributed to a reduction of viscosity of liquid film. The mechanism of oil transportation in these regions is dependent on shear force at the interface between gas and liquid phase. High viscosity of liquid film exerts high resistance, so the amount of retained oil increases with a rise of liquid viscosity. The viscosity of liquid film diminishes with an increase in solubility as the viscosity of liquid refrigerant is lower than that of oil. Solubility rises as pressure increases or temperature decreases. In case of superheat region of condenser, temperature of refrigerant decreases as the refrigerant passes through and this leads to an increment of solubility. The increment of solubility means a reduction of viscosity of liquid film. In the high quality region of condenser, the ratio of liquid refrigerant to total liquid rises as quality decreases. This also implies the decrement of viscosity of liquid film, so the volume fraction of oil in superheat region and high quality region of condenser goes down as the refrigerant becomes more distant from the condenser inlet. In contrast, the volume fraction of oil in the low quality region increases as quality decreases. Volume fraction of oil in this region was calculated using the void fraction, OCR and density of liquid mixture. Among these variables, OCR is constant and the density of liquid mixture almost does not change. However, the void fraction decreases as the quality becomes lower. Lower void fraction represents a higher amount of liquid,

which implies potential for higher volume fraction of oil. The volume fraction of oil in the subcooled region of condenser remains almost constant, which was calculated based on equation (2.11). Among variables on right hand side of equation (2.11), only density of liquid mixture changes slightly due to pressure drop. Therefore, volume fraction of oil in the subcooled region remains almost constant. The volume fraction of oil in horizontal and vertical liquid lines of refrigerant is fluctuates little, as the refrigerant becomes more distant from the inlet of liquid line (Fig. 2.6). This trend is similar to the subcooled region of condenser. In case of the volume fraction of oil in the evaporator, as in the condenser, volume fraction of oil in the low quality region reduces as quality increases due to a rise of void fraction. An increase in quality or temperature of refrigerant causes a rise of viscosity of liquid film, which leads to an increment of volume fraction of oil in the high quality and superheat regions of evaporator. In case of gas lines, the expression of 0 ~ 0.5 on the x-axis represents a vertical line and 0.5 ~ 1 indicates a horizontal line. Pressure drop occurs as the refrigerant and oil mixture flows, which leads to a reduction in temperature. Fig. 2.9 shows the viscosity of liquid film in relation to the dimensionless length in the gas lines of refrigerant. As the refrigerant flows through the gas lines of refrigerant, liquid film viscosity tends to increase. However, near the inlet, viscosity

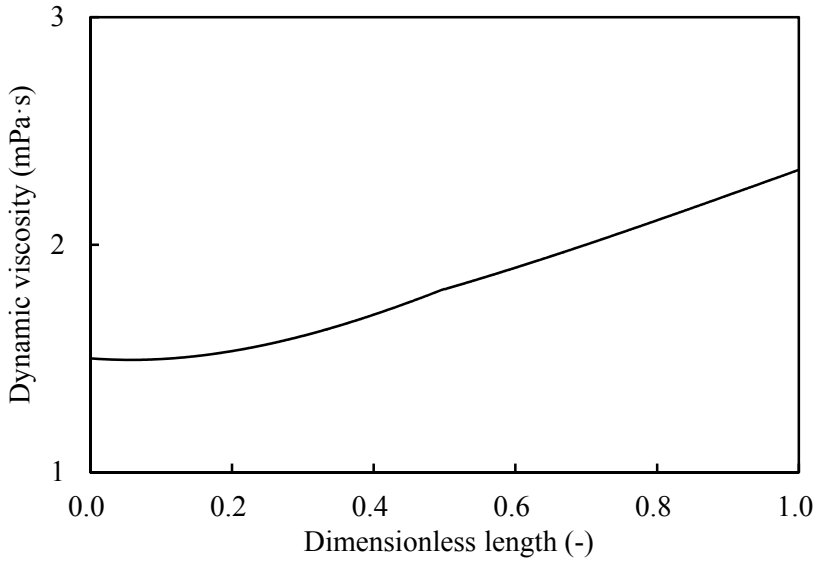

Fig. 2.9 Dynamic viscosity of liquid film in gas lines

decreases as the dimensionless length increases. Based on this tendency of viscosity of liquid film and dimensionless length, it is possible to explain the tendency of volume fraction of oil in vertical and horizontal gas lines of refrigerant. The volume fraction of oil changes sharply when the dimensionless length is 0.5 in gas lines. Viscosity of liquid film at the outlet of vertical line is nearly identical to the inlet of horizontal line, with the only difference being the existence of gravity force. Shear force only affects the transportation of liquid film in the horizontal line, while shear force and gravity force affect the transportation of liquid film in the vertical line. The directions of gravity force and shear force is opposite in vertical line, as gravity force hinders the transportation of liquid film. Therefore, the volume fraction of oil in the vertical line is higher than in the horizontal line under the same conditions, so the volume fraction of oil changes sharply when the pipe configuration changes.

Fig. 2.10 shows the oil retention amount in each component with respect to mass flux of refrigerant. The oil retention amount in each component reduces with the increment of mass flux. For the gas line of refrigerant, high mass flux induces high shear force on the interface between gas and liquid phases. Therefore, liquid film is transported easily under high mass flux condition. For the liquid line of refrigerant, the oil retention

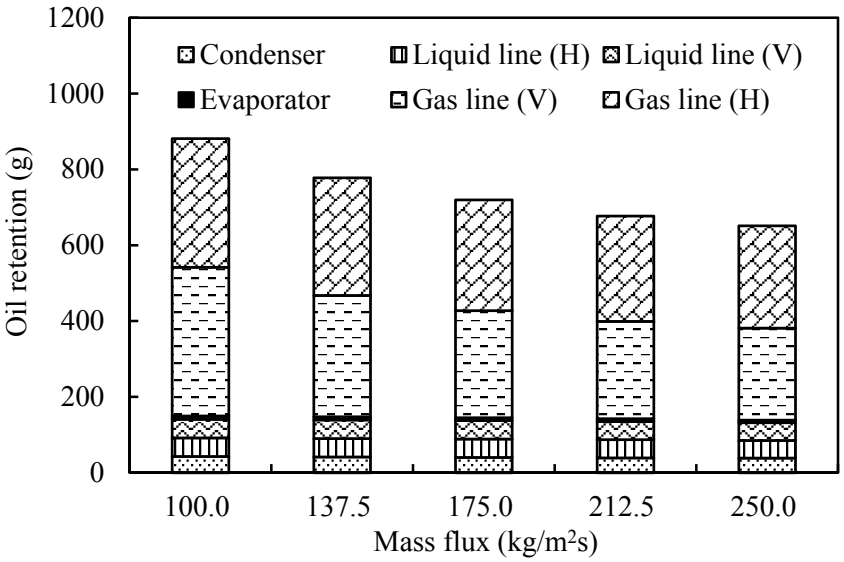

Fig. 2.10 Oil retention amount in each component with respect to the mass flux

amount is calculated using equation (2.11). OCR, volume of each section and void fraction are constant values, and the density of liquid changes slightly with respect to mass flux of refrigerant because of the pressure drop. Higher mass flux causes a higher pressure drop, and the density of liquid phase reduces as pressure drop increases. Therefore, oil retention amount in the liquid line of refrigerant slightly decreases as mass flux rises. The reduction of oil retention amount in heat exchangers may also be explained by the same reasons which mentioned above. Most of the discharged oil is retained in the gas lines of refrigerant. Under low mass flux conditions, the effect of gravity force is high and the oil retention amount in the vertical line is higher than the horizontal line. As mass flux increases, the effect of shear force becomes dominant and viscosity of liquid film rises due to the pressure drop. Under high mass flux conditions, the oil retention amount in the horizontal line is higher than that the vertical line. The total oil retention amount reduces from 881.1 g to 651.2 g as mass flux increases from 100 $kgm^{-2}s^{-1}$ to 250 $kgm^{-2}s^{-1}$. Fig. 2.11 shows the oil retention amount in each component with respect to the OCR. The oil retention amount in each component goes up as OCR rises. In case of liquid line of refrigerant, the oil retention amount is nearly proportional to OCR, and this tendency can be predicted based on equation (2.11). The oil retention amount for OCR of 0.9%

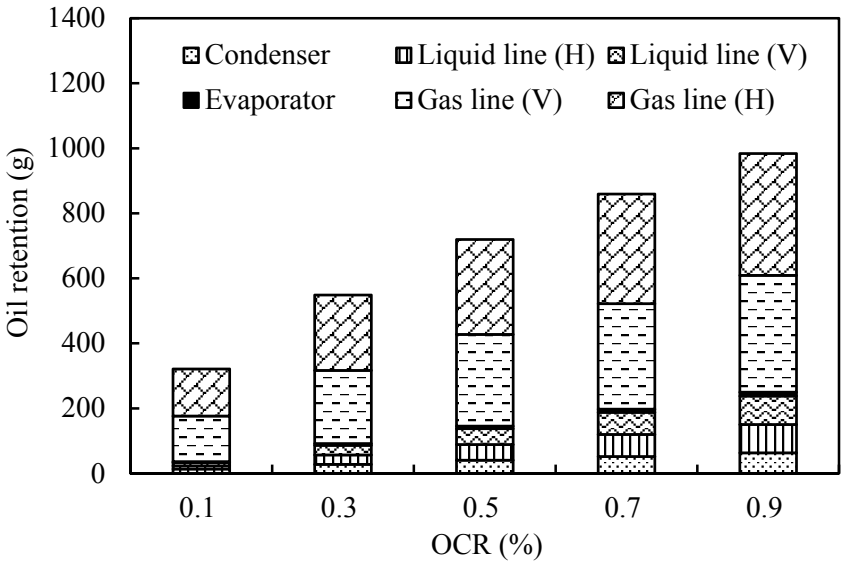

Fig. 2.11 Oil retention amount in each component with respect to OCR

in the liquid line of refrigerant is approximately 9 times higher than that of 0.1%. The oil retention amount in the gas line of refrigerant increases with OCR but not proportionally. The increase of oil retention amount is smaller as OCR rises. The oil retention amount for OCR of 0.9% in gas line of refrigerant is approximately 2.6 times higher than that of 0.1%. In case of heat exchangers, the model for calculating the oil retention amount is a combination of the models for gas and liquid phase regions. The oil retention amount of a heat exchanger lies between those of gas and liquid lines of refrigerant. The oil retention amount for OCR of 0.9% is approximately 4.7 times higher than that of 0.1% in condenser. In evaporator, the oil retention amount for OCR of 0.9% is approximately 3.9 times higher than that of 0.1%. Figs. 2.12 and 2.13 show the oil retention amount with respect to the length of horizontal and vertical lines. The oil retention amount increases as the length of line becomes longer. When the length of a horizontal line is 20 m, the oil retention amount in the horizontal gas line is higher than other components excluding the vertical gas line of refrigerant. When the length of a vertical line is 20 m, the oil retention amount in the vertical gas line is higher than other components excluding the horizontal gas line of refrigerant. The oil retention amount in gas lines of refrigerant is dominant even if the length of gas line of refrigerant is short.

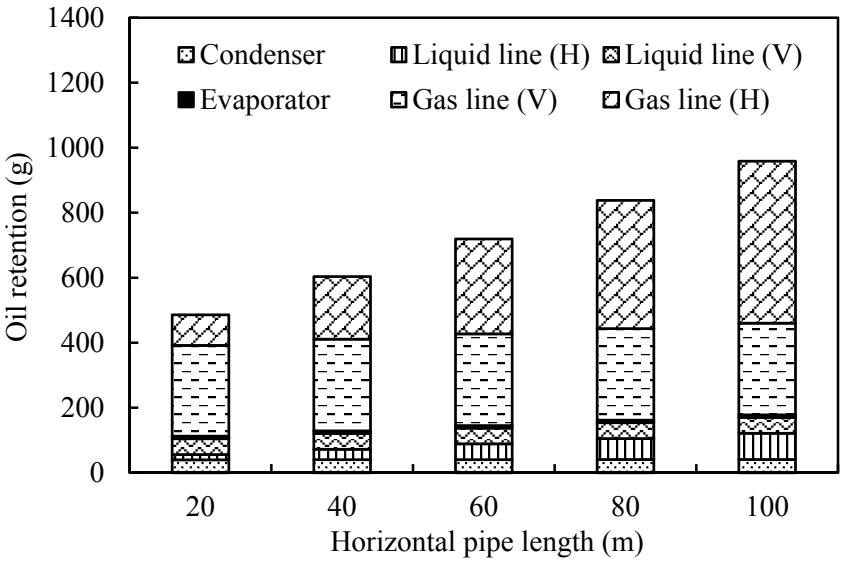

Fig. 2.12 Oil retention amount in each component with respect to horizontal pipe length

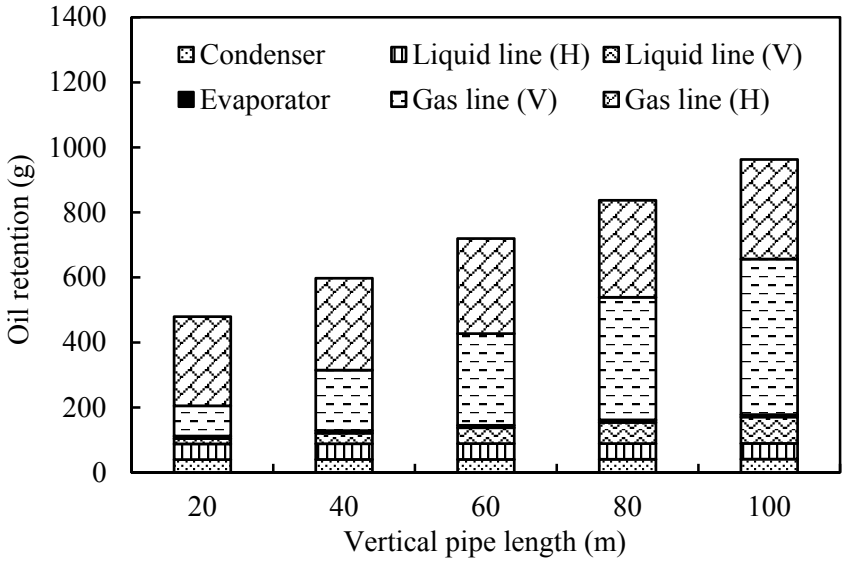

Fig. 2.13 Oil retention amount in each component with respect to vertical pipe length

From simulation results, it is possible to predict an oil retention amount that varies from 321.4 g to 983.8 g in the whole multi heat pump system. For the multi heat pump system of 29 kW with four indoor units and one outdoor unit, the compressor needs 983.8 g of oil (the amount of discharged oil from the compressor) + delta (the amount of oil for lubrication in the compressor) to work safely.

2.4 Conclusion

Models for predicting the oil retention amount in each component of a heat pump system have been suggested. Continuity and momentum equations were applied to the liquid film of annular flow to calculate the thickness of liquid film in the gas phase region. It was assumed that the liquid phase refrigerant and oil are totally mixed in liquid phase region, and model for oil retention amount in liquid phase region was suggested. In case of two phase regions of refrigerant, models for gas and liquid phase regions were combined to predict the oil retention amount.

The oil retention amount in 6 components that include condenser, horizontal and vertical liquid lines of refrigerant, evaporators, horizontal and vertical gas lines of refrigerant were predicted with respect to the mass flux

of refrigerant, oil circulation ratio (OCR), and length of horizontal and vertical lines. The oil retention amount in the whole system was reduced 26.1% and 67.3% as mass flux of refrigerant increased from 100 $kgm^{-2}s^{-1}$ to 250 $kgm^{-2}s^{-1}$ and oil circulation ratio diminished from 0.9% to 0.1%, respectively. Among the 6 components, the oil retention amounts in horizontal and vertical gas lines of refrigerant were significant.

Chapter 3. Experimental study on the oil retention and pressure drop

3.1 Introduction

The oil retention amount in heat pump system varies with the operating conditions and installation features. Among the oil retention amount in all components of heat pump system, the oil retention amount in gas lines of refrigerant is dominant. That is, prediction of oil retention amount in gas lines of refrigerant is important and the accuracy of the predicted oil retention amount in whole system is highly dependent on the accuracy of the predicted oil retention amount in gas lines of refrigerant.

There are many experimental studies on the flow characteristics of various refrigerant and oil mixtures. Lee (2003) used carbon dioxide and polyalkylene glocol (PAG). Cremaschi (2004) considered R22/BWMO (Blended white mineral oil), R410A/BWMO, R410A/POE, R134a/POE and R134a/PAG. Crompton *et al.* (2004) used R134a/POE, R134a/PAG, R134a/alkylbenzene, R22/alkylbenzene and R410A/POE. Zoellick and Hrnjak (2010) considered R410A and POE oil. Ramakrishnan and Hrnjak (2012) used R134a, R1234yf and R410A and POE oil. Although there have

been many experimental studies on the flow characteristics of various refrigerant and oil mixtures, there is little experimental study on flow characteristics of the R410A and PVE oil mixture under various operating conditions. To verify the numerical study on flow characteristics of R410A and PVE oil, the experimental data of R410A and PVE oil is necessary.

The main purpose of this chapter is to analyse the flow characteristics of R410A and PVE oil mixture in a compressor suction line quantitatively and to verify the numerical study by comparing the numerical results and experimental results. The experimental data of volume fraction of oil and pressure drop and flow visualization results in the compressor suction line are presented. The volume fraction of oil and pressure drop were measured with respect to refrigerant mass flux, oil circulation ratio (OCR) and pipe diameter for the horizontal and vertical pipe configurations. The flow visualization was conducted with respect to the refrigerant mass flux and OCR in horizontal pipe.

3.2 Experimental methodology

3.2.1 Experimental apparatus

This research developed two different experimental apparatus to

measure the volume fraction of oil under low and high mass flow rate of refrigerant conditions. In case of low mass flow rate condition, the experimental apparatus consists of gear pump, electric heater, condenser and so on. With this system, the condition of compressor suction line was simulated. The refrigerant becomes a liquid phase at condenser and the mass flow rate of refrigerant can be measured at the liquid line accurately. As mass flow rate of refrigerant increases, however, the energy consumption of chiller for condenser goes up and the experiment can't be conducted under high mass flow rate condition because of the limitation of chiller capacity. To predict the flow characteristics of refrigerant and oil mixture in the multi heat pump system, the experiment for high mass flow rate of refrigerant condition has to be conducted. So the experimental apparatus for high mass flow rate of refrigerant condition was also designed. This system consists of compressor, heat exchanger and expansion devices and so on. In this case, the refrigerant does not change from gas phase to liquid phase at heat exchanger so the load of chiller for heat exchanger decreases. Compare to the system for low mass flow rate of refrigerant, the experiment can be conducted under higher mass flow rate of refrigerant condition with the same chiller. However, there is a disadvantage of this system compare to the system for low mass flow rate of refrigerant. The refrigerant exists as a gas

phase at all components of experimental apparatus, and the mass flow meter has to be installed at the gas line of refrigerant. So the accuracy of refrigerant mass flow rate measurement is decreased because the measurement of the gas phase is less accurate and there is a small amount of liquid phase mist oil which is discharged from the compressor in gas phase refrigerant.

Fig. 3.1 shows the schematic of experimental apparatus for low mass flow rate condition and Fig. 3.2 shows pictures of each component of the experimental apparatus. There are refrigerant loop which consists of gear pump, mass flow meter, electric heater, oil retention test section, condenser, liquid receiver and subcooler and oil loop which consists of oil level sensor, oil tank, syringe pump and densimeter in the system. Gear pump speed was controlled by the control box of gear pump, and an electric heater which is made of cupper pipe was installed at the next to the mass flow meter. Slidacs was used to set the heating load of electric heater. Plate heat exchanger was used to condense the gas phase refrigerant, and temperature and mass flow rate of secondary flow which is a mixture of water and ethylene glycol were controlled by the control box in the chiller. A filter dryer was installed to remove the foreign material. Liquid receiver and subcooler were used to supply the liquid refrigerant to the gear pump. Two Coriolis mass flow meters were installed to measure the mass flow rate of the liquid phase

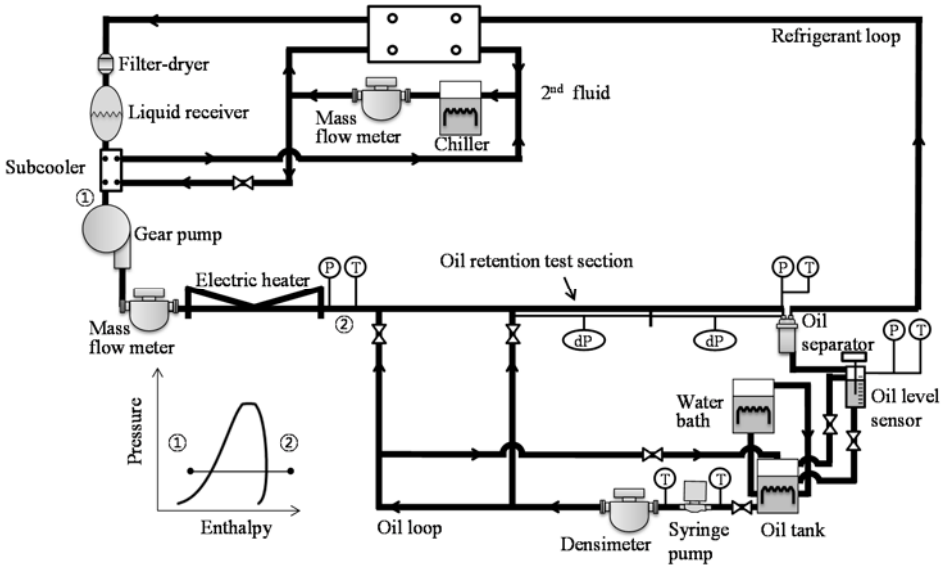

Fig. 3.1 Schematic of experimental apparatus for low mass flow rate condition

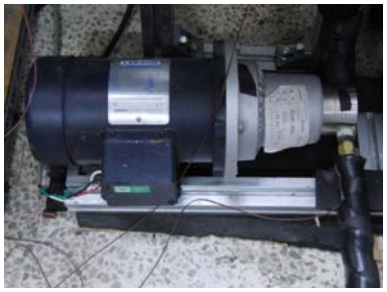

(a) Gear pump

(b) Electric heater

(c) Oil retention test section

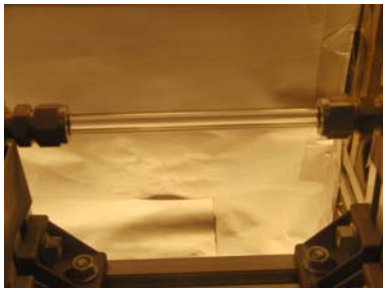

(d) Flow visualization section

Fig. 3.2 Pictures of experimental apparatus for low mass flow condition

(a) Slidacs

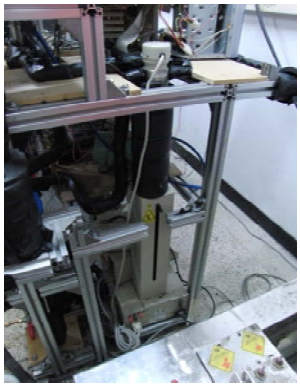

(b) Syringe pump

(c) Oil separator

(d) Level sensor

Fig. 3.2 Pictures of experimental apparatus for low mass flow condition, continued

refrigerant and the secondary fluid in the condenser. An oil separator is installed at the end of oil retention test section, and an oil level sensor is installed below the oil separator. A water bath was used to keep the set temperature of PVE oil in the oil tank. A Coriolis densimeter was installed to measure the density of liquid mixture during the injection.

The oil retention test section was length of 3.8 m. There were two oil injection ports in oil retention test section, and each port was located in 2 m and 3 m away from the oil separator. Two differential pressure transmitters were installed to measure the pressure drops at the sections of 2 ~ 1 m and 1 ~ 0 m away from the oil separator. T-type thermocouples and pressure transducers were used to measure the temperature and pressure at several points of experimental apparatus. Specifications of each component of experimental apparatus are shown in Table 3.1.

After finishing the experiment for low mass flow rate condition, the test section of experimental apparatus was changed to conduct the flow visualization. Fig. 3.3 shows the schematic of flow visualization section. To observe the flow pattern with respect to the mass flow rate and OCR, a quartz pipe was installed. The quartz pipe was length of 0.15 m, outer diameter of 10 mm and thickness of 2.5 mm. The picture of quartz pipe is shown in Fig. 3.2.

Table 3.1 Schematic of experimental apparatus for low mass flow rate condition

Gear pump	
Manufacture	Micropump
Model	219/56C
Flow rate range	0.425 ~ 11.75 LPM
Max. pressure	10342.1 kPa
Refrigerant mass flow meter	
Manufacture	Oval
Model	CT9301, CX006-0045
Range	0 ~ 100 g/s
Accuracy	±0.11%
Slidacs	
Manufacture	Daelim electronics
Range	0 ~ 240 V
Capacity	10 kVA

Table 3.1 Schematic of experimental apparatus for low mass flow rate condition, continued

Watt meter	
Manufacture	Yokogawa
Model	WT130
Range	0 ~ 600 V, 0 ~ 300 A
Accuracy	Voltage : ±0.2% F.S Current : ±0.3% F.S ±0.05 A (Clampmeter)
Electric Heater	
Material	Cupper pipe
Pipe size	9.52 mm (0.8t)
Length	20 m
Oil retention test section I	
Material	Cupper pipe
Pipe size	9.52 mm (0.8t)
Length	3.8 m

Table 3.1 Schematic of experimental apparatus for low mass flow rate condition, continued

Oil retention test section II	
Material	Cupper pipe
Pipe size	15.88 mm (0.9t)
Length	3.8 m
Differential pressure transmitter	
Manufacture	Druck
Model	STX 2100 series
Range	0 ~ 1 bar
Accuracy	±0.1%
Oil separator	
Manufacture	Henry technologies
Model	S-5581

Table 3.1 Schematic of experimental apparatus for low mass flow rate condition, continued

Oil level sensor	
Model	DT-200S2
Range	0 ~ 394 mm
Accuracy	F. S ±0.5%
Operating Temperature and Pressure	Max. 100^0C, Max. 1961 kPa
Oil tank	
Material	Stainless steel
Length	100 mm
Outer diameter	165 mm
Oil tank chiller	
Manufacture	DAIHAN Scientific Co.
Capacity	1.5 kW (Heating), 1/3 HP (Cooling)
Temp. accuracy	$\pm 0.1^0$C

Table 3.1 Schematic of experimental apparatus for low mass flow rate condition, continued

Syringe pump	
Manufacture	ISCO
Model	500D
Flow range	0.001 ~ 204 ml/min
Flow accuracy	0.5% of set point
Oil densimeter	
Manufacture	Oval
Model	CT9401, CN006-1629
Density range	0.3 ~ 2 g/ml
Density accuracy	±0.001 g/ml
Oil injection line	
Material	Cupper pipe
Pipe size	3.18 mm (0.7t)

Table 3.1 Schematic of experimental apparatus for low mass flow rate condition, continued

Condenser	
Manufacture	KOS MACHUNERY GROUP
Model	B25TH x 26
Capacity	5 RT
Water chiller	
Manufacture	Yescool
Model	YRC-5A
Capacity	5 RT
Water mass flow meter	
Manufacture	Oval
Model	CT9301, CX006-0045
Range	0 ~ 100 g/s
Accuracy	±0.11%

Table 3.1 Schematic of experimental apparatus for low mass flow rate condition, continued

Filter dryer	
Manufacture	ALCO CONTROLS
Type	ADK-053
Subcooler	
Manufacture	KOS MACHUNERY GROUP
Model	B10TH x 10
Capacity	0.75 RT
Pressure Transducer	
Manufacture	Sensotec
Model	FPA
Accuracy	$\pm 0.1\%$

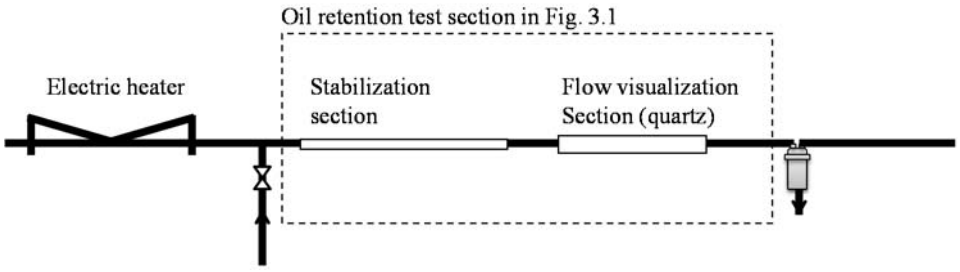

Fig. 3.3 Schematic of flow visualization section

Fig. 3.4 shows the schematic of experimental apparatus for high mass flow rate condition. The compressor speed was controlled by the speed control box. Two oil separators were installed at the outlet of compressor to minimize the amount of discharged oil from compressor, and a plate heat exchanger was used to cool the high temperature refrigerant coming from compressor. The refrigerant loop has a by-pass line and two expansion devices were installed. A filter-dryer was installed to remove the foreign substance in the refrigerant. Temperature and mass flow rate of secondary flow which is a mixture of water and ethylene glycol were controlled by the control box in the chiller. Two Coriolis mass flow meters were installed to measure the mass flow rate of the gas phase refrigerant and one Coriolis mass flow meter was installed to measure the mass flow rate of the secondary fluid in the plate heat exchanger.

Main components of the oil loop were oil separator, oil level and syringe pumps. A water bath was used to keep the set temperature of PVE oil in the oil tank. A Coriolis densimeter was installed to measure the density of liquid mixture during the injection.

Oil retention test section was 3 m in length and had three oil injection ports. Each oil injection port was located at 3 m, 2 m and 1 m away from the oil separator which was installed at the end of oil retention test section.

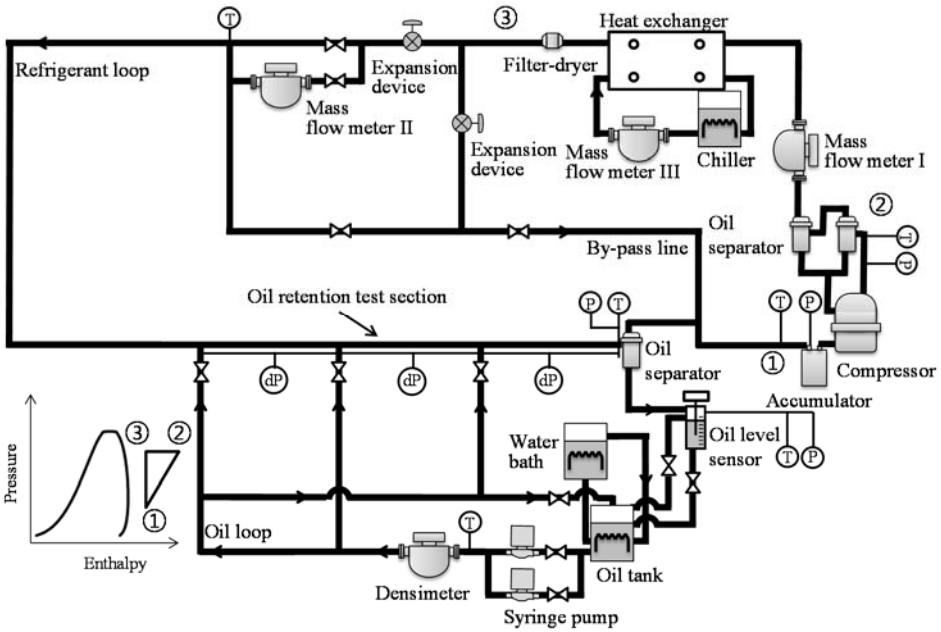

Fig. 3.4 Schematic of experimental apparatus for high mass flow rate condition

Pressure drops at each section 3 ~ 2 m, 2 ~ 1 m and 1 ~ 0 m away from oil separator were measured by differential pressure transmitters. Pressure transducers and T-type thermocouples were used to measure pressures and temperatures at several points of the system.

Chiller, mass flow meter for secondary fluid in heat exchanger, filter-dryer, differential pressure transmitters, water bath, oil level sensor and densimeter were the same with the components which were used in experimental apparatus for low mass flow rate condition. The specifications of rest components in experimental apparatus for high mass flow rate condition are shown in Table 3.2, and Fig. 3.5 shows the pictures of some components for high mass flow rate condition.

High pressure and high temperature refrigerant from a compressor is condensed at the heat exchanger in the general heat pump system. In this research, however, experimental apparatus was designed in such a way that the refrigerant from compressor is not condensed, which is illustrated in the pressure-enthalpy diagram of Fig. 3.4. The refrigerant is just cooled and maintained in a gas phase. In this case, the experiment can be conducted under high refrigerant mass flow rate condition. The disadvantage of this test apparatus is that the accuracy of refrigerant mass flow rate measurement is decreased.

Table 3.2 Schematic of experimental apparatus for high mass flow rate condition

Oil separator	
Manufacture	LG electronics
Model	MHH41401201
Accumulator	
Manufacture	LG electronics
Compressor	
Manufacture	LG electronics
Model	JBB055DAB
Refrigerant mass flow meter I	
Manufacture	Oval
Model	CT9401, CX015-ss-200k
Range	0 ~ 200 g/s
Accuracy	$\pm 0.55\%$

Table 3.2 Schematic of experimental apparatus for high mass flow rate condition, continued

Refrigerant mass flow meter II	
Manufacture	Oval
Model	CT9401, CX015-ss-200k
Range	0 ~ 200 g/s
Accuracy	±0.55%
Heat exchanger	
Manufacture	KOS MACHUNERY GROUP
Model	B25TH x 40
Capacity	7.5 RT
Expansion device	
Manufacture	Hoke
Model	2335G4Y
Max. Pressure	345 bar

(a) Accumulator

(b) Horizontal test section

(c) Compressor

(d) Vertical test section

Fig. 3.5 Pictures of experimental apparatus for high mass flow condition

3.2.2 Experimental procedure

The experimental procedures of two experimental apparatus are similar but there are some differences. In case of the low mass flow rate condition, the oil retention amount and pressure drop were measured with respect to the mass flux of refrigerant, oil circulation ratio (OCR) and pipe diameter. Among these variables, the definition of oil circulation ratio is the ratio of mass flow rate of oil to mass flow rate of total fluids which include refrigerant and liquid mixture (oil and solute refrigerant). The mass flow rate of refrigerant was measured using mass flow meter, and the volumetric flow rate of liquid mixture was measured using syringe pumps. Based on a solubility data, measured density and volumetric flow rate of liquid mixture, mass flow rates of oil and solute refrigerant were calculated. From the mass flow rates of refrigerant, oil and solute refrigerant, the oil circulation ratio was obtained. To conduct the experiment, at first, the speed of gear pump, heating load of electric heater and mass flow rate and temperature of secondary fluid in condenser were set. The mass flow rates of refrigerant was controlled by the speed controller of gear pump, and the temperature at the test section was set by the electric heater. As the refrigerant passes through the electric heater, the refrigerant vaporized from state 1 to state 2 in Fig. 3.1. Gas phase refrigerant went into the condenser and was condensed

from state 2 to state 1. The experimental apparatus was designed to simulate the compressor suction line, and the pressure of the system was maintained as the value of the compressor suction line. The system pressure was controlled by the temperature of secondary fluid in condenser. The water bath temperature was set to maintain the temperature of liquid mixture in oil tank as the same temperature of refrigerant at state 2 in Fig. 3.1. The temperature and pressure of state 2 were set as 20.9℃ and 906.4 kPa in this study. When the system became a steady state, syringe pump injected the liquid mixture to the oil retention test section. Volumetric flow rate and density of injected liquid mixture were measured by syringe pump and densimeter during the injection. Gas phase refrigerant and injected liquid mixture passed through the oil retention test section and entered the oil separator. At the oil separator, most of liquid mixture was separated and entered the oil level sensor. Real time volumetric flow rate of extracted liquid mixture was measured by oil level sensor. Gas phase refrigerant and unseparated liquid mixture circulated the refrigerant loop. By comparing the total amount of injected liquid mixture and extracted liquid mixture, the oil separator efficiency was calculated. Based on the volumetric flow rate and density of injected and extracted liquid mixture and the oil separator efficiency, the oil retention amount in the test section was calculated.

In case of high mass flow rate condition, this study measured the oil retention amount and pressure drop with respect to refrigerant mass flow rate, oil circulation ratio (OCR), pipe diameter and pipe configurations which include horizontal and vertical at the compressor suction line. The mass flow rates of refrigerant and the liquid mixture of oil and solute refrigerant were controlled by the speed controller of compressor and syringe pumps, respectively. To measure the oil retention amount and pressure drop at the set test condition, the compressor speed set, and then, refrigerant is compressed from state ① to ② as shown in Fig. 3.4. Refrigerant and oil are discharged from compressor and pass through the oil separators. At the oil separators, most of the oil is separated and the refrigerant with remaining amount of oil goes into the mass flow meter. The mass flow rate of gas phase refrigerant with this remaining oil was measured. The high temperature refrigerant enters the heat exchanger and is cooled from state ② to ③ as shown in Fig. 3.4. Mass flow rate of secondary flow was adjusted to control the temperature of state ③ as shown in Fig. 3.4. At the relatively low mass flow rate condition, mass flow rate of refrigerant which enters the oil retention test section is measured, and the rest of refrigerant flows to the accumulator through the by-pass line. In case of relatively high mass flow

rate condition, all the refrigerant goes to the oil retention test section. To control the liquid mixture temperature, the water bath temperature is set to the same as the refrigerant at state ① as shown in Fig. 3.4. The temperature and pressure of state ① were set as 20.7℃ and 905.2 kPa in this study. In this study, the effects of temperature and pressure on the oil retention amount were not considered, so the temperature and pressure conditions did not change. When the system was in a steady-state, syringe pumps injected the liquid mixture to the oil retention test section. During the injection, the volume flow rate of liquid mixture was controlled by syringe pumps and the density of liquid mixture was measured by densimeter. The refrigerant and liquid mixture flowed to the oil separator which was installed at the end of oil retention test section and the liquid mixture was separated. The refrigerant returned to the compressor and the oil level sensor measured the real time volume of extracted liquid mixture from the oil separator. Finally, the real time volume of liquid mixture in the oil retention test section was calculated by subtracting extracted volume from injected volume of the liquid mixture.

3.2.3 Data reduction

The oil injection ports are installed perpendicular to the flow of refrigerant in the oil retention test section. It is possible to presume that the flow near the injection port is not fully developed flow when the liquid mixture is injected. Fig. 3.6 shows the entry region and fully developed flow in a pipe, where the pressure drop at the fully developed flow region is linear because the velocity gradient does not change as the flow moves to flow direction. In case of entry region, however, the pressure gradient changes as the velocity gradient changes. The pressure drop of the entry region is higher than that of fully developed region, so it is possible to confirm the fully developed flow by comparing the pressure drops at several subsections. Fig. 3.7 shows pressure drop results with respect to the refrigerant mass flux when pipe inner diameter is 14.1 mm and OCR is about 2%. dP1, dP2 and dP3 mean the pressure drops at 0 ~ 1 m, 1 ~ 2 m and 2 ~ 3 m sections away from oil separator, respectively. IP2 and IP3 represent that the injection position is 2 m and 3 m away from the oil separator, respectively. Fig. 3.7 shows that dP3 is higher than dP1 and dP2, and the dP1 and dP2 is almost the same when the injection position is 3 m away from the oil separator. From the results, it is possible to confirm that the entrance length of flow is less than 1 m. When the injection position is 2 m, dP2 is higher than dP1,

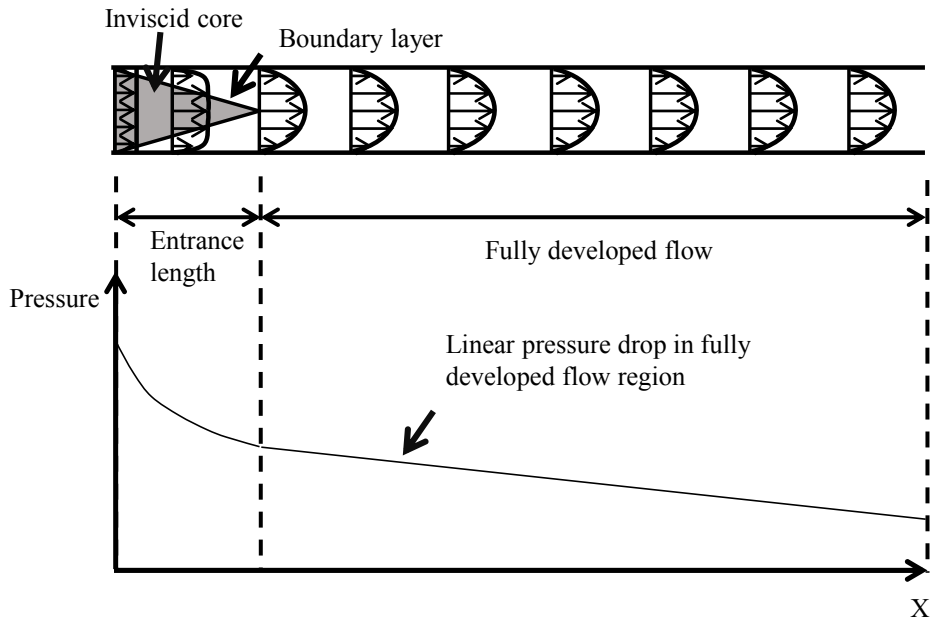

Fig. 3.6 Entry region and fully developed flow in a pipe

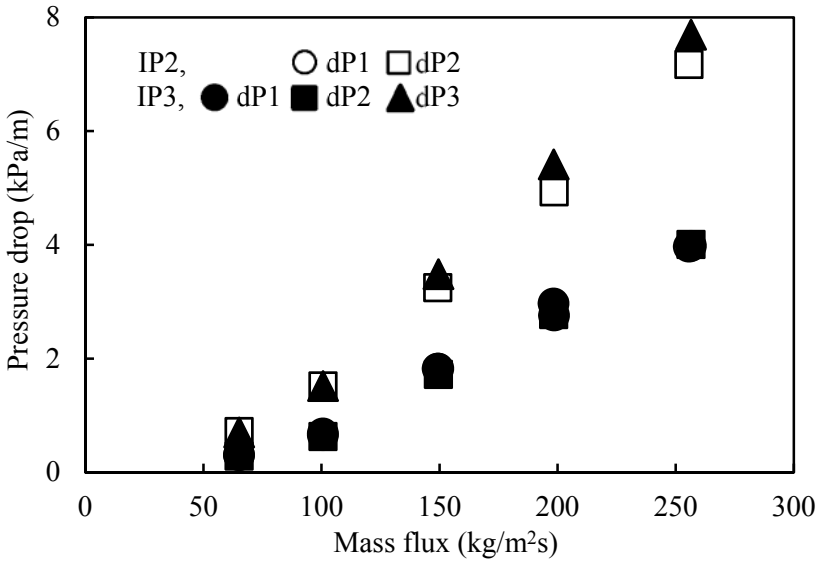

Fig. 3.7 Pressure drop for the tube with inner diameter of 14.1 mm and oil circulation ratio of 2%

and the dP1 is almost the same as the dP1 and dP2 for the case that the injection position is 3 m. These results also support that the entrance length is less than 1 m. dP3 for the case that the injection position is 3 m and dP2 for the case that the injection position is 2 m are similar and relatively higher than the other three pressure drop values because these two pressure drops were measured at the entry region of the flow. During the all experiments, pressure drops were measured. As a results, the tendency of pressure drop under all test conditions was just like Fig. 3.7. In case of the experiment for low mass flow rate condition, dP3 was not measured but the pressure drops at the other sections showed the same tendency. That is, dP1 and dP2 of IP3 and dP1 of IP2 were almost the same and dP2 of IP2 was higher than the other three pressure drops. This means that the entrance length is less than 1 m under all test conditions in this study.

Volumes of injected and extracted liquid mixture were measured by syringe pumps and oil level sensor, respectively, and Figs. 3.8 and 3.9 show the volume of the injected and extracted liquid mixture. To clean up the liquid mixture in the oil retention test section, the oil retention test section was flushed by pure refrigerant for approximately one hour after finishing the injection. As shown in Fig. 3.8, volume of extracted liquid mixture does not increase after cleaning the oil retention test section for 30 ~ 40 minutes

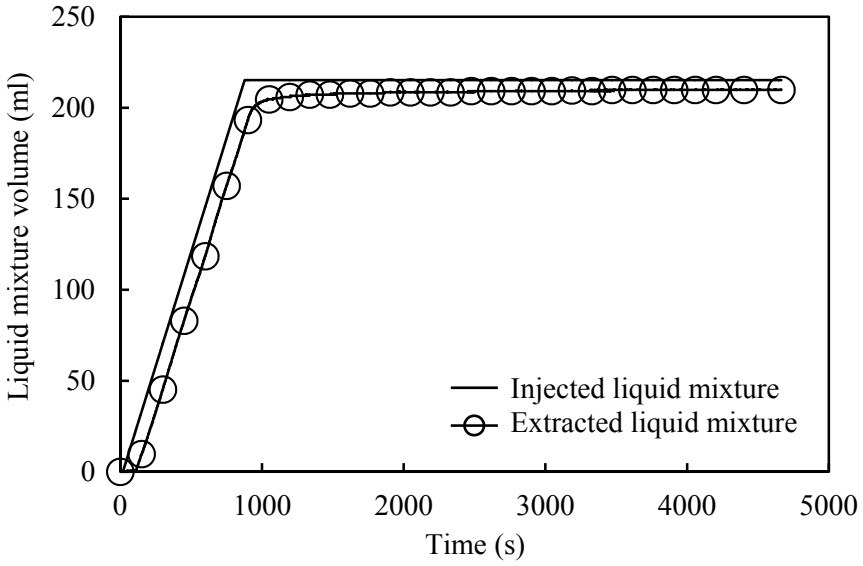

Fig. 3.8 Injected and extracted liquid mixture's (oil + solute refrigerant) volume at the experimental apparatus for low mass flow rate condition

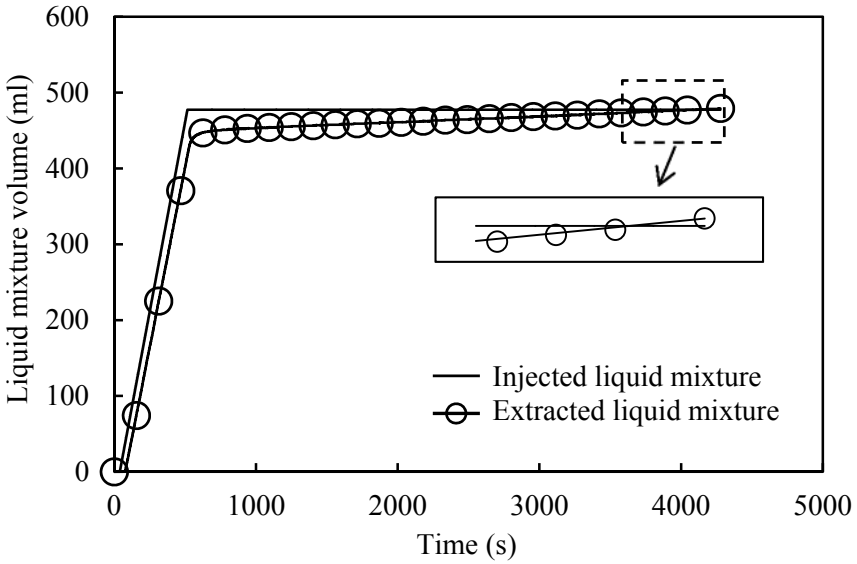

Fig. 3.9 Injected and extracted liquid mixture's (oil + solute refrigerant) volume at the experimental apparatus for high mass flow rate condition

and the volume of injected liquid mixture is higher than that of extracted liquid mixture. In Fig. 3.9, however, the liquid mixture was extracted until the last moment and the total volume of extracted liquid mixture was higher than that of injected liquid mixture. In case of the experimental apparatus for low mass flow rate condition, a gear pump was used while the experimental apparatus for high mass flow rate condition used a compressor to circulate the refrigerant. Unlike gear pump, compressor contains lubricant and the lubricant is discharged from the compressor. Small amount of discharged liquid mixture from the compressor is not separated in the oil separators which are installed at the outlet of compressor. The gas phase refrigerant and unseparated liquid mixture enters into the oil separator at the end of oil retention test section and the unseparated liquid mixture is separated there. So the level sensor detects the amount of this liquid mixture and this is the main reason why the volume of extracted liquid mixture is higher than that of injected liquid mixture in Fig. 3.9. To measure the oil retention amount, the consideration on the unseparated liquid mixture from oil separators of compressor outlet is necessary. Volumetric flow rate of the unseparated liquid mixture was calculated based on the gradient of extracted liquid mixture volume change in extension graph of Fig. 3.9. The volumetric flow rate of the oil (with solute refrigerant in the oil) at the oil separator discharge

line varied from 0.001 mls^{-1} to 0.019 mls^{-1} under all experimental conditions. The volume of extracted liquid mixture except the unseparated liquid mixture from compressor can be calculated by subtracting the volume of the unseparated liquid mixture from the total extracted volume of liquid mixture in Fig. 3.9. This result is shown in Fig. 3.10. The results of Fig. 3.10 is similar to that of Fig. 3.8. So the next steps to obtain the oil retention amount is the same. The mass of injected and extracted oil is obtained by using the density of liquid mixture and the R410A/PVE oil solubility data. The solubility is about 19.5% when temperature is 20.8℃ and pressure is 905.4 kPa. If efficiency of oil separator in oil retention test section is 100%, the total injected and extracted oil mass should be the same. Unfortunately, the oil separator efficiency is not 100% so the total extracted oil mass is lower than the total injected oil mass. The efficiency of oil separator at the end of oil retention test section is calculated by the following equation (3.1).

$$\varepsilon = \frac{m_{TEO}}{m_{TIO}} \tag{3.1}$$

Based on equation (3.1), the extracted oil mass when the oil separator efficiency is 100% was calculated. Fig. 3.11 can be obtained from the Fig. 3.10 by considering the oil separator efficiency. Unlike Fig. 3.10, Fig. 3.11 shows that the mass of extracted oil is equal to that of injected oil. The real time oil retention amount in the oil retention test section can be obtained by

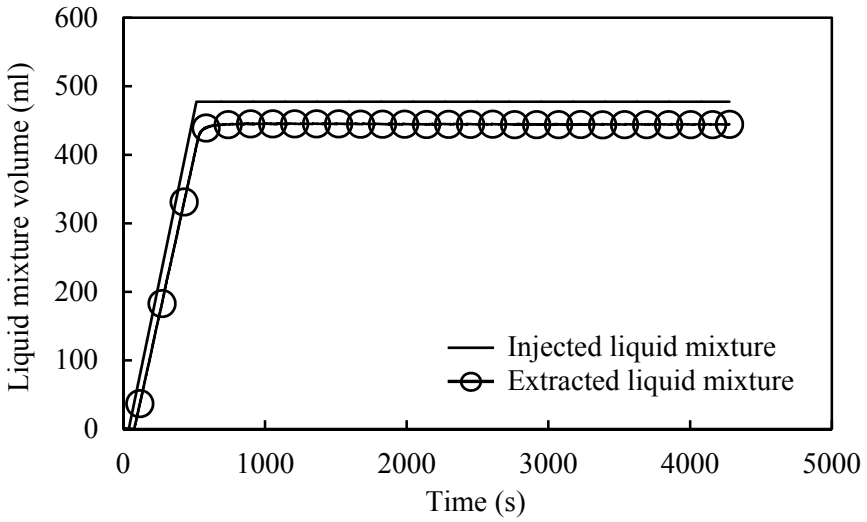

Fig. 3.10 Injected and extracted liquid mixture's (oil + solute refrigerant) volume with a consideration of the unseparated liquid mixture's volume from compressor

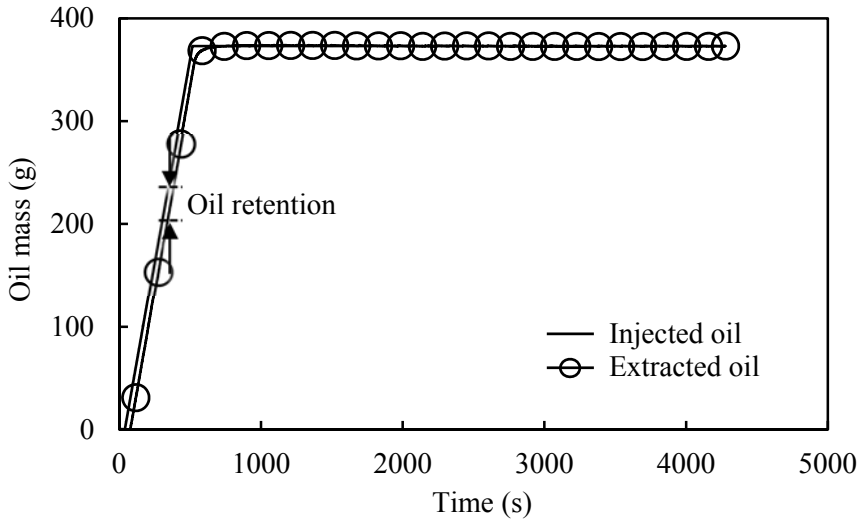

Fig. 3.11 Mass of injected and extracted oil with a consideration of the oil separator efficiency

subtracting the extracted oil mass from the injected oil mass as shown in Fig. 3.11. Under the same test condition, the oil retention amount and pressure drop were measured when liquid mixture was injected at the locations of 2 m and 3 m away from the oil separator. Then, the oil retention amount for 2 m and 3 m pipe length conditions and the pressure drop data were obtained. Because the entrance length is less than 1 m under all test conditions, the oil retention amount per unit length under fully developed flow can be calculated by subtracting the oil retention amount for 2 m pipe length condition from the oil retention amount for 3 m pipe length condition. In addition, the pressure drop per unit length under fully developed flow condition is obtained by computing the average of dP1 from 2 m pipe length condition and dP1 and dP2 from 3 m pipe length condition which are measured under fully developed flow. To confirm that the measured oil retention amount per unit length under fully developed flow condition is reliable, under some test conditions, the experiment was conducted when injection position is 1 m away from the oil separator. The oil retention amount per unit length under fully developed flow condition was also calculated by subtracting oil retention amount for 1 m pipe length condition from that for 2 m pipe length condition. Then, this results were compared with oil retention results from 2 m and 3 m pipe length conditions.

3.2.4 Uncertainty of measurements

Moffat (1988) presented a basic equation which is described in equation (3.2) for calculating the uncertainty of measurement

$$\delta R = \left\{ \sum_{i=1}^{N} \left(\frac{\partial R}{\partial X_i} \delta X_i \right)^2 \right\}^{1/2} \tag{3.2}$$

δR and δX_i are the uncertainty of overall measurement result and one variable, respectively.

This study conducted the experiment by using two different experimental apparatus. However, the volume fraction of oil was calculated by the same method. The injected and extracted oil volume, density and solubility data of liquid mixture under two different injection positions were used to calculate the volume fraction of oil. So, uncertainty of the measurement in volume fraction of oil can be expressed in equation (3.3).

$$\delta m_{OR} = \left\{ \sum_{i=1}^{8} \left(\frac{\partial m_{OR}}{\partial X_i} \delta X_i \right)^2 \right\}^{1/2} \tag{3.3}$$

Uncertainties of injected and extracted oil volume and density of liquid mixture are obtained from the accuracies of liquid flow rate indication given by the syringe pump, measurement by level sensor and densimeter.

Uncertainty of the solubility data is computed based on the accuracies of pressure and temperature measurements. The average and maximum uncertainty of the experimental volume fraction of oil were 5.8% and 11.4%, respectively.

3.3 Results and discussion

The experiment for low mass flow rate condition was conducted under horizontal pipe configuration with respect to the refrigerant mass flux and OCR. In case of high mass flow rate condition, the experiment was conducted under horizontal and vertical pipe configurations with respect to refrigerant mass flux and OCR. Volume fractions of oil at the suction line of compressor under fully developed flow are shown in Figs. 3.12 ~ 3.15. Experimental data in Fig. 3.12 was obtained from the experimental apparatus for low mass flow rate condition which is less than 10 g/s. Experimental data in Figs. 3.13 ~ 3.15 was obtained from the experimental apparatus for high mass flow rate condition which is more than 10 g/s. The experiment was conducted under three different pipe diameter conditions and Figs. 3.12 ~ 3.15 show each result for inner diameters of 8.0, 14.1, 17.3 and 26.0 mm. This study also conducted an experiment to observe the flow pattern of refrigerant and oil mixture in horizontal pipe. Flow visualization was

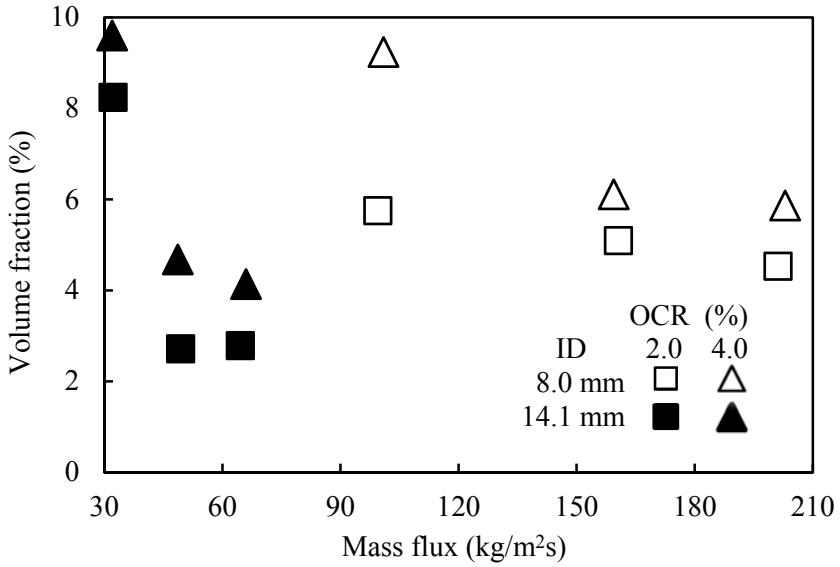

Fig. 3.12 Volume fraction of oil for the tube with inner diameter of 8.0 mm and 14.1 mm under low mass flow rate condition

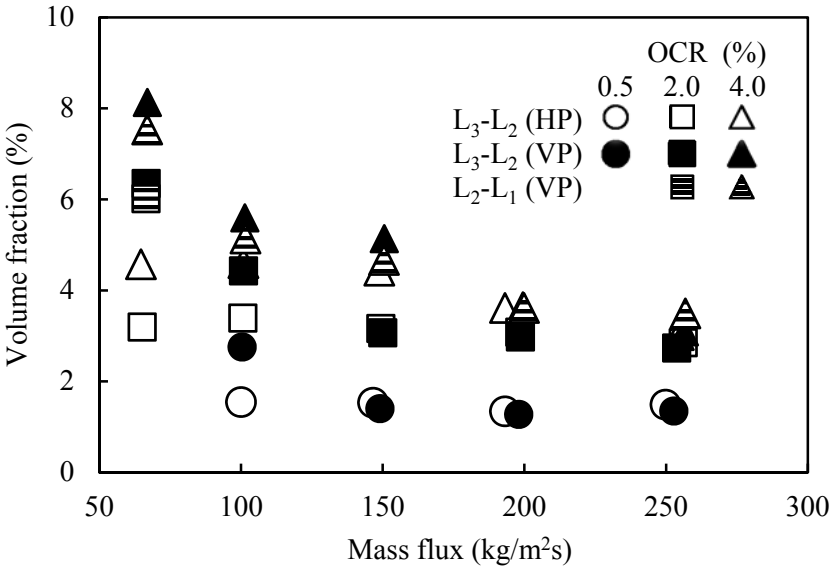

Fig. 3.13 Volume fraction of oil for the tube with inner diameter of 14.1 mm under high mass flow rate condition

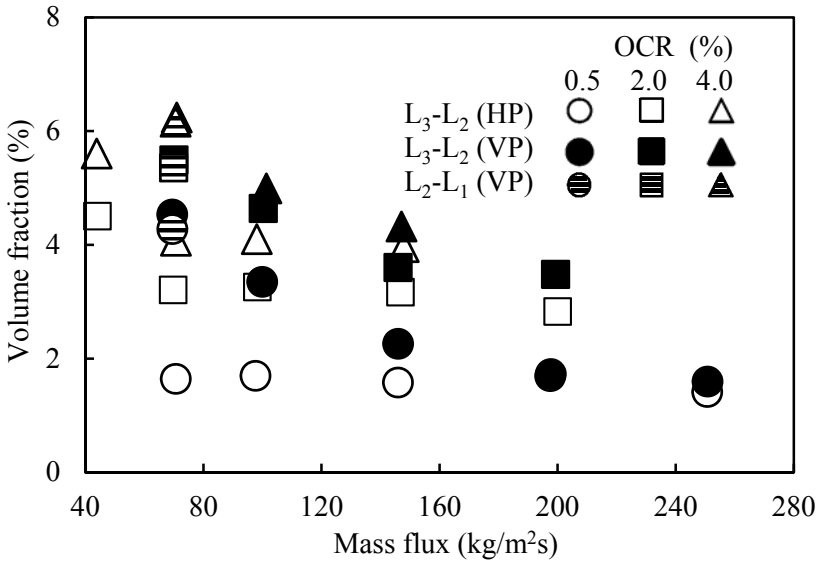

Fig. 3.14 Volume fraction of oil for the tube with inner diameter of 17.3 mm under high mass flow rate condition

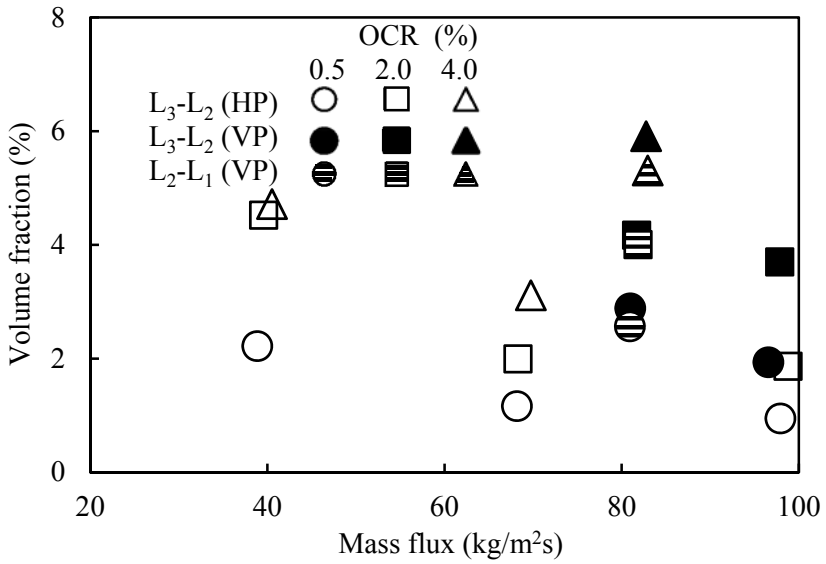

Fig. 3.15 Volume fraction of oil for the tube with inner diameter of 26.0 mm under high mass flow rate condition

conducted with respect to the mass flux of refrigerant and OCR. Fig. 3.16 shows the results of flow visualization. The flow pattern in the horizontal pipe when the superficial vapor velocity is higher than 3.2 ms^{-1} is annular flow. Many studies on the flow visualization and flow pattern of the refrigerant and lubricant mixture have been conducted. Among them, Ramakrishnan and Hrnjak (2010) showed that the flow pattern usually changes from stratified to annular flow when superficial vapor velocity is about 3 ~ 4 ms^{-1} in horizontal pipe. Based on the flow visualization results and previous studies, it is possible to presume that the flow patterns of the experimental conditions in horizontal pipe are stratified flow or annular flow. Figs. 3.12 ~ 3.15 shows that the oil retention amount reduces as the mass flux increases. The high refrigerant mass flux provides a high shear force on the interface between gas and liquid. Thus, the oil transportation rises as the refrigerant mass flux increases. There are some sections that the oil retention amount is almost constant with the mass flux in Figs. 3.12 ~ 3.15. When the change of oil retention amount is small, it is difficult to measure the slight change because of the error of measuring system. Thus, almost constant trend of oil retention amount with respect to the mass flux was measured.

In case of vertical upward flow, the liquid mixture flows up very slowly when the refrigerant mass flux is not sufficiently high. In this case, it takes a

(a) G : 101.7 kg/s·m^2

OCR : 1.9%

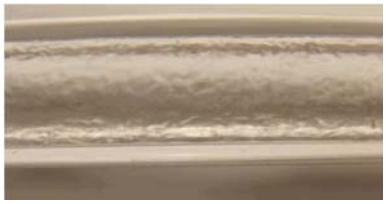

(a) G : 102.0 kg/s·m^2

OCR : 3.7%

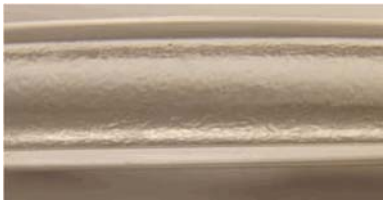

(c) G : 151.0 kg/s·m^2

OCR : 1.9%

(d) G : 155.8 kg/s·m^2

OCR : 3.6%

(e) G : 201.0 kg/s·m^2

OCR : 1.9%

(f) G : 205.6 kg/s·m^2

OCR : 3.7%

Fig. 3.16 Flow pattern in horizontal pipe

long time to extract the liquid mixture which is injected into the oil retention test section. Thus, it is necessary to find the mass flux limit for the acceptable amount of time required to extract the liquid mixture. In this experiment, the mass flux limit was obtained by varying the refrigerant mass flux. Figs. 3.17 and 3.18 show the injected and extracted liquid mixture volume under refrigerant mass flux of 63 and 67 $kgm^{-2}s^{-1}$when pipe inner diameter is 14.1 mm. In case of 63 $kgm^{-2}s^{-1}$condition, the liquid mixture was extracted very slowly and was not fully extracted until one hour after finishing the injection. As shown in Fig. 3.17, the liquid mixture was extracted rapidly when the refrigerant mass flow rate increased. Under this mass flux condition, it's not possible to predict the time for extracting all of injected liquid mixture. In case of 67 $kgm^{-2}s^{-1}$condition, however, the liquid mixture was totally extracted in 40 minutes after finishing the injection. In this case, the oil retention amount can be estimated. So this mass flux is defined as the mass flux limit for measuring oil retention amount at vertical upward flow in the inner diameter pipe of 14.1 mm. Similarly, the mass flux limits for inner diameter pipes of 17.3 mm and 26.0 mm were obtained, whose values are 70 $kgm^{-2}s^{-1}$ and 81 $kgm^{-2}s^{-1}$, respectively.

The oil retention results for vertical upward flow are shown in the Figs. 3.13 ~ 3.15. Under some test conditions, the volume fraction of oil was

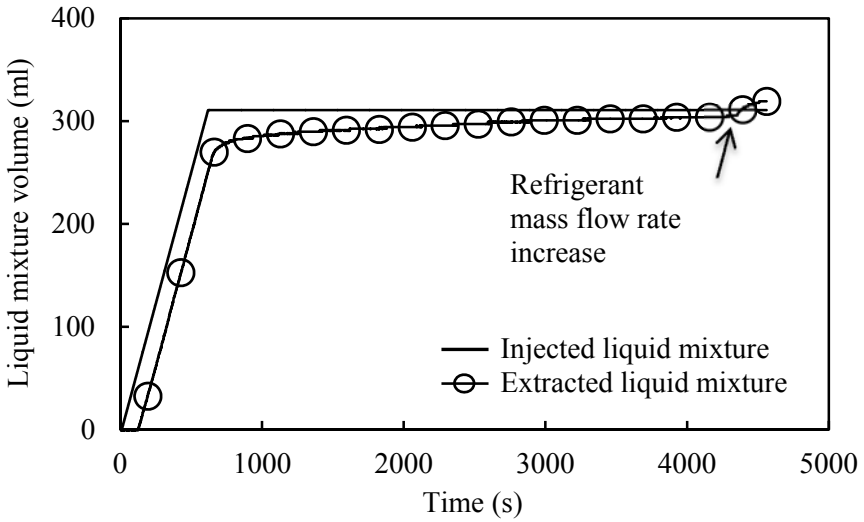

Fig. 3.17 Injected and extracted liquid mixture's (oil + solute refrigerant) volume in vertical upward flow under mass flux of 63 $kgm^{-2}s^{-1}$

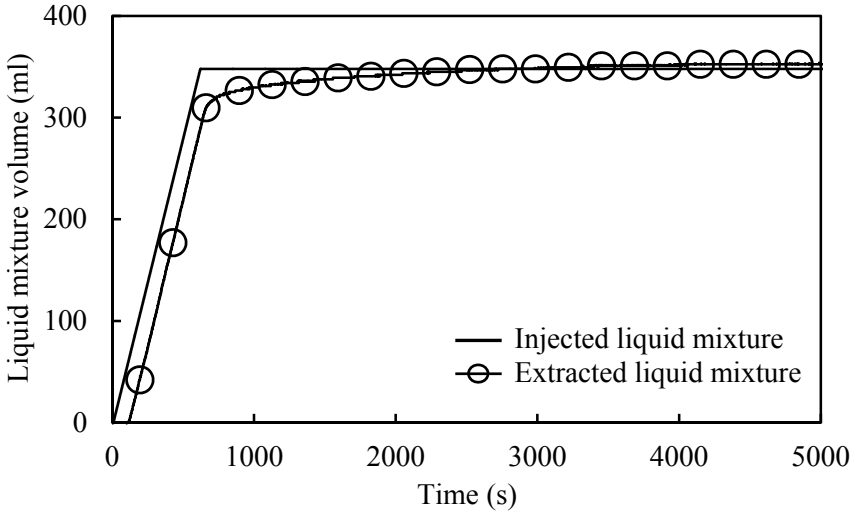

Fig. 3.18 Injected and extracted liquid mixture's (oil + solute refrigerant) volume in vertical upward flow under mass flux of 67 $kgm^{-2}s^{-1}$

measured when the liquid mixture was injected at 1 m away from oil separator. Then the oil retention amount per unit length was calculated by subtracting the oil retention amount for 1 m pipe length condition from the oil retention amount for 2 m pipe length condition. This value was compared with the oil retention result for 2 m and 3 m pipe length condition. As shown in Figs. 3.13 ~ 3.15, the volume fraction of oil for the 1 and 2 m pipe length conditions are similar to those for the 2 m and 3 m pipe length conditions. The average and maximum difference between two values were 6.5% and 13.0%, respectively. Many studies on flow visualization of refrigerant and lubricant mixture under vertical upward flow condition have shown that the flow pattern changes from churn flow to annular flow when the superficial vapor velocity is around 1.5 ~ 2.0 ms^{-1}. This research conducted the experiment when the mass flux is greater than 67 $kgm^{-2}s^{-1}$. Density of gas phase refrigerant is 31.1 kg/m^3, so the superficial vapor velocity of 67 $kgm^{-2}s^{-1}$ is about 2.2 m/s. Thus, it is possible to presume that the flow pattern is annular flow under all test conditions. In this case, as mentioned before, the increment of refrigerant mass flow rate leads to the decrement of oil retention amount. Figs. 3.13 ~ 3.15 show this tendency that volume fraction of oil in vertical upward flow tends to decrease as refrigerant mass flux increases.

Generally, the volume fraction of oil in vertical pipe is higher than that in horizontal pipe in Figs. 3.13 ~ 3.15. When the mass flux is large, however, the volume fractions of oil from horizontal and vertical pipe are almost the same. In case of horizontal pipe configuration, only shear force between gas and liquid affects the liquid film. Unlike the horizontal pipe configuration, two forces which including shear force and gravity force affect the liquid film in vertical pipe configuration. When refrigerant mass flux is low, the shear force between the interface of gas and liquid is small so the effect of gravity force on the liquid film is relatively large. So there is a large variation in the volume fractions of oil between horizontal and vertical pipe configuration under low mass flux condition. The effect of shear force is increased as refrigerant mass flux increases, and this leads to the reduction of the variation in the volume fractions of oil between horizontal and vertical pipe configurations. If refrigerant mass flux is large enough, the effect of gravity force is negligible because the shear force becomes dominant so the volume fractions of oil for horizontal and vertical pipes are almost the same.

Figs. 3.19 ~ 3.22 show pressure drop results with respect to the mass flux for pipe inner diameters of 8.0, 14.1, 17.3 and 26.0 mm. A high refrigerant mass flux means a high velocity gradient with respect to the radial direction, and a high velocity gradient causes a high pressure drop. So

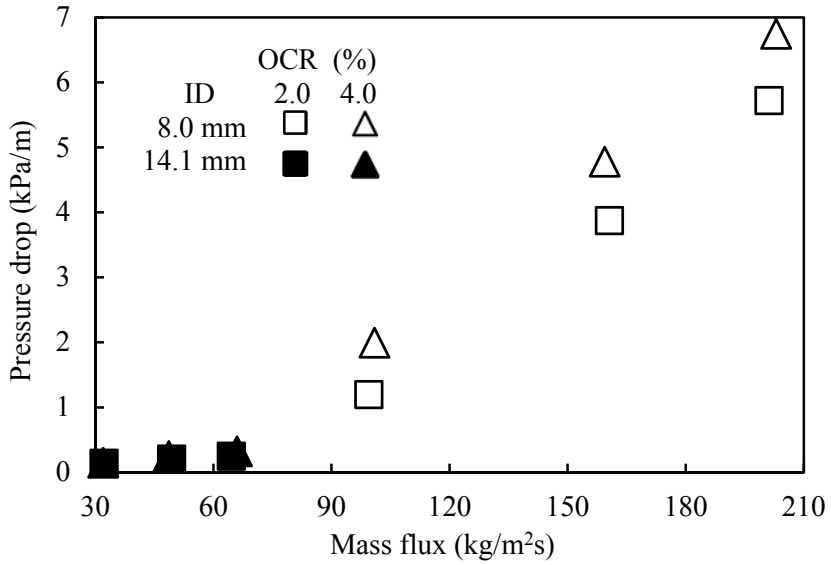

Fig. 3.19 Pressure drop per unit length in horizontal pipe of 8.0 and 14.1 mm

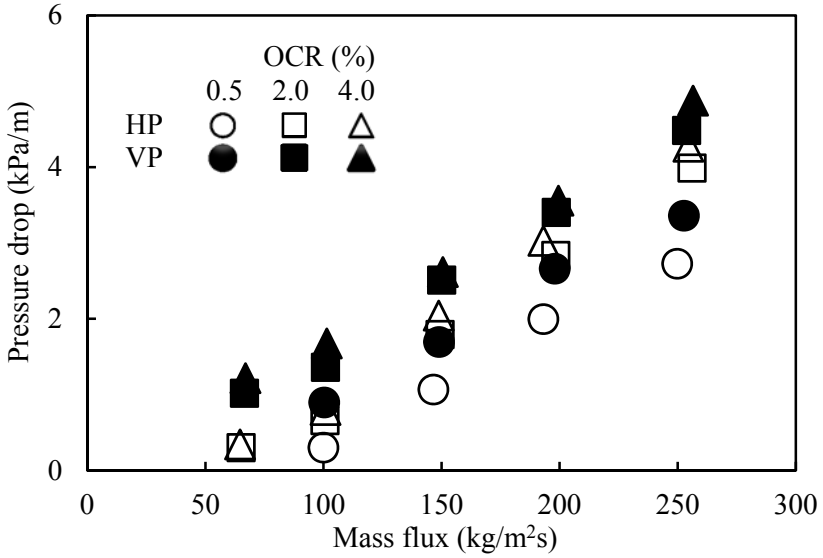

Fig. 3.20 Pressure drop per unit length in horizontal and vertical pipes of 14.1 mm

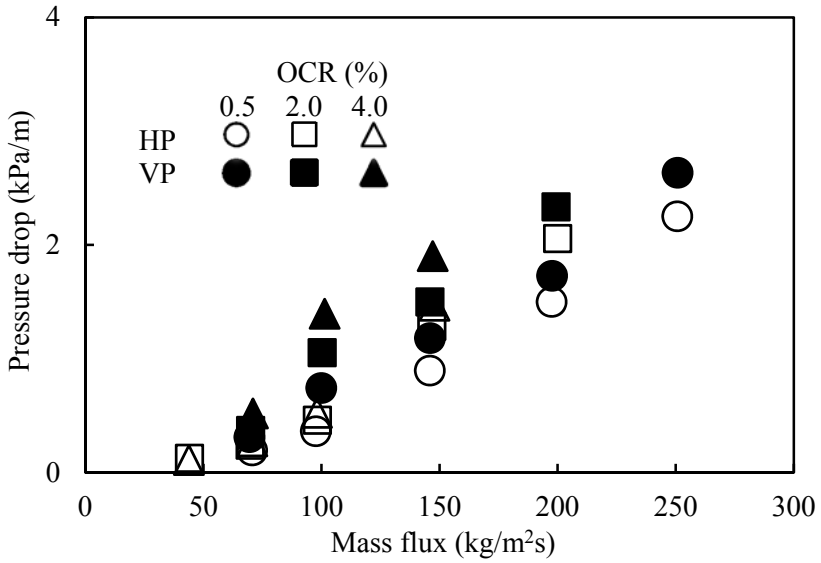

Fig. 3.21 Pressure drop per unit length in horizontal and vertical pipes of 17.3 mm

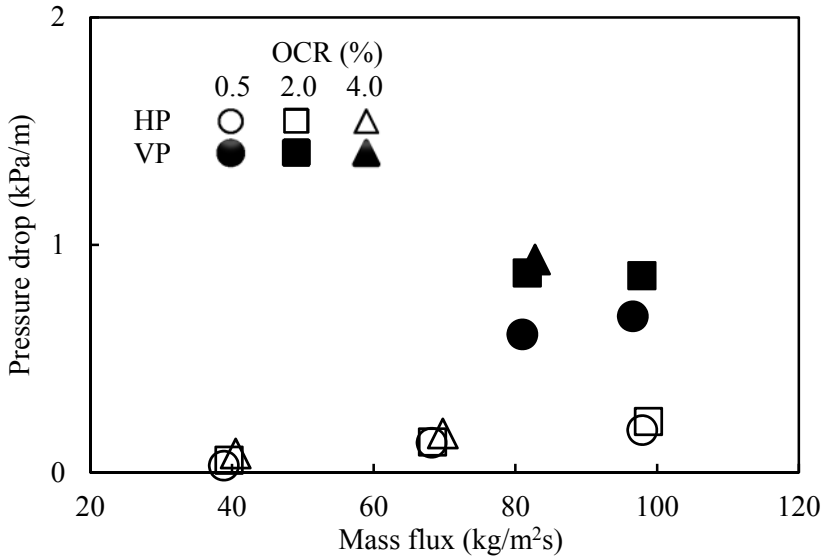

Fig. 3.22 Pressure drop per unit length in horizontal and vertical pipes of 26.0 mm

the pressure drop increases with an increment of mass flux. The pressure drop also increases with an increment of OCR. The viscosity of oil is higher than that of the refrigerant. High OCR means high oil retention amount in pipe, as shown in oil retention results, and this means an increment of the thickness of high viscosity layer. In addition, the velocity of gas phase rises as the thickness of oil increases. So the increment of OCR leads to the rise of pressure drop. Pressure drop changes slightly as oil circulation ratio increases when mass flux is low at horizontal pipe configurations. Pressure drop was almost constant with mass flux at the oil circulation ratio of 2% in vertical pipe of 26.0 mm. The pressure drop under these conditions has to show the increasing trend just like other cases. However, these changes of pressure drop may not be clearly measured by the differential pressure transmitters which the accuracy is 0.1 kPa under these circumstances because the changes were so small. Overall tendency of pressure drop is predictable, but the experimental pressure drop data is important to predict the flow characteristics in suction line more accurately and to understand the flow characteristic quantitatively.

3.4 Verification of numerical study

The model for predicting the oil retention amount in gas line of refrigerant was suggested at the chapter 2. With some assumptions, momentum and continuity equation were applied to the liquid film of annular flow. Empirical correlation from Wallis (1969) was used to calculate the interfacial friction factor between gas core and liquid film of annular flow. From the results of chapter 2, it was presumed that the ratio of oil retention amount in the gas line of refrigerant to the whole system will be high, even when the length of gas line is not long. The accuracy of predicted oil retention amount for the whole system is primarily affected by the accuracy of predicted oil retention amount in the gas line of refrigerant. Therefore, the comparison between predicted and experimental oil retention amount in the horizontal and vertical gas lines of refrigerant is important.

The experimental results of volume fractions of oil in horizontal and vertical gas lines of refrigerant were compared to the predicted volume fraction of oil from numerical calculation. As mentioned in chapter 2, the oil retention amount in gas line of refrigerant was calculated with an assumption that the flow pattern is annular flow. From the flow visualization results and previous studies, it was possible to know that the flow pattern of horizontal and vertical gas lines is annular flow when the superficial velocity of gas

phase refrigerant is higher than 3.2 $m^{-1}s$. So the experimental results which the superficial velocity of refrigerant is higher than 3.2 $m^{-1}s$ were used for the verification. Fig. 3.23 shows the comparison between predicted and experimental volume fraction of oil in horizontal and vertical gas lines of refrigerant. The mean absolute percentage error of predicted and experimental values was 15.0%. This demonstrates that predictions of chapter 2 were conducted with good reliability.

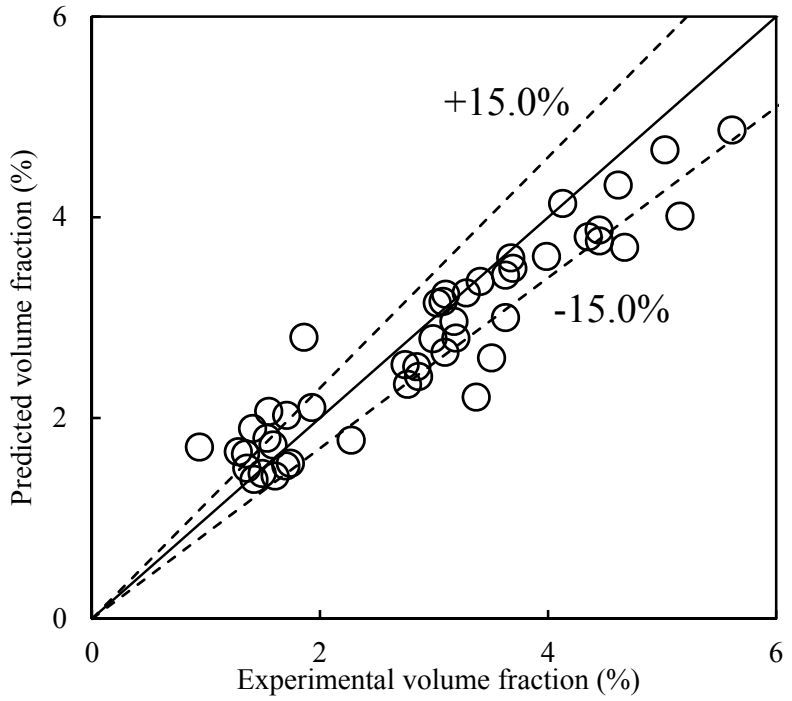

Fig. 3.23 Comparison of experimental and predicted volume fraction of oil in gas lines

3.5 Conclusion

The volume fraction of oil and pressure drop of refrigerant and oil mixture in compressor suction line were measured experimentally and the model for predicting the oil retention amount in the horizontal and vertical suction pipes were verified. The uncertainty in measuring average and maximum experimental volume fraction of oil were 5.8% and 11.4%, respectively. The volume fraction of oil and pressure drop data were obtained with respect to the mass flux, oil circulation ratio (OCR) and pipe diameter in horizontal and vertical suction pipes. The volume fraction of oil tends to decrease with the increment of refrigerant mass flux and the reduction of oil circulation ratio. Generally, the volume fraction of oil in vertical pipe was higher than that in horizontal pipe. However, the difference of volume fractions of oil in the horizontal and vertical pipe was reduced as the mass flux increases because the shear force becomes dominant. The pressure drop results show the increasing trend with the increment of mass flux and OCR.

Based on the experimental data, the numerical model was verified. The experimental volume fraction of oil when the flow pattern is annular flow were compared to the predicted volume fraction of oil. The mean absolute percentage error of predicted and experimental values was 15.0%.

Chapter 4. Study on the flow characteristics in oil separator

4.1 Introduction

The oil circulation ratio highly affects the oil retention amount and pressure drop in each component of heat pump system. As the oil circulation ratio increases, the oil retention amount and pressure drop rise. That is, increment of oil circulation ratio denotes decrement of the performance of heat pump system and the increment of the initial charge amount of lubricant. Therefore, reduction of oil circulation ratio is very important to enhance the system performance and reduce the initial charge amount of lubricant.

The oil separator is installed at the outlet of compressor to prevent the oil from circulating the system. Unfortunately, the efficiency of oil separator is not 100% so small amount of oil circulates the whole system. The oil circulation ratio is determined by the performance of the oil separator. So the development of high performance oil separator is required to enhance the system performance and reduce the initial charge amount of lubricant.

There are many kinds of gas-liquid separator, among them cyclone separator is widely used in heat pump system. There have been many studies

on the cyclone separator, and most of them focused on the gas-solid cyclone separator. Some studies considered gas-liquid separator and suggested model for predicting the flow characteristics in the separator. However, there is little research which considered the cyclone separator for multi heat pump system.

The main purpose of this chapter is to analyse the flow characteristics in the oil separator quantitatively and propose models for predicting the flow characteristics in oil separator. Experiment was conducted to measure the efficiency of oil separator and pressure drop with respect to mass flow rate of gas phase refrigerant and liquid circulation ratio. Mass flow rate and liquid circulation ratio were varied from 30 to 150 gs^{-1} and 1.5 to 4.5%, respectively. Seven different designs of oil separator were considered. R410A and PVE oil were used as refrigerant and lubricant. Based on the experimental results, the models for predicting the performance of various oil separators were suggested.

4.2 Experimental methodology

4.2.1 Experimental apparatus

The efficiency of oil separator is defined as a ratio of mass flow rate of

separated oil at the oil separator to mass flow rate of oil at the inlet of oil separator. According to the ASHRAE standards, mass flow rate of oil at the inlet of oil separator was measured by using mass flow meter and the mass flow rate of separated oil was calculated by dividing the time of experiment into mass change of a tank which contains separated oil during the experiment. A tank should be detached from experimental setup to measure its mass and this method takes many time. So, more convenient method to measure the efficiency of oil separator with a good accuracy is suggested.

Fig. 4.1 shows the experimental apparatus for measuring the efficiency and pressure drop of oil separator. There are refrigerant loop and oil loop. Refrigerant loop consists of compressor, oil separators, mass flow meter, test oil separator, heat exchanger, expansion devices and accumulator. Speed controller in compressor was used to control mass flow rate of refrigerant. To minimize the amount of discharged oil from compressor, two oil separators were installed. A mass flow meter was installed to measure the mass flow rate of gas phase refrigerant and heat exchanger was used to cool down the high temperature and high pressure refrigerant. Secondary fluid of heat exchanger was a mixture of water and ethylene glycol and the temperature and mass flow rate of the secondary fluid were controlled by the

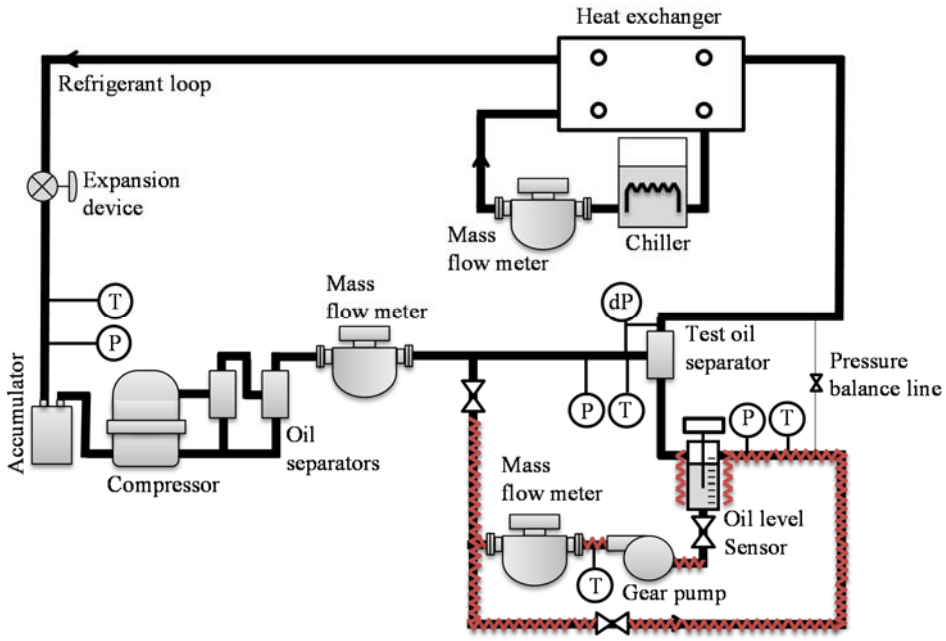

Fig. 4.1 Experimental apparatus for measuring the efficiency and pressure drop of oil separator

control box of chiller. This study considered seven different test oil separators and Fig. 4.2, Tables 4.1 and 4.2 show the design and specification of oil separators. Specification of reference oil separator was designed based on an oil separator which is used for commercial multi heat pump system. Compare to the reference oil separator, fat and tall oil separators were designed to measure the efficiency and pressure drop with respect to diameter and length of oil separator. Oil loop consists of oil level sensor, gear pump and mass flow meter. Oil level sensor was used to measure the mass flow rate of unseparated oil at the test oil separator. Mass flow rate of oil was controlled by gear pump and mass flow rate and density of oil were measured by mass flow/densimeter. Oil separator is usually installed at the outlet of compressor, and this means that the fluids which enter the oil separator is high temperature and high pressure condition. The oil in the pipe of oil loop and level sensor has to be maintained as high temperature and high pressure condition. So, pipe of oil loop and level sensor were wrapped in line heater. Temperature of line heater was controlled by using thyristor power regulator (TPR) and digital indicating temperature controller.

T-type thermocouples and pressure sensors were attached some points of experimental apparatus and a differential pressure transmitter was installed to measure the pressure drop at test oil separator. Oil injection port

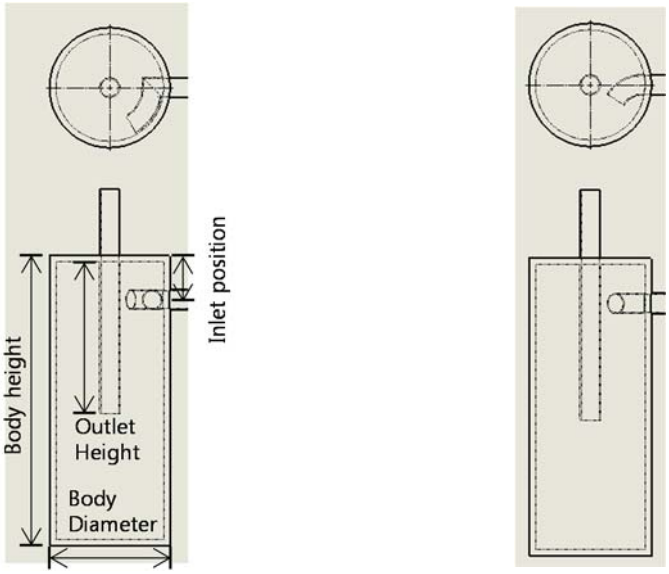

(a) Type 1 (b) Type 2

Fig. 4.2 Design of oil separator

Table 4.1 Specification of reference oil separator

Parameter	Reference model
BD (mm)	85.0
BH (mm)	85.0
Inlet OD (mm)	220.0
Inlet ID (mm)	15.9
INP (mm)	14.1
Outlet OD (mm)	30.0
Outlet ID (mm)	15.9
OH (mm)	14.1
IC	Tp1 and Tp2

Table 4.2 Normalized specification of various oil separators

Parameter	Refer	DS1	DS2	DS3	DS4	DS5
BD*	1.00	1.20	1.41	1.00	1.00	0.55
BH*	1.00	1.00	1.00	1.18	1.36	0.59
Inlet OD*	1.00	1.00	1.00	1.00	1.00	0.80
Inlet ID*	1.00	1.00	1.00	1.00	1.00	0.79
INP*	1.00	1.00	1.00	1.00	1.00	0.47
Outlet OD*	1.00	1.00	1.00	1.00	1.00	0.80
Outlet ID*	1.00	1.00	1.00	1.00	1.00	0.79
OH*	1.00	1.00	1.00	1.00	1.00	0.72
IC	Tp1 and Tp2	Tp1	Tp1	Tp1	Tp1	Tp2

is installed at 2 m away from test oil separator.

Most of the experimental components for measuring the efficiency and pressure drop of oil separator were the same with those for measuring the oil retention amount. Only level sensor was changed because the pressure limit of former level sensor is 1961 kPa. Level sensor which the pressure limit is 2942 kPa and temperature limit is 100°C was used.

In a typical heat pump system, gas phase refrigerant from a compressor becomes a liquid phase when it passes through a condenser. Mass flow meter measures the mass flow rate of fluid which is single phase precisely. So the mass flow meter is usually installed at liquid line to measure the mass flow rate accurately because there's always a small amount of oil from compressor. However refrigerant emits heat energy to secondary fluid at condenser, and the energy capacity becomes higher as the mass flow rate of refrigerant increases. A chiller was used to maintain the temperature of secondary fluid in this research, and it was possible to predict that the experiment can't be conducted at high mass flow rate of refrigerant condition due to the limitation of the chiller capacity. So the refrigerant from compressor was not condensed and just cooled down at the heat exchanger. The energy consumption at chiller was reduced and the experiment was conducted under high mass flow rate condition. However, there is a

disadvantage of this method. Mass flow meter has to be installed at gas line of refrigerant because the refrigerant exists as a gas phase in all components of experimental apparatus. The accuracy of mass flow meter at gas line of refrigerant decreases because the measurement of the gas phase is less accurate than that of liquid phase and small amount of oil in gas phase refrigerant has a negative influence on the mass flow meter.

4.2.2 Experimental procedure

The efficiency and pressure drop of oil separator were measured with respect to mass flow rate of refrigerant and liquid circulation ratio (LCR). Liquid circulation ratio is defined as a ratio of mass flow rate of liquid mixture which is oil and solute refrigerant to mass flow rate of total fluids which include refrigerant and liquid mixture at the inlet of oil separator. Mass flow rate of refrigerant and liquid mixture which is oil and solute refrigerant were controlled by the speed control box of the compressor and gear pump, respectively. Pressure and temperature at the inlet of oil separator were controlled by the opening of expansion device and mass flow rate of secondary fluid of heat exchanger. Before the system became a steady-state condition, the refrigerant and liquid mixture circulated the refrigerant loop

and the oil loop. While the liquid mixture circulated the oil loop, temperature of liquid mixture was maintained as a set temperature by the line heater. Temperature and pressure at the inlet of oil separator were set as 70.0℃ and 2611.3 kPa or 79.9℃ and 2809.8 kPa in this study. When the system became a steady-state, the liquid mixture in level sensor was injected into the refrigerant loop. Refrigerant and liquid mixture passed through the pipe which was length of 2 m and entered the test oil separator. Refrigerant and most of injected liquid mixture were separated at the oil separator, and refrigerant and small amount of unseparated liquid mixture circulated refrigerant loop and separated liquid mixture entered level sensor. During the injection, mass flow rate and density of injected liquid mixture were measured and volume of liquid mixture in level sensor was measured.

4.2.3 Data reduction

Fig. 4.3 shows an experimental result of reference oil separator under mass flow rate of 90 gs^{-1}, liquid circulation ratio of 3% condition. When system was a steady-state, liquid mixture was injected and the volume of liquid mixture in level sensor was measured for about 20 minutes. After finishing injection, the system was operated for about 1 hour to clean up the

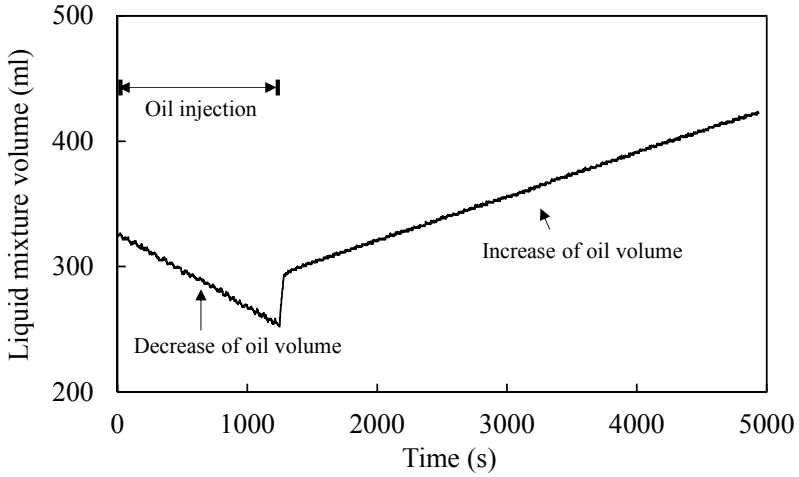

Fig. 4.3 Experimental results (MFR=90 gs^{-1}, LCR=3%, reference model)

pipe and oil separator and measure the amount of liquid mixture from the compressor. As shown in Fig. 4.3, the volume of liquid mixture in level sensor decreased while the liquid mixture was injected and then increased after finishing the injection. Although two oil separators were installed at the outlet of compressor, small amount of liquid mixture was unseparated at the oil separators. The small amount of liquid mixture entered the test oil separator with gas phase refrigerant and was separated. This separated liquid mixture entered the level sensor, so the volume of liquid mixture in level sensor increased after finishing the injection. If the efficiency of test oil separator was 100%, the volume of liquid mixture in level sensor would increase during the injection because the amount of liquid mixture which entered the level sensor is the summation of the amount of liquid mixture which came out from level sensor and compressor. However, the efficiency of test oil separator was not 100%, so the volume of liquid mixture in level sensor decreased during the injection. From the result of Fig. 4.3, the gradients of the volume of liquid mixture in level sensor during the injection and after finishing the injection were calculated. Then, mass changes of liquid mixture per second were obtained by multiplying the density of liquid mixture by the gradients of volume of liquid mixture. As mentioned before, the oil separator efficiency is defined as equation (4.1).

$$\varepsilon = \frac{\dot{m}_{separated}}{\dot{m}_{injected}} = \frac{\dot{m}_{injected} - \dot{m}_{unseparated}}{\dot{m}_{injected}} = 1 - \frac{\dot{m}_{unseparated}}{\dot{m}_{injected}} \quad (4.1)$$

The mass flow rate of injected liquid mixture was measured by mass flow meter. The mass flow rate of liquid mixture which was unseparated at the test oil separator can be obtained by subtracting the mass change per second of liquid mixture in level sensor during the injection from that in level sensor after finishing the injection. This can be expressed as following equation (4.2).

$$\dot{m}_{unseparated} = \dot{m}_{increase} - \dot{m}_{decrease} \quad (4.2)$$

By the result of equation (4.2), the efficiency in equation (4.1) was calculated.

To measure pressure drop of oil separator during the injection, a differential pressure transmitter was used.

4.2.4 Uncertainty of measurements

The experimental results always contain uncertainties because errors of the measurements exist. Moffat (1988) suggested an equation to calculate the uncertainty of overall measurement. This equation is described as in equation (4.3).

$$\delta R = \left\{ \sum_{i=1}^{N} \left(\frac{\partial R}{\partial X_i} \delta X_i \right)^2 \right\}^{1/2} \tag{4.3}$$

δR and δX_i are the uncertainty of overall measurement and each variable, respectively.

The efficiency of oil separator was calculated by the equation (4.1). This study measured $\frac{\dot{m}_{unseparated}}{\dot{m}_{injected}}$, so uncertainty of this measurement was considered. The mass flow rate of injected liquid mixture, volume change per second during the injection and after finishing the injection and density of liquid mixture were used to calculate the efficiency of test oil separator. The overall uncertainty of the measurement in the efficiency of oil separator is expressed in equation (4.4).

$$\delta R_{EOS} = \left\{ \sum_{i=1}^{4} \left(\frac{\partial R_{EOS}}{\partial X_i} \delta X_i \right)^2 \right\}^{1/2} \tag{4.4}$$

Each uncertainty of mass flow rate of injected liquid mixture, volume changes per second during the injection and after finishing the injection and density of liquid mixture were obtained from the accuracies of mass flow meter, level sensor and densimeter. The average and maximum uncertainty of the overall measurement were 2.2% and 11.8%, respectively.

4.3 Results and discussion

The experiment was conducted for oil separators of seven different designs with respect to mass flow rate of refrigerant and liquid circulation ratio. Most of experiment was conducted under temperature of 79.9℃ and pressure of 2809.8 kPa. In case of reference model with inlet configuration of type 1, the experiment was conducted when temperature and pressure were 70.0℃ and 2611.3 kPa. Figs. 4.4 ~ 4.11 show the separation efficiency of each oil separator.

When the gas phase refrigerant and liquid mixture enter the oil separator, the liquid mixture is sprayed out in fine droplets. Centrifugal force which is caused by the gas phase refrigerant pushes the droplets to the wall of oil separator, and drag force affects the droplets to the opposite direction of centrifugal force. If a droplet reaches to the wall, the droplet is separated, and if droplet don't reach to the wall, the droplet is unseparated. Centrifugal force increases as the angular velocity of gas phase refrigerant goes up. In case of drag force, the drag force per unit particle mass is expressed as following equation (4.5).

$$F_D = \frac{18\mu C_D \,\mathrm{Re}}{24\rho_{oil} d_{oil}^2}\left(u - u_p\right) \tag{4.5}$$

In equation (4.5), C_D is drag coefficient and is a function of Reynolds

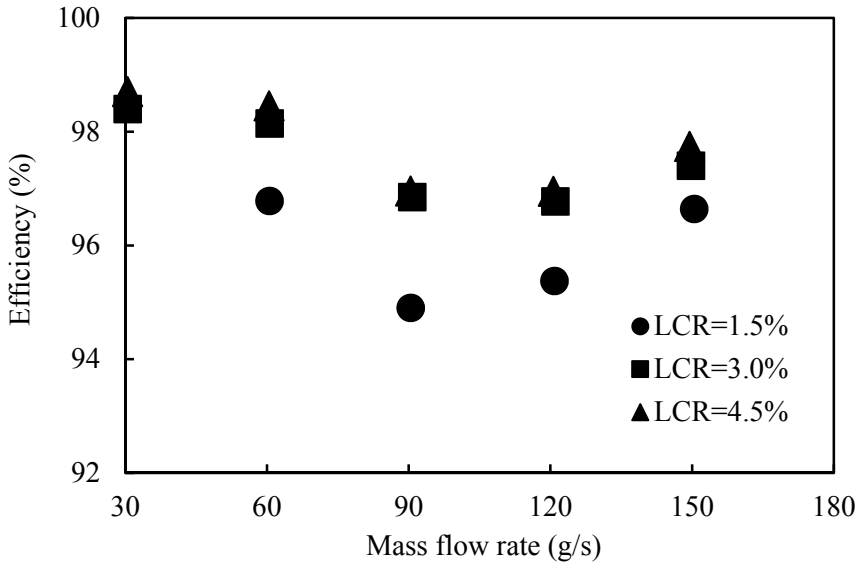

Fig. 4.4 Separation efficiency of reference model (inlet configuration of type 1, 2611.3 kPa and 70.0℃ condition)

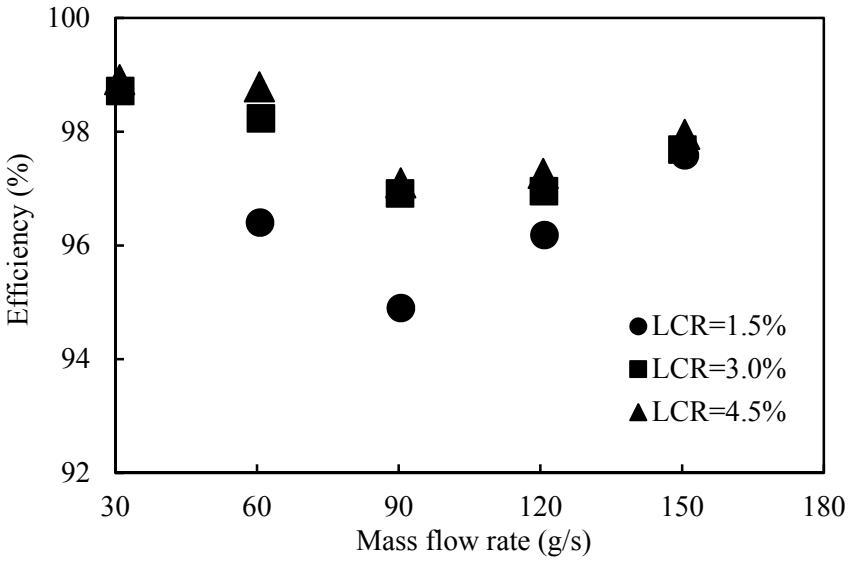

Fig. 4.5 Separation efficiency of reference model (inlet configuration of type 1, 2809.8 kPa and 79.9℃ condition)

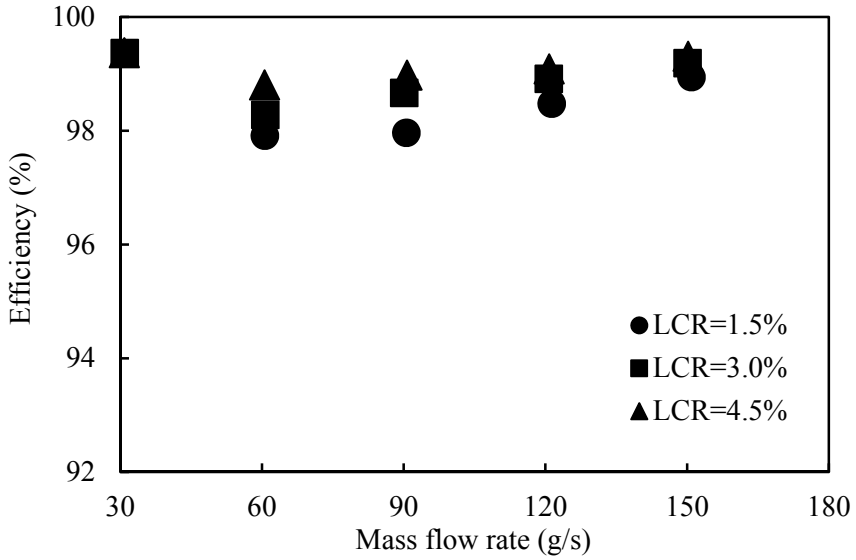

Fig. 4.6 Separation efficiency of design 1 model (inlet configuration of type 1, 2809.8 kPa and 79.9℃ condition)

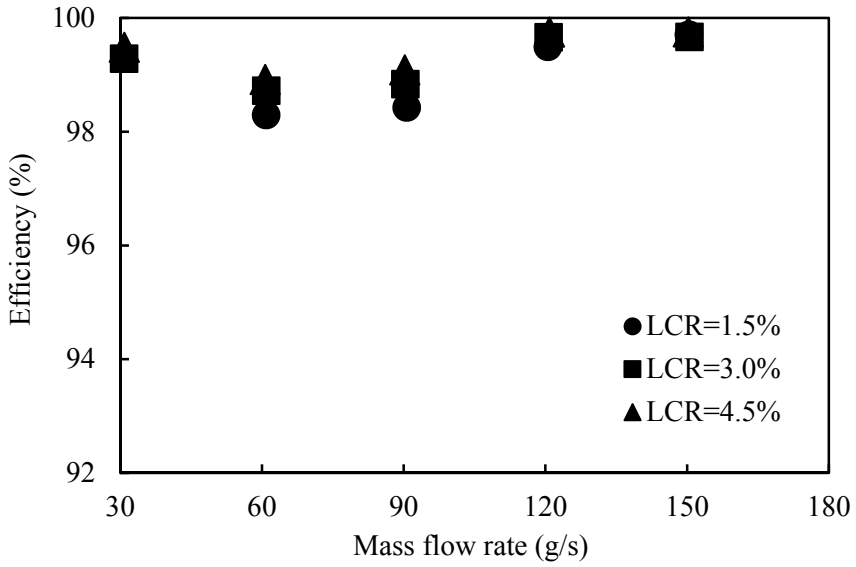

Fig. 4.7 Separation efficiency of design 2 model (inlet configuration of type 1, 2809.8 kPa and 79.9℃ condition)

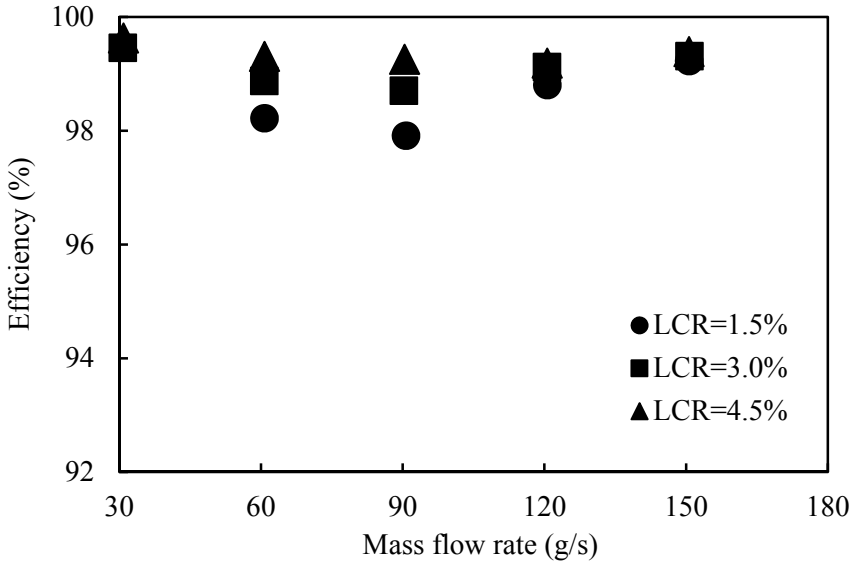

Fig. 4.8 Separation efficiency of design 3 model (inlet configuration of type 1, 2809.8 kPa and 79.9℃ condition)

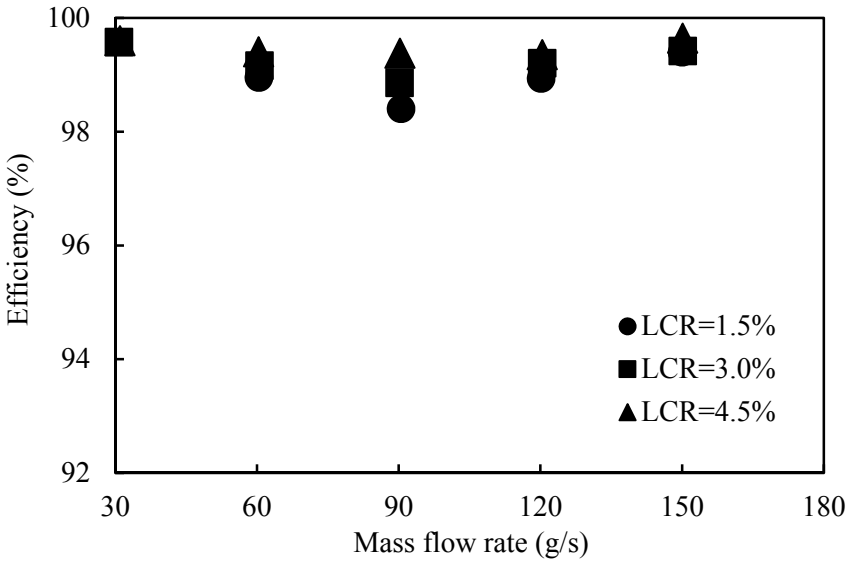

Fig. 4.9 Separation efficiency of design 4 model (inlet configuration of type 1, 2809.8 kPa and 79.9℃ condition)

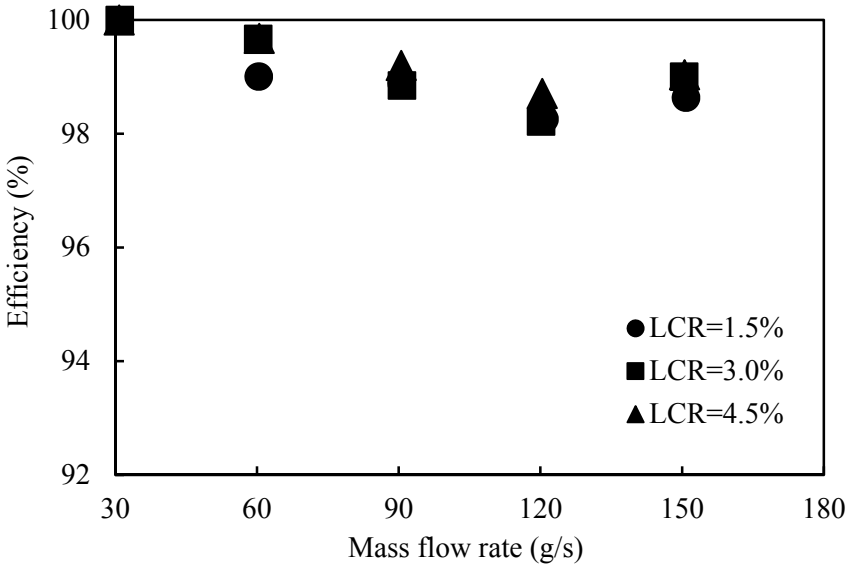

Fig. 4.10 Separation efficiency of reference model (inlet configuration of type 2, 2809.8 kPa and 79.9℃ condition)

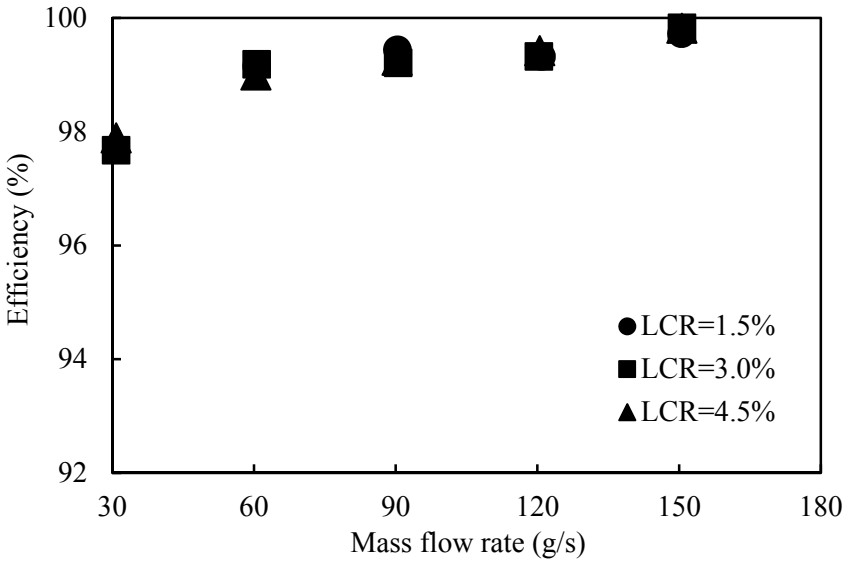

Fig. 4.11 Separation efficiency of design 5 model (inlet configuration of type 2, 2809.8 kPa and 79.9℃ condition)

number. The drag force per unit particle mass reduces as the droplet size increases. Murakami *et al.* (2006) suggested an experimental correlation for predicting the droplet size distribution of liquid mixture which is oil and solute refrigerant in the oil separator. In this study, they showed that the droplet size decreases as mass flow rate of gas phase refrigerant goes up under the same oil circulation ratio condition. Hede *et al.* (2008) reviewed on the studies for two fluid spray atomization. In this study, they showed that the droplet size decreases as mass flow rate of gas phase increases under the same air/liquid mass ratio condition. In addition, they showed that the droplet size goes up as mass flow rate of liquid increases under the same mass flow rate of gas phase condition. The separation efficiency increases under high centrifugal force and low drag force condition. As the mass flow rate of gas phase refrigerant increases, the centrifugal force goes up and the drag force per unit mass also increases because of reduction of droplet size. That is, positive effect which is increment of centrifugal force and negative effect which is increment of drag force occur at the same time as the mass flow rate of gas phase refrigerant increases. If the effect of centrifugal force is dominant, the separation efficiency will increase as the mass flow rate of gas phase refrigerant increases. If the effect of drag force is dominant, the separation efficiency will decrease as the mass flow rate of gas phase

refrigerant increases.

Figs. 4.4 ~ 4.5 show the separation efficiency of reference model with inlet configuration of type 1, and each figure shows the experimental results under temperature and pressure of 70.0℃, 2611.3 kPa and 79.9℃, 2809.8 kPa. The separation efficiency diminishes as the mass flow rate increases until the mass flow rate of 90 gs^{-1}, thereafter, the separation efficiency goes up with the increment of mass flow rate. From the results, it is possible to presume that the rise of drag force mainly affects the separation efficiency under low mass flow rate condition and the increment of centrifugal force is dominant under high mass flow condition. The separation efficiency goes up as the liquid circulation ratio increases because high liquid circulation ratio denotes large droplet size which causes low drag force. By comparing the results of Figs. 4.4 and 4.5, it is possible to know that the separation efficiency is slightly higher under the experimental condition of Fig. 4.5. Compare to the condition of Fig. 4.4, density of gas phase refrigerant and viscosity of liquid mixture which is oil and solute refrigerant increase. As the density of gas phase refrigerant increases the velocity of gas phase refrigerant reduces under the same mass flow rate condition, and this means reduction of centrifugal force. In case of increment of liquid viscosity, Hede *et al.* (2008) showed that high liquid viscosity denotes large droplet size.

That is, drag force per unit mass diminishes as the liquid viscosity increases. Therefore, centrifugal and drag forces per unit mass of experimental condition for Fig. 4.5 are relatively lower than those for Fig. 4.4. From the results of Figs. 4.4 and 4.5, it can be surmised that the effect of reduction of drag force more affects the separation efficiency compare to the decrement of centrifugal force.

Figs. 4.6 and 4.7 show the separation efficiency of the oil separators of design 1 and design 2. Body diameters of design 1 and design 2 are larger than body diameter of reference model about 20% and 41%, respectively, and the other specifications are the same. Figs. 4.5 ~ 4.6 show that large body diameter denotes high separation efficiency. Inlet pipe diameters of each separator are equal, so the droplet size distribution and initial velocity of gas phase are the same. Liquid mixture droplets are separated when gas phase refrigerant circulates and moves downward at the near the wall of oil separator. As the body diameter of oil separator increases, the distance that gas phase refrigerant travels becomes longer because gas phase refrigerant move around the wall. So the liquid mixture droplets which are not separated under relatively small body diameter condition are separated during the additional travel distance under large body diameter condition. Therefore the separation efficiency goes up as body diameter becomes larger.

Figs. 4.8 and 4.9 show the separation efficiency of oil separators of design 3 and design 4. Body heights of design 3 and design 4 are longer than body height of reference model about 18% and 36%, respectively, and the other specifications are the same. From the results of Figs. 4.5, 4.8 and 4.9, it was confirmed that the separation efficiency is high under tall body height condition. The gas phase refrigerant more circulates along the wall as the height of separator increases. So liquid mixture droplets which are not separated under relatively small body height condition are separated during the additional circulation under tall body height condition. Thus the separation efficiency of taller body height condition is high.

Figs. 4.10 and 4.11 show the separation efficiency of reference model with inlet configuration of type2 and design 5. In case of the inlet configuration of type 1, the gas phase refrigerant and liquid mixture spray from inlet pipe and circulate around the wall of oil separator. In case of the inlet configuration of type 2, however, the gas phase refrigerant and liquid mixture spray from inlet pipe and hit the wall of oil separator and then circulate around the wall. Figs. 4.5 and 4.10 show that the separation efficiency of type 2 is higher than that of type 1. From this results, it is possible to surmise that large amount of liquid mixture is separated when the fluids which are gas phase refrigerant and liquid mixture hit the oil

separator's wall when the fluids spray from the inlet pipe. Fig. 4.11 shows the separation efficiency of small oil separator. The velocity of gas phase refrigerant in oil separator of design 5 is higher than that of other designs because of relatively small diameter of inlet pipe. This denotes high centrifugal force. As the velocity of gas phase refrigerant increases, as mentioned before, the drag force per unit mass increases because of small droplet size. As shown in other experimental results, the change of centrifugal force mainly affects the separation efficiency under high velocity condition. So, in case of oil separator of design 5, increment of centrifugal force largely affects the separation efficiency compare to the increment of drag force because the speed of refrigerant is relatively high due to small inlet pipe diameter. Thus, the separation efficiency of small size oil separator goes up as the mass flow rate of refrigerant increases.

Fig. 4.12 shows the pathlines of gas phase refrigerant in the oil separator. The gas phase refrigerant circulates and flows downward near the wall of oil separator until it reaches to the bottom of oil separator. When it reaches to the bottom of oil separator, circulation near the wall converts to the inner circulation near the outlet pipe. With consideration of conservation of angular momentum during this conversion, equation (4.6) can be applied.

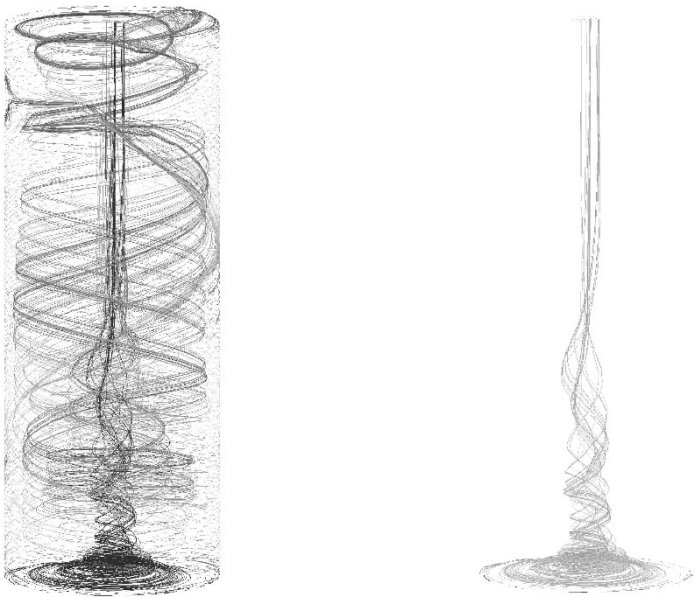

(a) Pathlines in the oil separator

(b) Pathlines near the bottom and outlet pipe of oil separator

Fig. 4.12 Pathlines of gas phase refrigerant in cyclone separator

$$\vec{r}_1 \times (m\vec{u}_1) = \vec{r}_2 \times (m\vec{u}_2) \tag{4.6}$$

$\vec{r}_1$, $\vec{u}_1$, $\vec{r}_2$ and $\vec{u}_2$ denote radius and tangential velocity of outer circulation and radius and tangential velocity of inner circulation. With Bernoulli equation which is $\frac{P}{\rho} + gh + \frac{1}{2}u^2 = C$, it is possible to know that the pressure of the inner circulation is lower than that of outer circulation due to the transformation of energy which is from pressure to velocity. As shown in Fig. 4.12, the inner circulation dissipates at near the outlet pipe. If there is no wall friction, dissipated energy is $\frac{1}{2}\rho u_2^2$. If the wall friction is very large, outer circulation is dissipated by the wall and the dissipated energy becomes $\frac{1}{2}\rho u_1^2$. Because u_1 is smaller than u_2, pressure drop under high wall friction is lower than pressure drop under low wall friction.

Figs. 4.13 ~ 4.20 show the pressure drop results of various oil separators. As shown in these results, the pressure drop diminishes as the liquid circulation ratio increases. High liquid circulation ratio denotes large amount of liquid mixture in oil separator, and liquid mixture is a resistance to the gas phase refrigerant. As the liquid circulation ratio goes up, therefore, the frictional loss during the outer circulation increases and energy dissipation of inner circulation decreases. As mentioned above, effect of

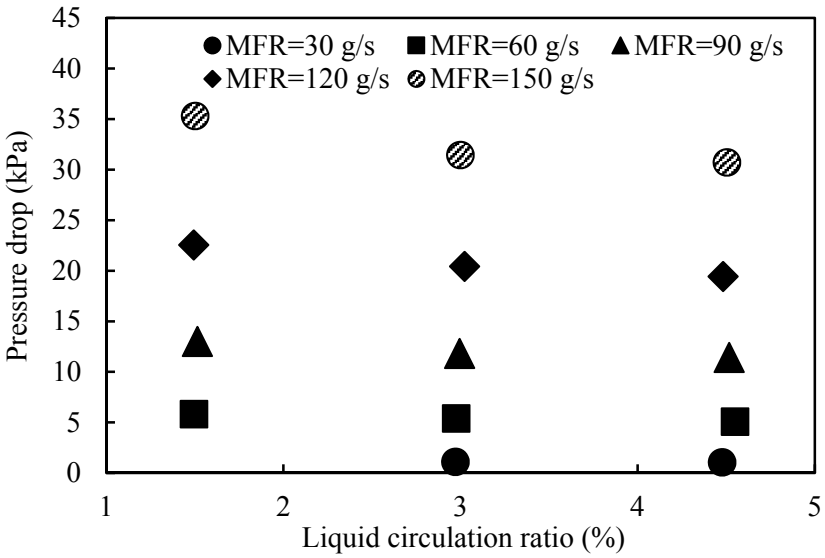

Fig. 4.13 Pressure drop of reference model (inlet configuration of type 1, 2611.3 kPa and 70.0°C condition)

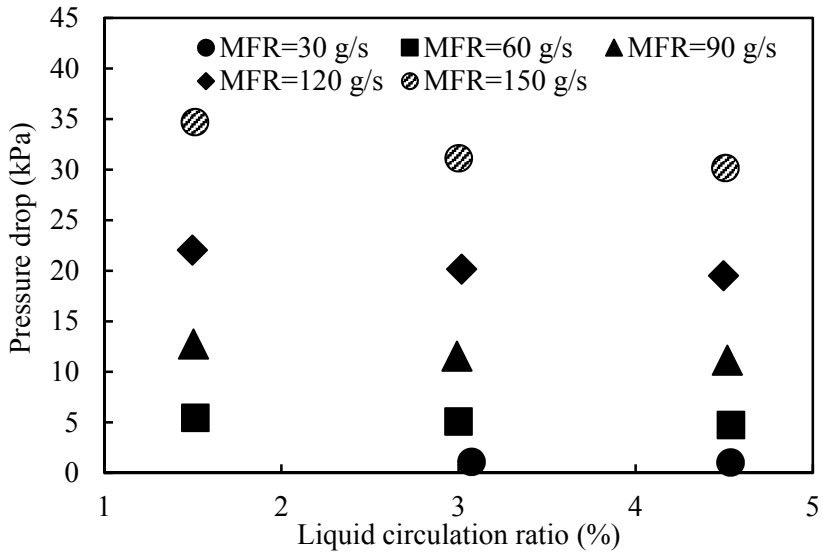

Fig. 4.14 Pressure drop of reference model (inlet configuration of type 1, 2809.8 kPa and 79.9°C condition)

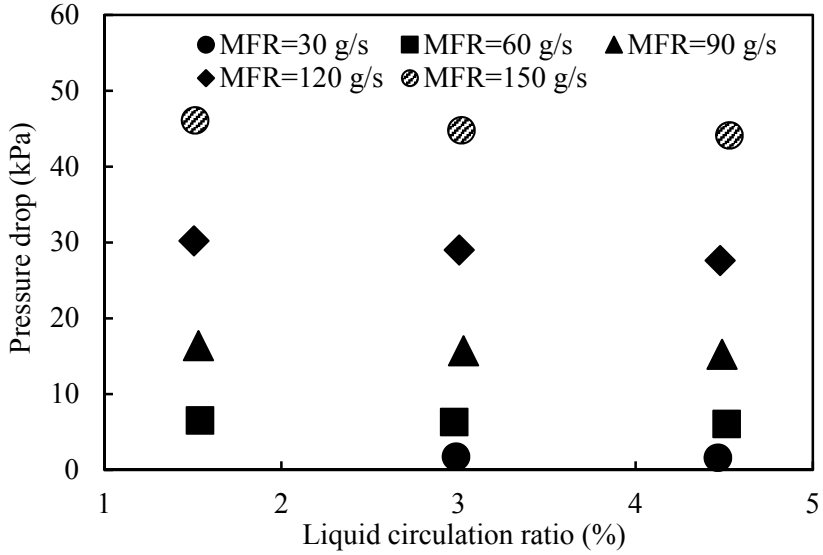

Fig. 4.15 Pressure drop of design 1 model (inlet configuration of type 1, 2809.8 kPa and 79.9°C condition)

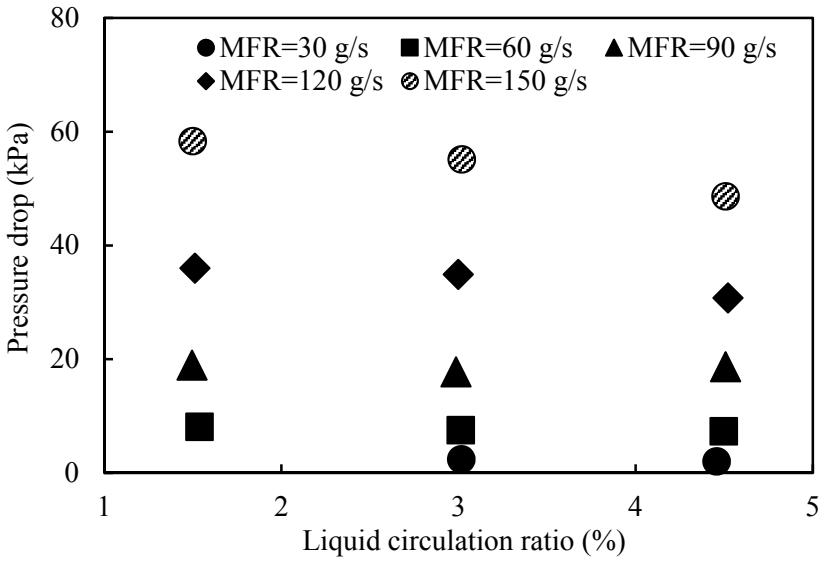

Fig. 4.16 Pressure drop of design 2 model (inlet configuration of type 1, 2809.8 kPa and 79.9°C condition)

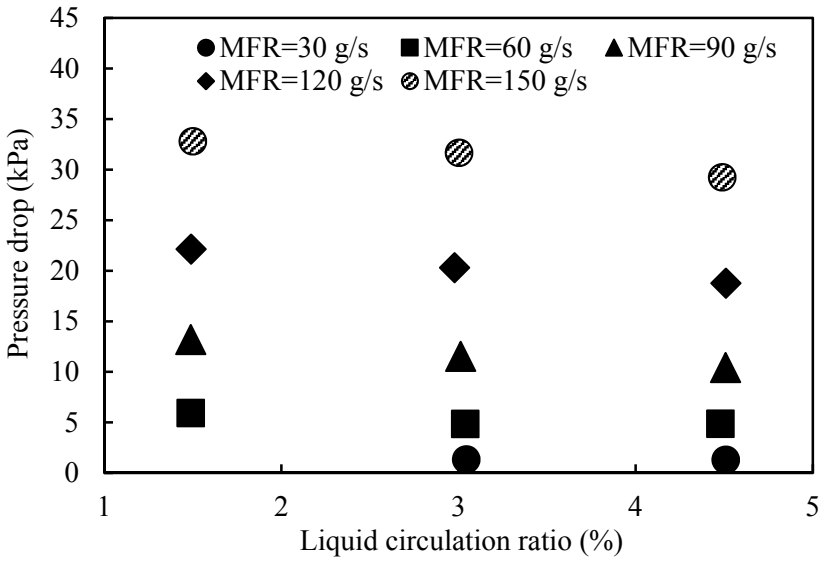

Fig. 4.17 Pressure drop of design 3 model (inlet configuration of type 1, 2809.8 kPa and 79.9°C condition)

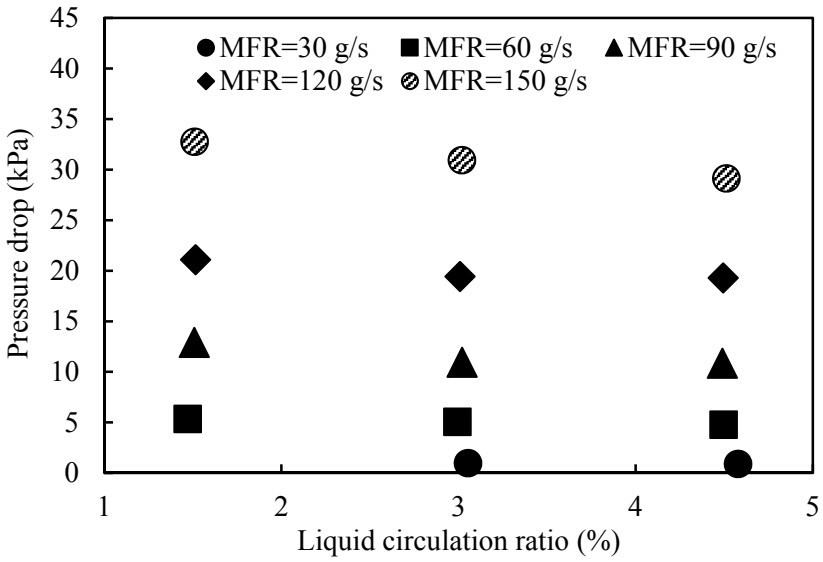

Fig. 4.18 Pressure drop of design 4 model (inlet configuration of type 1, 2809.8 kPa and 79.9°C condition)

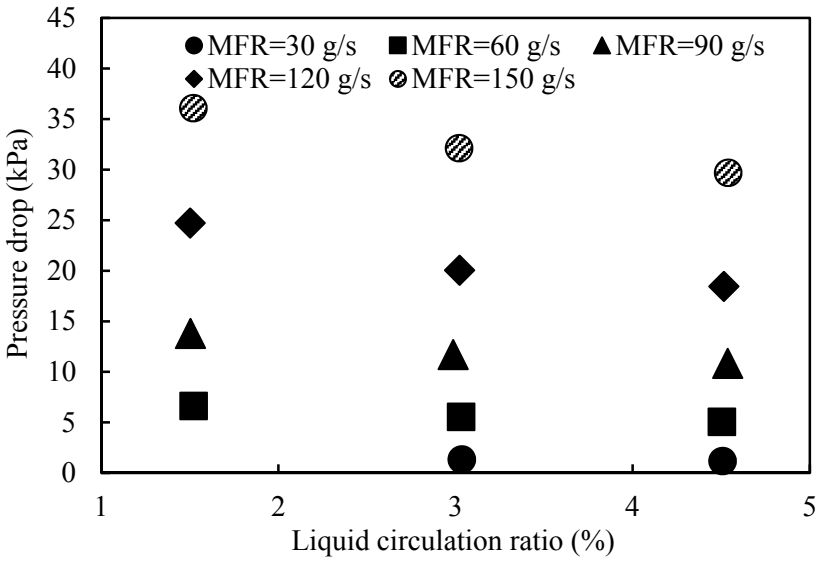

Fig. 4.19 Pressure drop of reference model (inlet configuration of type 2, 2809.8 kPa and 79.9°C condition)

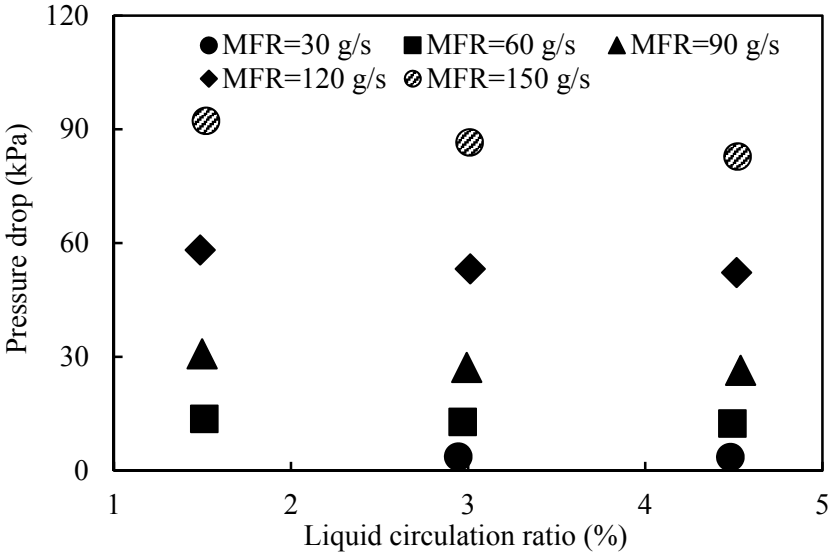

Fig. 4.20 Pressure drop of design 5 model (inlet configuration of type 2, 2809.8 kPa and 79.9°C condition)

energy dissipation at near the outlet pipe is larger than energy loss during the outer circulation. So the pressure drop is low under high liquid circulation ratio condition.

In Figs. 4.13 and 4.14, pressure drop under temperature and pressure of 70.0℃ and 2611.3 kPa is slightly higher than those of 79.9℃ and 2809.8 kPa. Gas phase velocity mainly affects the pressure drop, and pressure drop rises as the gas phase velocity increases. As mentioned before, density of gas phase refrigerant under temperature and pressure of 70.0℃ and 2611.3 kPa is slightly lower than those of 79.9℃ and 2809.8 kPa. That is, velocity of refrigerant of Fig. 4.13 is slightly higher than that of Fig. 4.14.

Figs. 4.14 ~ 4.16 show pressure drop results at the oil separators with different body diameters. Results show that large body diameter denotes high pressure drop. Outer circulation converts to the inner circulation at the bottom of oil separator. From equation (4.6), the tangential velocity of inner circulation is proportional to the radius of outer circulation. That is, dissipation energy at near the outlet pipe goes up as the radius of outer circulation becomes longer. The radius of outer circulation is almost the same with the radius of body diameter. Thus, high pressure drop occurs at the oil separator of large body diameter.

Figs. 4.14, 4.17 and 4.18 show pressure drop results at the oil separators with different body heights. Theoretically, the tangential velocity of outer circulation diminishes as the gas phase refrigerant circulates and flow downward near the wall. So tangential velocity of outer circulation becomes lower as the body height goes up, and the dissipation energy at near the outlet pipe reduces. Therefore, the pressure drop is low under tall body height condition. In real system, however, pressure drop slightly reduces or almost constant as the body height becomes taller. From the results, it is possible to surmise that reduction of tangential velocity at the outer circulation is not enough to affect the pressure drop.

Figs. 4.19 and 4.20 show the pressure drop results of oil separators with inlet configuration of type 2. In case of Fig. 4.19, pressure drop is similar to the pressure drop of reference model with inlet configuration of type 1. Although the energy loss at near the inlet pipe changes with respect to the inlet configuration, this change almost does not affect the pressure drop. Fig. 4.20 shows the pressure drop at the small oil separator. Compare to the other oil separator, pressure drop is very high. The velocity of gas phase refrigerant in small oil separator is high due to the small diameter of inlet pipe. In addition, pressure drop at the inlet and outlet pipe also increases compare to the other oil separator because of small diameter.

4.4 Modeling of the flow characteristics in oil separator

Models for predicting the efficiency and pressure drop of the oil separator are necessary to design the optimal oil separator for various operating condition. There have been many studies on the modeling of cyclone separator. Among them, Muschelknautz method is famous. Based on this method, various correlations for predicting efficiency and pressure drop of cyclone separator were proposed by many studies. Most of the studies focused on the gas-solid cyclone separator, but Muschelknautz and Dahl (1994) proposed modeling for predicting the performance of vapor and liquid cyclone separator. Hoffmann and Stein (2007) reviewed and introduced the model of Muschelknautz and Dahl (1994).

Fig. 4.21 shows the schematic of oil separator with some notations for modeling of oil separator. Generally, the efficiency of cyclone separator for a specific particle diameter is expressed as following equation (4.7).

$$\eta = \frac{1}{1+\left(\frac{d_{50}}{d_i}\right)^m} \tag{4.7}$$

d_{50} and d_i denote cut size and particle size, respectively. In case of gas-liquid cyclone separator, Hoffmann and Stein (2007) suggested ‘m’ of 3 in

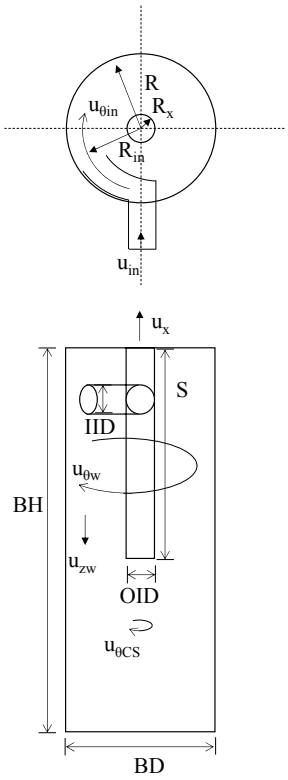

Fig. 4.21 Schematic of the oil separator with various notations for modeling

equation (4.7). In cyclone separator, 'Mass loading' occurs when inlet loading is larger than the limit loading. Inlet loading is a mass ratio of mass of solid or liquid to mass of gas at the inlet of cyclone. Limit loading is calculated by empirical correlation which is described in equation (4.8)

$$c_{oL} = 0.0078\left(\frac{d_{50}}{d_{mm}}\right)\left(10c_o\right)^k$$

(4.8)

In equation (4.8), k is defined as following equation (4.9).

$$k = 0.07 - 0.16\ln(c_o) \tag{4.9}$$

If the mass loading does not occur, the efficiency of cyclone separator is obtained by equation (4.10).

$$\eta = \sum_{i=1}^{N} \eta_i \times \Delta MF_i \tag{4.10}$$

If the mass loading occurs, the separation in cyclone separator becomes two-stages which include immediate separation at near the inlet pipe and separation during the circulation of gas phase in the separator. In this case, the efficiency of cyclone separator is calculated by equation (4.11).

$$\eta = \left(1 - \frac{c_{oL}}{c_o}\right) + \frac{c_{oL}}{c_o}\sum_{i=1}^{N} \eta_i \times \Delta MF_i \tag{4.11}$$

The liquid is sprayed out in various sizes of droplet, so droplet size distribution is necessary to calculate the efficiency of oil separator. Murakami *et al.* (2006) proposed experimental dimensionless droplet size

distribution which is a gamma distribution in an oil separator. The dimensionless droplet size is defined as d/d_1.

Based on the experimental results of the oil separator with inlet configuration of type 1, empirical correlations for d_{50} and d_1 are suggested as following equations (4.12) and (4.13).

$$d_{50} = 5.18\mu^{0.375}\rho^{0.25}u_{rCS}^{0.875}\left(\frac{(\rho_p-\rho)u_{\theta CS}^2}{R_x}\right)^{-0.625}\left(\frac{BD_{Refer}}{BD}\cdot\frac{BH_{Refer}}{BH}\right)^{0.97} \quad (4.12)$$

$$d_1 = 4.02\cdot10^{-6} + 2.04\cdot10^{-5}\cdot LCR^{0.52}\cdot \mathrm{Re}^{-0.04}\cdot\frac{v_{liquid}}{v_{Refer}} \quad (4.13)$$

Hoffmann and Stein (2007) showed Muschelknautz method, and described a correlation for $u_{\theta CS}$ and $u_{\theta w}$ in Fig. 4.21. Based on the equations from (4.7) to (4.13), the efficiency of oil separator is predicted. The predicted results are compared to the experimental results, and Fig. 4.22 shows the comparison results. As shown in Fig. 4.22, maximum error between predicted and experimental values is less than 2% and mean absolute percentage error is 0.4%.

Pressure drop occurs at the inlet pipe, outer circulation in separator, near the outlet pipe and outlet pipe. In case of inlet pipe, gas phase refrigerant and liquid mixture flows in the pipe and the flow pattern is annular flow as shown in chapter 3. So equations (2.8) to (2.10) were used to predict the pressure drop at the inlet pipe. In case of outlet pipe, most of

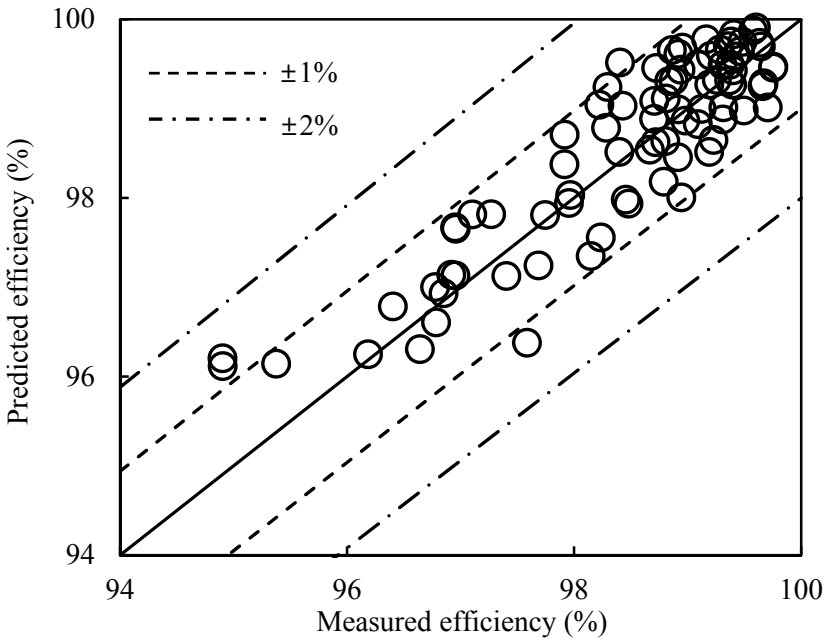

Fig. 4.22 Comparison of experimental and predicted efficiency of oil separator with inlet configuration of type 1

liquid mixture is separated at the oil separator and very small amount of liquid mixture flows with gas phase refrigerant. This case is similar to the single gas phase flow. Thus the pressure drop at the outlet pipe is calculated by the friction factor correlation of petukhov. Pressure drops during the outer circulation and at near the outlet pipe are obtained by subtracting calculated pressure drops at the inlet and outlet pipe from measured pressure drop at the oil separator. Hoffmann and Stein (2007) described correlation for predicting pressure drop at the cyclone body and near the outlet pipe. Based on the previous correlation, this study suggested a correlation which is shown in equation (4.14) for predicting the pressure drop at drop at the cyclone body and near the outlet pipe.

$$\Delta P = \left(\frac{0.38 f A_R \rho_g \left(u_{\theta w} u_{\theta cs} \right)^{1.71}}{2Q} + \frac{1}{2}\left(1 + \left(\frac{u_{\theta cs}}{u_x} \right)^{0.76} \right)\left(\frac{1}{2}\rho_g u_x^2 \right) \right)\left(\frac{BD}{BD_{Refer}} \right)^{1.35} \quad (4.14)$$

Some exponents and coefficients in equation (4.14) were obtained based on the experimental results. Fig. 4.23 shows the comparison of experimental and predicted pressure drop at oil separator with inlet configuration of type 1, and mean absolute percentage error is 7.8%.

In case of oil separators with inlet configuration of type 2, the inlet diameters are different and this feature was added to the correlation. In equations (4.12) and (4.13), term of dimensionless inlet diameter was added

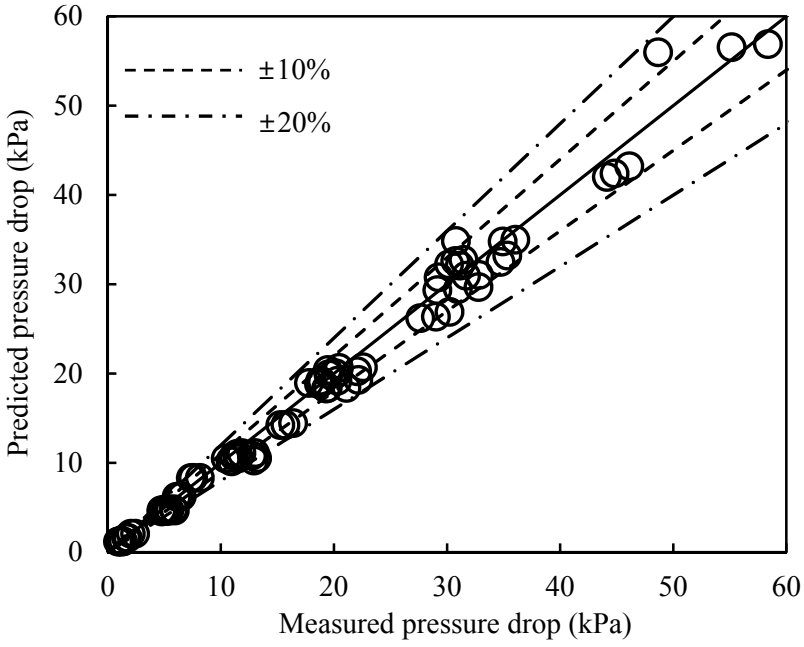

Fig. 4.23 Comparison of experimental and predicted pressure drop of oil separator with inlet configuration of type 1

and new equations for inlet configuration of type 2 are described in equations (4.15) and (4.16).

$$d_{50} = 5.18\mu^{0.375}\rho^{0.25}u_{rCS}^{0.875}\left(\frac{(\rho_p-\rho)u_{\theta CS}^2}{R_x}\right)^{-0.625}\left(\frac{BD_{Refer}}{BD}\cdot\frac{BH_{Refer}}{BH}\right)^{0.97}\left(\frac{IID}{IID_{refer}}\right)^{11.72} \tag{4.15}$$

$$d_1 = 1.17\cdot10^{-6} + 6.70\cdot10^{-3}\cdot LCR^{0.36}\cdot \mathrm{Re}^{-0.48}\cdot\frac{v_{liquid}}{v_{Refer}}\cdot\left(\frac{IID}{IID_{Refer}}\right)^{26.67} \tag{4.16}$$

Compare to the inlet configuration of type 1, the gas phase refrigerant and liquid mixture hit the wall after spraying out from inlet pipe. This means the effect of mass loading goes up, so the correlation for limit loading slightly changes. Equation (4.17) shows the limit loading equation for inlet configuration of type 2.

$$c_{oL} = 0.0013\left(\frac{d_{50}}{d}\right)(10c_o)^k \tag{4.17}$$

Exponents and coefficients of pressure drop correlation were slightly changed based on the experimental data of the oil separators with inlet configuration of type 2 and a term of body height was added. Pressure drop correlation for type 2 is shown in equation (4.18).

$$\Delta P = \left(\frac{0.078\,fA_R\rho_g\left(u_{\theta w}u_{\theta cs}\right)^{1.88}}{2Q} + \left(0.5+3.95\left(\frac{u_{\theta cs}}{u_x}\right)^{0.5}\right)\left(\frac{1}{2}\rho_g u_x^2\right)\right)\left(\frac{BD}{BD_{Refer}}\cdot\frac{BH_{Refer}}{BH}\right)^{1.06} \tag{4.18}$$

From these equations, the efficiency and pressure drop of oil separator with inlet configuration of type 2 were predicted. Figs. 4.24 and 4.25 show the comparisons between predicted and measured efficiency and pressure drop of oil separator with inlet configuration of type 2. Mean absolute percentage errors of efficiency and pressure drop are 0.3% and 7.6%, respectively.

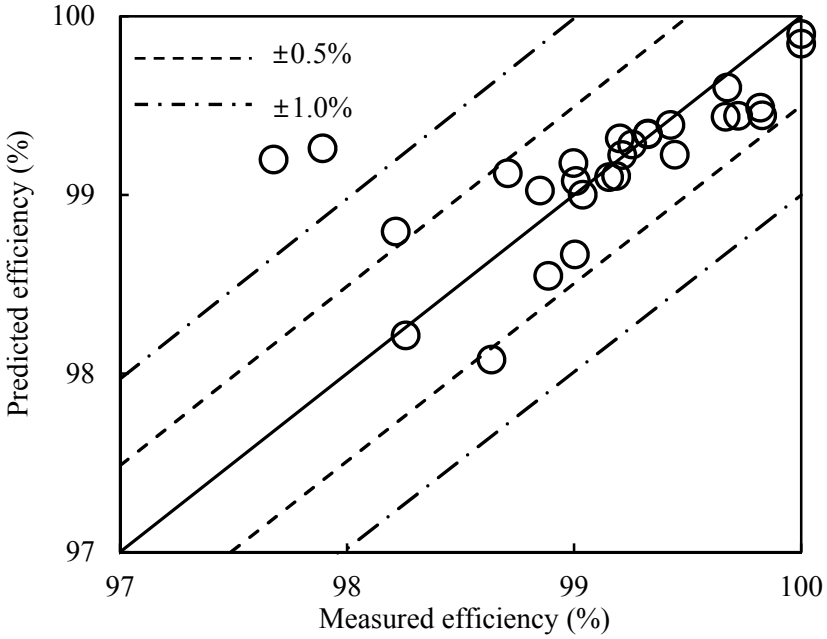

Fig. 4.24 Comparison of experimental and predicted efficiency of oil separator with inlet configuration of type 2

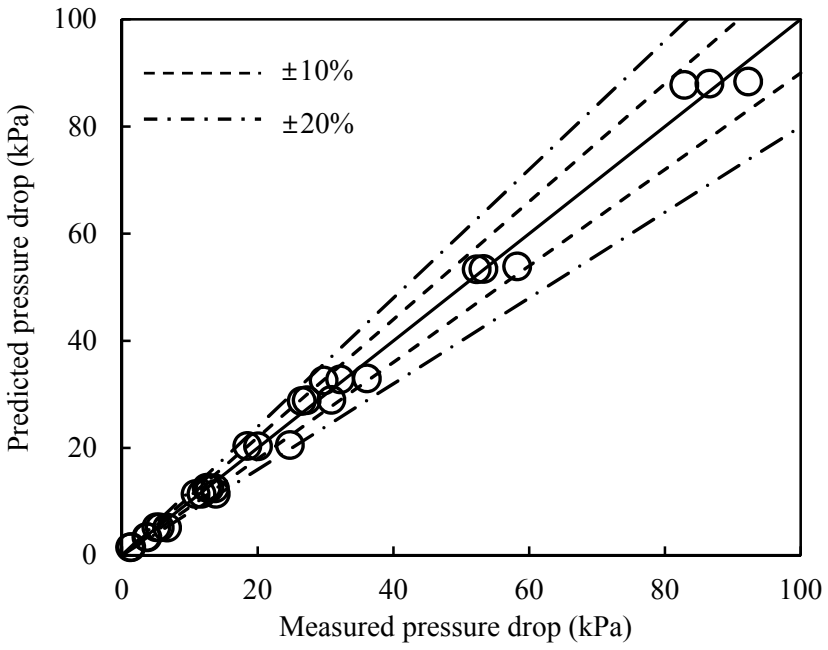

Fig. 4.25 Comparison of experimental and predicted pressure drop of oil separator with inlet configuration of type 2

4.5 Conclusion

The efficiency and pressure drop of the oil separator were measured. Seven oil separators were used to analyze the flow characteristics in oil separator with respect to size of oil separator and configuration of inlet pipe.

The efficiency of oil separator diminishes as the mass flow rate of refrigerant goes up under low mass flow rate condition. However, the efficiency of oil separator goes up as the mass flow rate of refrigerant increases under high mass flow rate condition. From the results, it can be presumed that the reduction of droplet size due to the rise of mass flow rate mainly affect the separation efficiency and increment of centrifugal force due to the rise of mass flow rate is dominantly affect the separation efficiency under low and high mass flow rate condition, respectively. Compare to the reference model, the fatter body diameter or the taller body height denotes the higher separation efficiency. In addition, inlet configuration of type 2 showed high separation efficiency compare to that of type 1.

Pressure drop decreases as the liquid circulation ratio goes up because of increment of friction during the outer circulation. Pressure drop goes up as the body diameter becomes fatter because pressure loss at near the outlet pipe increases due to high tangential velocity of inner circulation.

Theoretically, as the body height increases, pressure drop diminishes because the friction loss during outer circulation goes up. From the experimental results, however, it was confirmed that this effect is not significant. Configuration of inlet pipe also almost does not affect pressure drop.

Based on the experimental data, empirical correlations for predicting the efficiency and pressure drop of the oil separator were proposed. In case of inlet configuration of type 1, the mean absolute percentage errors between the measured and predicted efficiency and pressure drop were 0.4% and 7.8%, respectively. As for inlet configuration of type 2, those were 0.3% and 7.6%, respectively.

Chapter 5. Concluding remarks

Lubricant in a compressor of heat pump system is discharged due to the refrigerant which passes through the compressor. Even though the oil separator is installed to return the discharged oil to the compressor, small amount of oil is not separated and circulates the whole heat pump system with refrigerant. This causes reduction of heat transfer, increment of pressure drop and durability problem of compressor. To prevent these problems, studies on the oil retention in each component of heat pump system and the performance of oil separator are required.

Models for predicting the oil retention amount in a heat pump system are suggested. This study divided the heat pump system into 3 sections based on the phase of refrigerant; gas phase region, liquid phase region and two phase region. Models for each region were proposed. Based on the models, the oil retention amount in 6 components (condenser, horizontal and vertical gas lines, evaporators, horizontal and vertical liquid lines) of multi heat pump system were predicted under various operating conditions. The oil retention amount in heat pump system diminished 26.1% and 67.3% with the increment of mass flux from 100 $kgm^{-2}s^{-1}$ to 250 $kgm^{-2}s^{-1}$ and reduction of oil circulation ratio from 0.9% to 0.1%, respectively. Portion of oil retention

amount in gas lines of refrigerant was the highest compare to that in other components. Thus, the accuracy of the prediction for gas lines highly affects the accuracy of prediction of oil retention amount in whole system.

To verify the model for gas phase region, experiment was conducted. The oil retention amount was measured with respect to the mass flux of refrigerant, oil circulation ratio and pipe diameter in horizontal and vertical suction lines. The oil retention amount reduces as the mass flux increases or oil circulation ratio diminishes. Due to the gravity force, the oil retention amount in vertical line was higher than that in horizontal line. As mass flux increases, however, the effect of shear force between gas and liquid phases becomes dominant. Thus the oil retention amounts in horizontal and vertical lines are almost the same under high mass flux condition. From the experimental results, the model for predicting the oil retention amount in gas phase region was verified. The mean absolute percentage error between predicted and experimental oil retention amount was 15.0%.

To reduce the oil circulation ratio, high performance oil separator is necessary. In order to design the high performance oil separator, the experiment was conducted. This study focused on the effect of body diameter, body height and inlet configuration on the separation efficiency and pressure drop of oil separator. As body diameter or height increases, the

separation efficiency goes up. In case of pressure drop, large body diameter denotes high pressure drop and body height almost does not affect the pressure drop. In case of inlet configuration of type 2, the separation efficiency was higher than the separation efficiency of inlet configuration of type 1 and pressure drop was similar to the pressure drop of type 1. Based on the experimental results, the correlations for predicting the separation efficiency and pressure drop were suggested. Different correlations were proposed based on the inlet configuration. In case of inlet configuration of type 1, the mean absolute percentage errors of models for efficiency and pressure drop were 0.4% and 7.8%, respectively. As for type 2, those were 0.3% and 7.6%.

References

[1] ANSI/ASHRAE 69-1990, 1990, Methods of Testing Discharge Line Refrigerant-Oil Separators, pp. 1-16.

[2] Azadi, M., Azadi, M. and Mohebbi, A., 2010, A CFD Study of the Effect of Cyclone Size on its Performance Parameters, *Journal of Hazardous Materials*, Vol. 182, No. 1-3, pp. 835-841.

[3] Bankoff, S. G., 1960, A Variable Density Single Fluid Model for Two-Phase Flow with Particular Reference to Steam-Water, *Journal of Heat Transfer*, Vol. II, pp. 265-272.

[4] Ben A., 2002, Two Phase Flow: Accounting for the Presence of Liquids in Gas Pipeline Simulation, *PSIG Annual Meeting*, Portland, U. S. A., pp. 1-21.

[5] Brennan, M., Holtham, P. and Narasimha, M., 2009, CFD Modeling of Cyclone Separators: Validation against Plant Hydrodynamic Performance, *Seventh International Conference on CFD in the Minerals and Process Industries*, CSIRO, Melbourne, Australia, pp. 1-6.

[6] Chen, S. L., Gerner, F. M. and Tien, C. L., 1987, General Film Condensation Correlations, *Experimental Heat Transfer*, Vol. 1, pp. 93-107.

[7] Chisholm, D., 1972, An Equation for Velocity Ratio in Two-Phase Flow, NEL Report 535.

[8] Cho, M. K., 2013, Study on Liquid Film Thickness Measurement of Annular Flow with Image Processing, Master thesis, Seoul National University, Korea.

[9] Cremaschi, L., 2004, Experimental and Theoretical investigation of Oil Retention in Vapor Compression Systems, Ph. D. thesis, University of Maryland, U.S.A.

[10] Crompton, J. A., Newell, T. A. and Chato, J. C., 2004, Experimental Measurement and Modeling of Oil Holdup, Air Conditioning and Refrigeration Center, Univ. of Illinois, Urbana-Champaign, U.S.A., ACRC TR-226.

[11] Dittus, F. W. and Boelter, L. M. K., 1930, Heat transfer in automobile radiators of the tubular type, University of California Publications in Engineering, Vol. 2, pp. 443-461.

[12] Elsayed, K. and Lacor, C., 2011, The Effect of Cyclone Inlet Dimensions on the Flow Pattern and Performance, *Applied Mathematical Modelling*, Vol. 35, No. 4, pp. 1952-1968.

[13] Fore, L. B., Beus, S. G. and Bauer, R. C., 2000, Interfacial Friction in Gas-Liquid Annular Flow: Analogies to Full and Transition Roughness,

International Journal of Multiphase Flow, Vol. 26, No. 11, pp. 1755-1769.

[14] Friedel, L., 1979, Improved Friction Pressure Drop Correlations for Horizontal and Vertical Two-Phase Pipe Flow, European Two-Phase Flow Group Meeting, Ispra, Italy, June, Paper E2.

[15] Fukuta, M., Yanagisawa, T., Shimasaki, M., and Ogi, Y., 2006, Real-time measurement of mixing ratio of refrigerant/refrigeration oil Mixture, *International Journal of Refrigeration*, Vol. 29, pp. 1058-1065.

[16] Gao, X., Zhao, Y., Yang, X., Chang, Y. and Peng, X., 2012, The Research on the Performance of Oil-gas Cyclone Separators in Oil Injected Compressor Systems with Considering the Collision and Breakup of Oil Droplets, International compressor Engineering Conference, Paper 1407, pp. 1-10.

[17] Gil, A., Romeo, L. M. and Cortes, C., 2002, Effect of the Solid Loading on a Pressurized Fluidized Bed Combustors Cyclone with Pneumatic Extraction of Solids, *Chemical engineering and Technology*, Vol. 25, No. 4, pp. 407-415.

[18] Gnielinski, V., 1976, New Equations for Heat and Mass Transfer in Turbulent Pipe and Channel Flow, *International Journal of Chemical Engineering*, Vol. 16, pp. 359-368.

[19] Grőnnerud, R., 1972, Investigation in Liquid Holdup, Flow Resistance and Heat Transfer in Circular Type Evaporators, Part IV: Two-Phase Resistance in Boiling Refrigearants, *Bulletin de I Ἰnst. Du Froid*, Annexe 1972-1.

[20] Gungor, K. E. and Winterton, R. H. S., 1986, A General Correlation for Flow Boiling in Tubes and Annuli, *International Journal of Heat and Mass Transfer*, Vol. 29, No.3, pp. 351-358.

[21] Gungor, K., E. and Winterton, R. H. S., 1987, Simplified General Correlation for Saturated Flow Boiling and Comparisions with Data, *Chemical Engineering Research and Design*, Vol. 65, pp. 148-156.

[22] Guo, T, Lee, W., Do, S. and Jeong, J. H., 2012, Suction Pipe Criterion for R-134a Refrigerators to Secure Oil Return to Compressor, *International Journal of Air-Conditioning and Refrigeration*, Vol. 20, No. 4, Paper 1250018, pp. 1-9.

[23] Hede, P. D., Bach, P. and Jensen, A. D., 2008, Two-fluid spray atomisation and pneumatic nozzles for fluid bed coating/agglomeration purposes: A review, *Chemical Engineering Science*, Vol. 63, No. 14, pp. 3821-3842.

[24] Hoffmann, A. C. and Stein, L. E., 2007, Gas Cyclones and Swirl Tubes, Springer.

[25] Hwang, Y., Lee, J. P., Rademche,r R. and Pereira, R. H., 2000, An Experimental Investigation On Flow Characteristics Of Refrigerant/Oil Mixture In Vertical Upward Flow, *International Refrigeration and Air Conditioning Conference at Purdue*, West Lafayette, Paper 491, pp. 265-272.

[26] Incropera, F. P., Dewitt, D. P., Bergman, T. L. and Lavine, A. S., 2007, Introduction to Heat Transfer, Fifth ed., John Wiley & Sons, New York, U.S.A.

[27] Lebreton, J. M. and Vuillame, L., 2001, Oil Concentration Measurement In Saturated Liquid Refrigerant Flowing Inside A Refrigeration Machine, *International Journal of Applied Thermodynamics*, Vol. 4, No. 1, pp. 53-60.

[28] Lee, J. P., 2003, Experimental and Theoretical Investigation of Oil Retention in a Carbon Dioxide Air Conditioning System, Ph. D. thesis, University of Maryland, U.S.A.

[29] Levi, S., 1967, Forced Convection Subcooled Boiling Prediction of Vapor Volumetric Fraction, *International Journal of Heat and Mass Transfer*, Vol. 10, pp. 951-965.

[30] Lockhart, R. W. and Martinelli, R. C., 1949, Proposed Correlation Data for Isothermal Two-Phase, Two-Component Flow in Pipes, *Chemical engineering Progress*, Vol. 45, No. 1, pp. 39-48.

[31] Luz III, R. M., 2005, Design of an Ultraviolet Absorption Spectroscopy Oil Concentration Sensor for Online HVAC Measurements, Master thesis, Massachusetts Institute of Technology, U.S.A.

[32] Matsuzaki, K., Ushijima, H., Munekata, M. and Ohba, H., 2006, Numerical Study on Particle Motions in Swirling Flows in a Cyclone Separator, *Journal of Thermal Science*, Vol. 15, No. 2, pp. 181-185.

[33] Mehendale, S. S. and Radermacher, R., 2000, Experimental and Theoretical Investigation of Annular Film Flow Reversal In a Vertical Pipe : Application To Oil Return In Refrigeration Systems, *HVAC&R Research*, Vol. 6, No. 1, pp. 55-74.

[34] Műller-Steinhagen, H. and Heck, K., 1986, A Simple Friction Pressure Drop Correlation for Two-Phase Flow in Pipes, *Chemical Engineering and Processing: Process Intensification*, Vol. 20, No. 6, pp. 297-308.

[35] Murakami, H., Wakamoto, S. and Morimoto, O., 2006, Performance Prediction of a Cyclone Oil Separator, *International Refrigeration and Air Conditioning Conference at Purdue*, Paper R028, pp. 1-8.

[36] Ould Didi, M. B., Kattan, N. and Thome, J. R., 2002, Prediction of Two-Phase Pressure gradients of Refrigerants in Horizontal Tubes, *International Journal of Refrigeration*, Vo. 25, No. 7, pp. 935-947.

[37] Pe´rez-Lombard, L., Ortiz, J. and Pout, C., 2008, A review on buildings energy consumption information, *Energy and Buildings*, Vol. 40, No. 3, pp. 394-398.

[38] Ramakrishnan, A. and Hrnjak, P. S., 2012, Oil Retention and Pressure Drop of R134a, R1234yf and R410A with POE 100 in Suction Lines, *International Refrigeration and Air Conditioning Conference at Purdue*, West Lafayette, U.S.A., Paper 2508, pp. 1-10.

[39] Safikhani, H., Behabadi, M. A., Shams, M. and Rahimyan, M. H., 2010, Numerical Simulation of Flow Field in Three Types of Standard Cyclone Separators, *Advanced Powder Technology*, Vol. 21, No. 4, pp. 435-442.

[40] Shedd, T. A. and Newell, T. A., 1997, An Automated Optical Liquid Film Thickness Measurement Method, Air Conditioning and Refrigeration Center, Univ. of Illinois, Urban- Champaign, U.S.A., ACRC TR-134.

[41] Sheth, V. P. and Newell, T. A., 2005, Refrigerant and Oil Migration and Retention in Air Conditioning and Refrigeration Systems, Air

Conditioning and Refrigeration Center, Univ. of Illinois, Urbana-Champaign, U.S.A., ACRC TR-240.

[42] Smith, S. L., 1969, Void Fractions in Two-Phase Flow. A Correlation Based on an Equal Velocity Heat Model, *Proceeding of Institution of Mechanical Engineers*, Vol. 184, No. 36, pp. 647-664.

[43] Thome, J. R., 2004, Engineering Data Book III, WOLVERINE TUBE, INC., Chap. 5, pp. 3-4.

[44] Wallis, G. B., 1969, *One Dimensional Two-Phase Flow*, McGraw-Hill, New York.

[45] Wang, B., Xu, D. L., Chu, K. W. and Yu, A. B., 2006, Numerical Study of Gas-Solid Flow in a Cyclone Separator, *Applied Mathematical Modelling*, Vol. 30, No. 11, pp. 1326-1342.

[46] Wang, C. C. and Chi, K. Y., 2000, Heat Transfer and Friction Characteristics of Plain Fin and Tube Heat Exchangers, Part I: New Experimental Data, *International Journal of Heat and Mass Transfer*, Vol. 43, No. 15, pp. 2681-2691.

[47] Wang, C. C., Chi, K. Y. and Chang, C. J., 2000, Heat Transfer and Friction Characteristics of Plain Fin and Tube Heat Exchangers, Part II: Correlation, *International Journal of Heat and Mass Transfer*, Vol. 43, No. 15, pp. 2693-2700.

[48] Wang, C. C., Lee, C. J., Chang, C. T. and Lin, S. P., 1998, Heat Transfer and Friction Correlation for Compact Louvered Fin and Tube Heat Exchangers, *International Journal of Heat and Mass Transfer*, Vol. 42, No. 11, pp. 1945-1956.

[49] Wang, C. C., Lee, W. S. and Sheu, W. J., 2001, A Comparative Study of Compact Enhanced Fin and Tube Heat Exchangers, *International Journal of Heat and Mass Transfer*, Vol. 44, No. 18, pp. 3565-3573.

[50] Winterton, R. H. S., 1998, Where did the Dittus and Boelter equation come from?, *International Journal of Heat and Mass Transfer*, Vol. 41, No. 4-5, pp. 809-810.

[51] Wongwises, S. and Kongkiatwanitch, W., 2001, Interfacial Friction Factor in Vertical Upward Gas-Liquid Annular Two-Phase Flow, *International Communications in Heat and Mass Transfer*, Vol. 28, No. 3, pp. 323-336.

[52] Zivi, S. M., 1964, Estimation of Steady-State Steam Void Fraction by Means of the Principle of Minimum entropy Generation, *Journal of Heat Transfer*, Vol. 86, pp. 247.252.

[53] Zoellick, K. F. and Hrnjak, P. S., 2010, Oil Retention and Pressure Drop in Horizontal and Vertical Suction Lines with R410A/POE, *International Refrigeration and Air Conditioning Conference*, Paper 2327, pp. 1-8.

국 문 초 록

본 연구에서는 히트펌프시스템 내를 순환하는 냉매/오일 혼합물의 유동특성에 대한 연구를 수행하였다. 히트펌프시스템 내의 주요 구성요소 중 하나인 압축기에는 구동부가 존재하고, 이 구동부에서 발생하는 마찰을 감소시키기 위해 오일을 이용한 윤활이 필수적이다. 하지만 윤활을 위한 오일 중 일부는 압축기를 통과하는 냉매에 의해 압축기로부터 토출된다. 토출된 오일을 다시 압축기로 회수하기 위해 압축기 출구에 오일분리기를 설치한다. 하지만 오일분리기의 효율이 100%가 아니기 때문에 일부의 오일은 냉매와 함께 히트펌프시스템 전체를 순환하게 된다. 이상적으로 냉매만 히트펌프시스템을 순환하는 경우와 비교할 때, 냉매와 오일이 함께 순환하는 경우 압력강하 증대와 열전달 둔화 등의 문제가 발생할 수 있다. 또한 많은 양의 오일이 시스템을 순환할 경우 압축기 윤활에 필요한 오일이 부족하여 압축기 내구성 문제를 야기할 수 있다. 이러한 문제 중 압축기 내구성 문제의 경우, 시스템 전체를 순환하는 오일의 양을 정확히 예측하여 최적의 압축기 오일 충전량을 제시하여 예방할 수 있다. 초기 압축기 오일 충전량은 압축기 윤활을 위해 필요한 오일과 시스템을 순환하는 오일의 양을 합친 것과 같다. 이 중 시스템을 순환하는 오일량은 히트펌프시스템 각 구성요소에서의 오일 축적량을 계산하여 예측할 수 있다. 본 연구에서는 히트펌프시스템 각 구성요소에서의 오일 축적량을 예측할 수 있는 모델을 제시하였고, 이를 바탕으로 다양한 운전 조건 및 시스템 설치 조건에 따른 각 구성요소에서의 오일 축적량을 예측하였다. 이를 통해 기상배관에서의 오일 축적량이 전체 오일 축적량 대비 매우 높은 비중을 차지한다는 것을 파악하였다. 따라서 본 연구에서는 실험적 연구를 통해 기상 배관인 압축기 흡입관에서의 오일 축적량 및 압력 강하를 측정하였다. 이를 통해 확보한 실험 결과를

해석을 통해 예측한 결과와 비교하여 제시한 오일축적량 예측 모델의 타당성을 검증하였다. 초기 오일 충전량과 관련된 문제 외에 압력강하 증대 및 열전달 둔화 등의 시스템 성능저하와 관련된 문제의 경우, 시스템을 순환하는 오일량을 감소시킴으로써 개선할 수 있다. 이를 위해서는 압축기 출구 측에 설치되는 오일분리기의 효율 향상이 필요하다. 때문에 본 연구에서는 다양한 형상의 오일분리기에 대한 실험을 수행하여 오일분리기 형상에 따른 오일분리기의 효율 및 오일분리기에서의 압력강하를 측정하였다. 이를 통해 오일분리기 내부를 통과하는 냉매/오일 혼합물의 유동특성을 예측하여 다양한 조건에 따라 최적 오일분리기 형상을 제안할 수 있는 모델을 제시하였다.

주요어: 오일축적량, 압력 강하, 오일분리기, 멀티히트펌프시스템, R410A, PVE 오일

학 번: 2011-31291